

FUJI ELECTRIC REVIEW

2017
Vol.63 No.

4

Power Semiconductors Contributing in Energy Management



FUJI ELECTRIC REVIEW

2017
Vol.63 No.

4

Power Semiconductors Contributing in Energy Management

Efforts to curb CO₂ emissions are very important to address global warming. Measures are thus actively being taken to save energy, expand renewable energy, including photovoltaic and wind power generation, and introduce electrically driven vehicles, such as hybrid electric vehicles (HEVs) and electric vehicles (EVs). In this situation, expectations are increasingly raised for power semiconductors as key devices for power electronics to use electric energy efficiently and stably. Fuji Electric has developed and commercialized power semiconductors that facilitate downsizing and efficiency improvement of power electronics equipment intended for many fields.

This special issue presents the latest technologies and products of Fuji Electric's power semiconductors.

Cover Photo:

(1) "PrimePACK™" of 7th-Generation "X Series" 1,700-V IGBT modules, (2) All-SiC 2-in-1 module (Type 3L), (3) "HPnC" high-current SiC hybrid module, (4) "M660" high-power IGBT module for automotive applications, (5) 6.5th-generation automotive pressure sensor



FUJI ELECTRIC REVIEW vol.63 no.4 2017

date of issue: December 30, 2017

editor-in-chief and publisher KONDO Shiro

Corporate R & D Headquarters
Fuji Electric Co., Ltd.
Gate City Ohsaki, East Tower,
11-2, Osaki 1-chome, Shinagawa-ku,
Tokyo 141-0032, Japan
<http://www.fujielectric.co.jp>

editorial office Fuji Electric Journal Editorial Office
c/o Fuji Office & Life Service Co., Ltd.
1, Fujimachi, Hino-shi, Tokyo 191-8502,
Japan

Fuji Electric Co., Ltd. reserves all rights concerning the republication and publication after translation into other languages of articles appearing herein.

All brand names and product names in this journal might be trademarks or registered trademarks of their respective companies.

Contents

Power Semiconductors Contributing in Energy Management	
All-SiC Modules Equipped with SiC Trench Gate MOSFETs NAKAZAWA, Masayoshi DAICHO, Norihiro TSUJI, Takashi	204
3.3-kV All-SiC Modules for Electric Distribution Equipment TANIGUCHI, Katsumi KANEKO, Satoshi KUMADA, Keishiro	209
“PrimePACK™” of 7th-Generation “X Series” 1,700-V IGBT Modules YAMAMOTO, Takuya YOSHIWATARI, Shinichi OKAMOTO, Yujin	214
“HPnC” High-Current SiC Hybrid Module SEKINO, Yusuke MITSUMOTO, Takahiro MORIYA, Tomohiro	218
7th-Generation “X Series” RC-IGBT Module Line-Up for Industrial Applications YAMANO, Akio TAKASAKI, Aiko ICHIKAWA, Hiroaki	223
“M660” High-Power IGBT Module for Automotive Applications OSAWA, Akihiro HIGUCHI, Keiichi NAKANO, Hayato	228
6.5th-Generation Automotive Pressure Sensors UZAWA, Ryohei NISHIKAWA, Mutsuo TANAKA, Takahide	232
“FA8A80 Series” 650-V PWM Power Supply Control ICs HIASA, Nobuyuki ENDO, Yuta KARINO, Taichi	237
“Super J MOS S2 Series” and “Super J MOS S2FD Series” for DFN 8 × 8 Packages SHIMATO, Takayuki WATANABE, Sota MATSUMOTO, Kazunori	242
New Products	
“PrimePACK™” of 7th-Generation “X Series” 1,700-V IGBT Modules	246
I-Type “PrimePACK™” of 3-Level IGBT Modules	249
“SUPER ECO MOLTRA II” Cast Resin Transformer Achieving Super High Efficiency	252
6.5th-Generation Automotive Pressure Sensors	255

All-SiC Modules Equipped with SiC Trench Gate MOSFETs

NAKAZAWA, Masayoshi* DAICHO, Norihiro* TSUJI, Takashi*

ABSTRACT

There are increasing expectations placed on products that utilize SiC modules to achieve higher efficiency, smaller size and larger capacity in power conversion equipment. Fuji Electric has been producing products that incorporate All-SiC modules with a rated capacity of up to 1,200 V/100 A in a package with a new structure. This package achieves higher performance and higher reliability for SiC modules. In order to expand the rated capacity, Fuji Electric has recently developed a large-capacity package with a new structure. This new package utilizes an All-SiC module with a rated capacity of 1,200 V/400 A, being equipped with an SiC trench gate MOSFET that achieves both low on-resistance and high-speed switching characteristics.

1. Introduction

In order to mitigate environmental problems such as global warming and achieve a low-carbon society, it is necessary to develop energy-saving power conversion equipment and actively utilize renewable energies. Power semiconductors play a major role in efficient power conversion. Up until now, silicon (Si) has been used as a major semiconductor material. However, in spite of characteristic improvement efforts for Si semiconductor devices, their performance is already approaching the theoretical limit determined by the physical properties. It is against this backdrop that wide band gap semiconductor silicon carbide (SiC) has been focused as a next generation semiconductor material. SiC devices can achieve significantly lower loss than Si devices, it is thus expected that they will contribute to further energy savings.

Fuji Electric commenced operation of the industry's first 6-inch SiC wafer production line at the Matsumoto Factory in 2013 as shown in Fig. 1. In 2014, Fuji Electric developed and started producing an All-SiC chopper module that combined SiC metal-oxide-semiconductor field-effect transistor (SiC-MOSFET) and SiC Schottky barrier diode (SiC-SBD) for the booster circuit used in mega solar power conditioning systems (PCSs).⁽¹⁾ This All-SiC chopper module has achieved the world's highest level of conversion efficiency at 98.8% while also contributing to miniaturization of about 60% when compared to conventional PCSs. Furthermore, Fuji Electric developed an All-SiC 2-in-1 module in 2016 and has utilized its features (low loss, high-temperature working guarantee, high reliability and low thermal resistance) to successfully develop a totally-enclosed self-cooled inverter (IP65 in-



Fig.1 6-inch SiC wafer

verter).⁽²⁾




Fuji Electric has already developed an All-SiC module with a maximum rated capacity of 1,200 V/100 A.⁽³⁾ In order to meet the demand for further expansion of power module capacity, Fuji Electric developed a large-capacity package with a new structure. This new package utilizes an All-SiC 2-in-1 module with a rated capacity of 1,200 V/400 A, being equipped with a 1st-generation SiC trench gate MOSFET that achieves both low on-resistance and high-speed switching characteristics. The following sections introduce this module.

2. Line-Up of All-SiC 2-in-1 Modules

Table 1 shows the line-up of All-SiC 2-in-1 modules. A line-up of Type 1, Type 2 and Type 3L newly structured packages are provided for their respective rated current. Compared with the conventionally highest rated Type 2 module of 1,200 V/100 A, the current product development utilizes a newly developed

* Electronic Devices Business Group, Fuji Electric Co., Ltd.

Table 1 Line-up of All-SiC 2-in-1 modules

		Type 1	Type 2	Type 3L
External dimensions (mm)		W68 × D26 × H13	W68 × D26 × H13	W126 × D45 × H13
External appearance				
Rating	Voltage (V)	1,200		
	Current (A)	25, 50	75, 100	200, 300, 400
Terminal	Main terminal	Solder pin		Screw terminal
	Auxiliary terminal	Solder pin		
Connection point	Main terminal	Printed circuit board		Bus bar
	Auxiliary terminal	Printed circuit board		

large-capacity Type 3L package to achieve a 2-in-1 module with a maximum rating of 1,200 V/400 A.

3. All-SiC Module Elemental Technologies

3.1 Newly structured large-capacity package

Figure 2 shows a comparison of the newly structured package developed for All-SiC modules and the conventionally structured package for Si-IGBT mod-

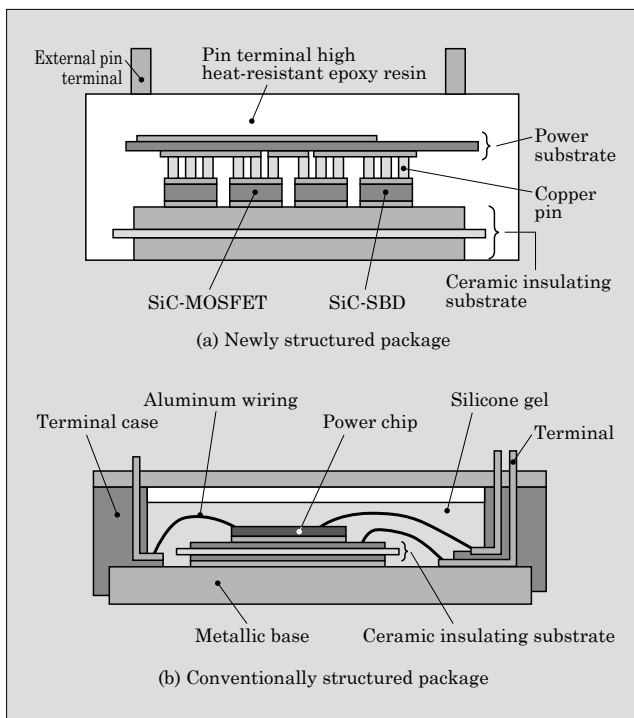


Fig.2 Comparison of package structures

ules.⁽⁴⁾ The conventional package utilizes aluminum bonding wire for the wiring, silicone gel resin for the insulation sealing resin and a thin copper ceramic insulating substrate for the insulating substrate. In contrast to this, the newly structured package utilizes implant pins for the wiring, high heat-resistant epoxy resin for the sealing resin and a thick copper ceramic insulating substrate for the insulating substrate. As a result, it facilitates high-density mounting in which multiple SiC chips are connected in parallel, while also achieving reduced internal inductance, low thermal resistance and high reliability.

The large-capacity newly structured package is based on these technological characteristics and is distinguished by the following 3 development points:

- Making it easy to connect the main terminals and laminated bus bar
- Making it easy to connect the auxiliary terminals and the printed circuit board
- Securing an isolating distance between terminals, and between terminals and ground, while simultaneously achieving low inductance

Laminated bus bar is preferred to achieve low inductance when connecting an input power supply with a power module. This large-capacity newly structured package utilizes a screw terminal structure for connecting the laminated bus bar and the power module. The screw terminal structure is designed by laser welding together the external pin terminals and a copper bar with a threaded hole located on the top part of the external pin terminals.

Furthermore, to achieve high-speed high-frequency switching, it is necessary to reduce gate-source wiring inductance. Therefore, a solder pin is used for the auxiliary terminals to enable direct connection with the circuit board via soldering. This made it possible to arrange the gate driver circuit in the vicinity of the module.

In addition, it is necessary to secure a sufficient isolating distance to comply with IEC 60077 and IEC 62497 for the insulation while also obtaining an external shape that enables expansion of the absolute maximum rated voltage to 1,700 V. However, in this respect, there was the issue of increasing the package size. Furthermore, to suppress surge voltage during high-speed turn off current, there was the issue of reducing internal inductance of the module. Therefore, external shape of this package has the same low height as the conventional Type 2 package to secure a sufficient isolating distance, shorten the main circuit path and achieve low inductance.

3.2 SiC trench gate MOSFET with rated withstand voltage of 1,200V

Fuji Electric has been providing the market with All-SiC modules equipped with planar gate MOSFET. As is well known, one effective way to further reduce on-resistance per unit area for planar gate MOSFET is

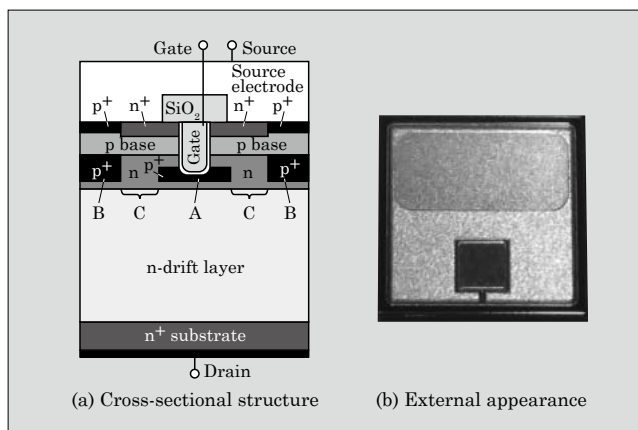


Fig.3 SiC trench gate MOSFET cross sectional structure and chip external appearance

to reduce the cell pitch. However, excessive reduction of the cell pitch can lead to increased junction field-effect transistor (JFET) resistance. As a result, on-resistance can't be lower.

Therefore, the trench gate MOSFET is adopted to suppress the increase in the JFET resistance resulting from reduction of the cell pitch, and thus, make it possible to achieve low on-resistance. Figure 3 shows the cross sectional structure of the recently developed SiC trench gate MOSFET and the external appearance of the chip.⁽⁵⁾

In order to simultaneously establish a low on-resistance and a high threshold voltage that does not induce malfunction, the cell pitch was reduced, and the channel length was also optimized. Furthermore, to improve the reliability of the oxide film, a p-well is used to enclose the gate oxide film at the bottom of the trench to help ease the high electric field on the gate oxide film. Moreover, as shown in Fig. 3, the JFET region (see C in the figure) that is between the p-well at the bottom of the trench (see A in the figure) and the p-well connected to the source (see B in the figure) was optimized.

By adopting the above-mentioned trench gate MOSFET and optimizing various parameters, the development of an SiC MOSFET with a rated withstand voltage of 1,200 V with the world's highest-level of on-resistance at $3.5 \text{ m}\Omega \cdot \text{cm}^2$ and a threshold voltage of 5 V has been achieved.

4. Characteristics of 1,200-V/400-A All-SiC 2-in-1 Module

4.1 Output characteristics

Figure 4 shows the output characteristics of All-SiC module (1,200-V/400-A rated product) that is achieved by the large-capacity newly structured package equipped with the trench gate MOSFET and 7th-generation "X Series" Si-IGBT module (1,200-V/450-A rated product).⁽⁶⁾ Because MOSFETs have no built-in voltage unlike as IGBTs, the steady-state loss during

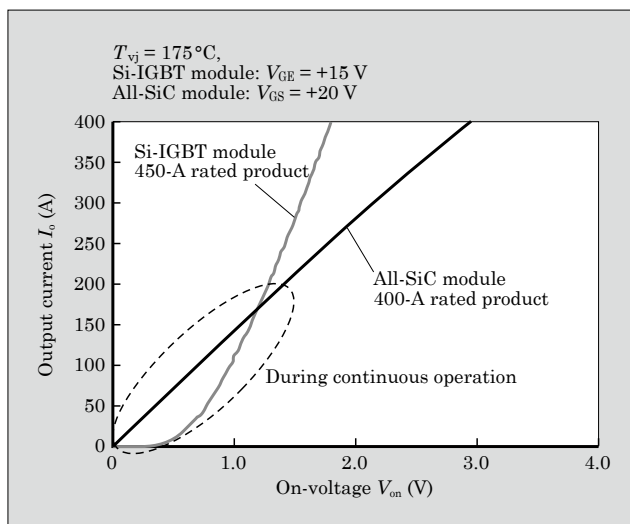


Fig.4 Comparison of output characteristics

continuous operation of the All-SiC module is lower than that of the Si-IGBT module.

4.2 Switching characteristics

Figure 5 shows the turn-on, turn-off and reverse recovery switching waveforms of the All-SiC module. The waveforms are stable and that there is no malfunction.

Figure 6 shows a comparison of turn-on losses, Fig. 7, turn-off losses, Fig. 8, reverse recovery loss, and Fig. 9, total switching losses. Compared with the 7th-generation Si-IGBT module, the All-SiC module reduces turn-on loss by approximately 87%, turn-off loss

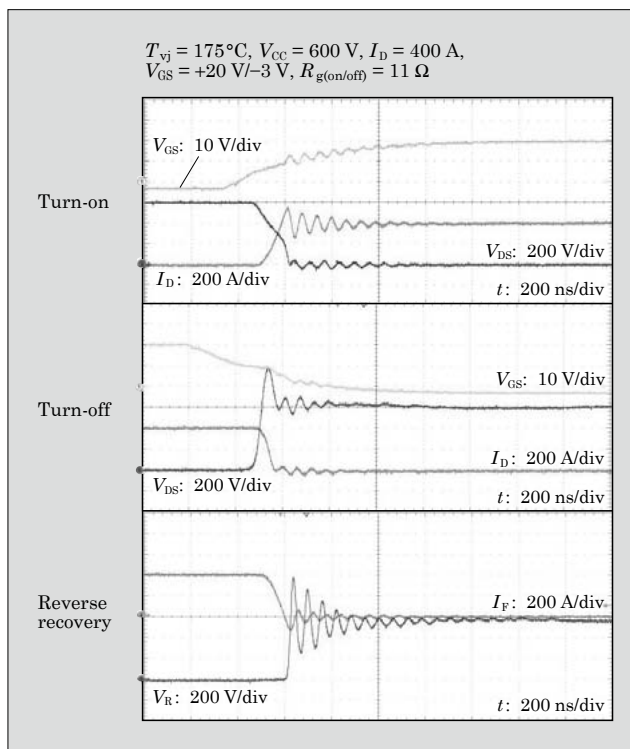


Fig.5 All-SiC module switching waveforms (1,200 V/400 A)

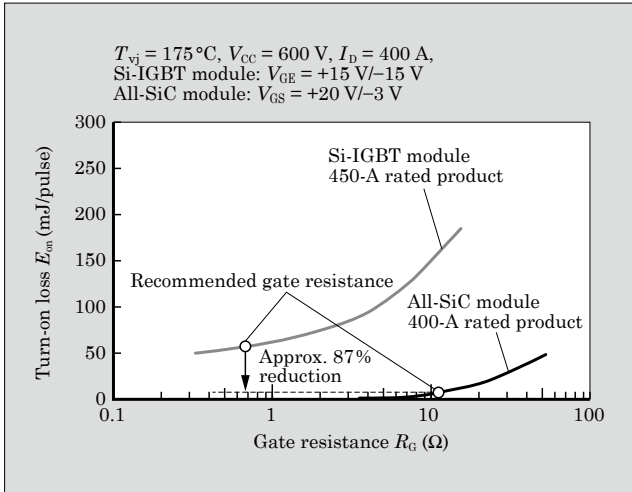


Fig.6 Turn-on loss

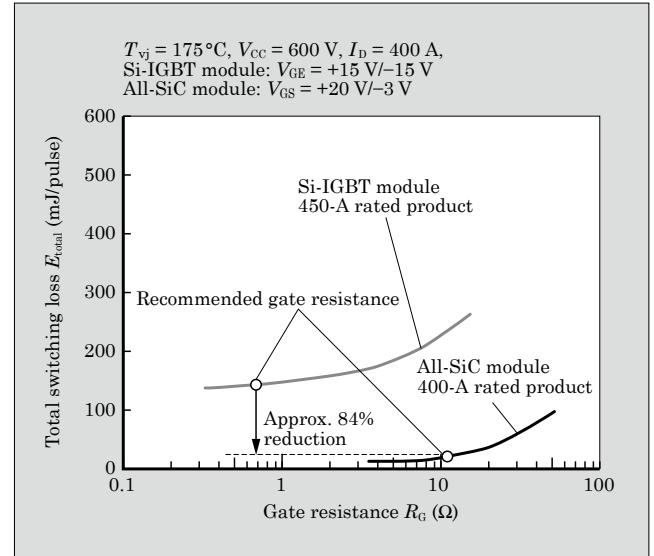


Fig.9 Total switching loss

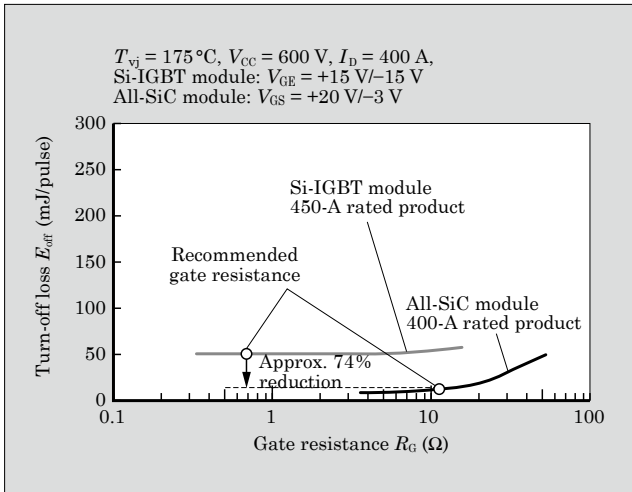


Fig.7 Turn-off loss

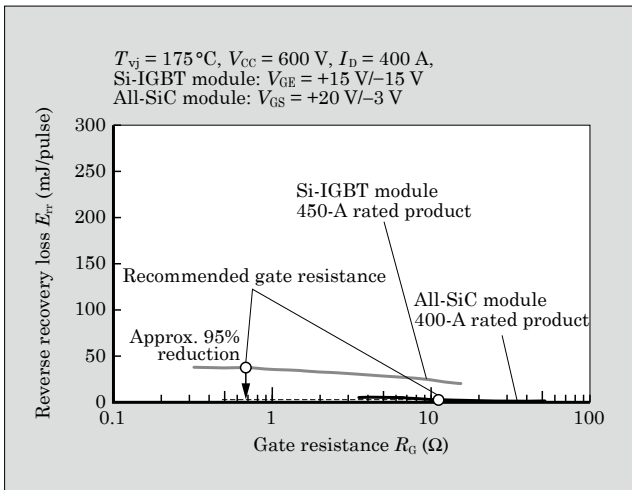


Fig.8 Reverse recovery loss

by approximately 74% and reverse recovery loss by approximately 95%. As a result, total switching loss was reduced by about 84%.

4.3 Inverter loss simulation

Figure 10 shows the simulation results for inverter loss under general use conditions for the inverter mounted All-SiC module and 7th-generation “X Series” Si-IGBT module. Compared with the Si-IGBT module, the All-SiC module reduced inverter loss for the inverter by approximately 57%.

Figure 11 shows the simulation results with respect to the carrier frequency dependence of the inverter loss. Compared with the Si-IGBT module, the switching loss for the All-SiC module was extremely low. The results shows that using the All-SiC module with high carrier frequency can lead to the significant miniaturization of passive components such as DC reactors and isolation transformers. As one example, the auxiliary power supplies of electrical rolling stock can achieve device weight savings and miniaturization of about 50% compared with conventional utility frequency link

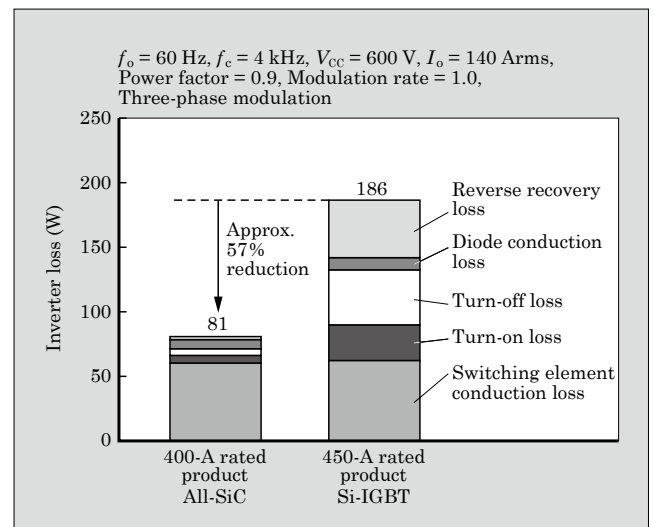


Fig.10 Inverter loss simulation results

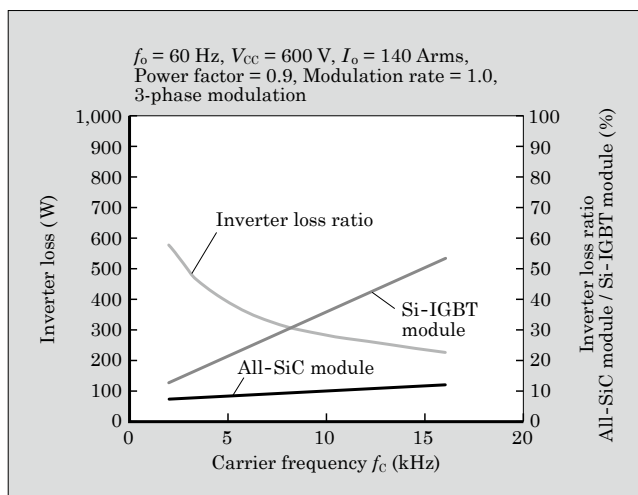


Fig.11 Inverter loss carrier frequency dependence

system.

5. Postscript

In this paper, All-SiC module that comes equipped with SiC trench gate MOSFETs was introduced. By equipping the newly developed large-capacity package with a new structure with SiC trench gate MOSFETs, 2-in-1 module with a rated capacity of 1,200 V/400 A has been successfully developed. In the future, we

plan to increase the power density and expand our line-up of All-SiC modules to contribute to the miniaturization, high-efficiency and high-reliability of various types of power conversion equipment.

Some of the development work has been carried out as part of a project of the joint research body Tsukuba Power Electronics Constellations (TPEC). We would like to conclude by expressing our appreciation to all those involved in the project.

References

- (1) Oshima, M. et al. Mega Solar PCS Incorporating All-SiC Module "PVI1000 AJ-3/1000". FUJI ELECTRIC REVIEW. 2015, vol.61, no.1, p.11-16.
- (2) Chonabayashi, M. et al. All-SiC 2-in-1 Module. FUJI ELECTRIC REVIEW. 2016, vol.62, no.4, p.222-226.
- (3) Iwasaki, Y. "All-SiC Module with 1 st Generation Trench Gate SiC MOSFETs and New Concept Package". PCIM Europe 2017.
- (4) Nakamura, H. et al. All-SiC Module Packaging Technology. FUJI ELECTRIC REVIEW. 2015, vol.61, no.4, p.224-227.
- (5) Tsuji, T. et al. 1.2-kV SiC Trench MOSFET. FUJI ELECTRIC REVIEW. 2016, vol.62, no.4, p.218-221.
- (6) Yoshida, K. "Power Rating extension with 7th generation IGBT and thermal management by newly developed package technologies", PCIM Europe 2017.

3.3-kV All-SiC Modules for Electric Distribution Equipment

TANIGUCHI, Katsumi* KANEKO, Satoshi* KUMADA, Keishiro*

ABSTRACT

Fuji Electric has partnered with the New Energy and Industrial Technology Development Organization (NEDO) in a project to develop electric distribution equipment and control systems that contribute to power grid stabilization when distributed energy sources such as solar power generation are massively introduced. For electric distribution equipment, an All-SiC module with a withstand voltage of 3.3 kV has been developed in that purpose. Compared to conventional Si-IGBT modules, it reduces the generated loss of inverters by 64%. As a result, our electric distribution equipment becomes so small and lightweight that they can be mounted to a single utility pole, which was not possible for conventional Si-IGBT modules due to size restrictions.

1. Introduction

There has been growing demand to reduce emission of greenhouse gases such as CO₂ in order to mitigate global warming. To achieve this, it is necessary to use renewable energies actively and adopt energy-saving power electronics equipment. Playing a major role in power conversion for power electronics equipment is power semiconductors. Up until now, the technological advance of silicon (Si) devices has made them widely popular, but they are already nearing the performance limit of their physical properties. Against this backdrop, it is expected that next-generation silicon carbide (SiC) semiconductor devices will enable even greater reductions in power loss while simultaneously contributing to energy savings and the reduction of size and weight of power electronics equipment.

In September 2014, Fuji Electric began working with the New Energy and Industrial Technology Development Organization (NEDO) in the “Demonstration Project for Constructing a Distributed Energy Next-Generation Electric Power Network.” We have been developing next-generation voltage regulators (electric distribution equipment) and applicable control systems such as a static var compensator (SVC) that uses SiC power semiconductors. This development is aimed at supporting the expanded installation of renewable energies such as photovoltaic power generation and also support to maintain and improve Japan’s international competitiveness in the electric power equipment and systems industry.

2. All-SiC Power Semiconductor Modules for Electric Distribution Equipment

In the “Demonstration Project for Constructing a Distributed Energy Next-Generation Electric Power Network” that we have been participating in with NEDO, one of the goals has been to facilitate the large-scale adoption of distributed energy sources such as photovoltaic power generation to electric distribution systems. In this regard, we have been developing electric distribution equipment and applicable control systems to deal with many technological challenges, such as the generation of surplus power, lack of power for frequency adjustment and voltage rise in distribution wires (see Fig. 1). Particularly in Japan, the increased adoption of household photovoltaic power generation would create challenges such as power loss caused by reverse power flow at times of voltage rise in 6.6-kV distribution systems and output suppression of photovoltaic power generation. Therefore, it is necessary to utilize electric distribution equipment for these 6.6-kV distribution systems. In this respect, it would be necessary for them to be compact and lightweight so that they could be mounted to existing utility poles (single poles) and be self-cooling because they would not be able to support water or air based cooling systems.

Electric distribution systems with conventional Si power semiconductor were susceptible to large amounts of loss and required large heat sinks for dissipating heat generated by the module, thus making it impossible to achieve size reductions and weight savings. Therefore, it was necessary to install dedicated infrastructure for double utility poles,⁽¹⁾ and as a result, the adoption of these systems was infeasible due to the problem of installation space and cost factors.

However, size reduction, weight savings and single pole mounting can be achieved for electric distribution

* Electronic Devices Business Group, Fuji Electric Co., Ltd.

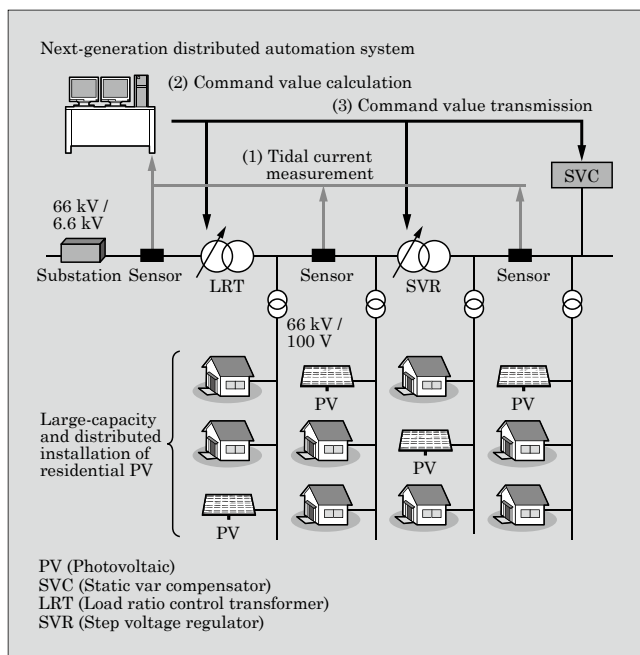


Fig.1 Overview of NEDO's "Demonstration Project for Constructing a Distributed Energy Next-Generation Electric Power Network"

equipment equipped with our newly developed All-SiC power semiconductor modules. Furthermore, they can be operated at high-frequency (13 kHz or higher), which is higher than the audible frequency of humans, thus making it possible to install the equipment in residential areas and accelerate adoption of them. Figure 2 shows the recently developed 3.3-kV All-SiC module for electric distribution equipment and the external appearance of an SVC mounted with the module. This paper describes the structure and characteristics of the 3.3-kV All-SiC 1-in-1 module developed for electric distribution equipment.

The All-SiC module contains SiC metal-oxide-semiconductor field-effect transistor (SiC-MOSFET) and SiC Schottky barrier diode (SiC-SBD) chips. Since

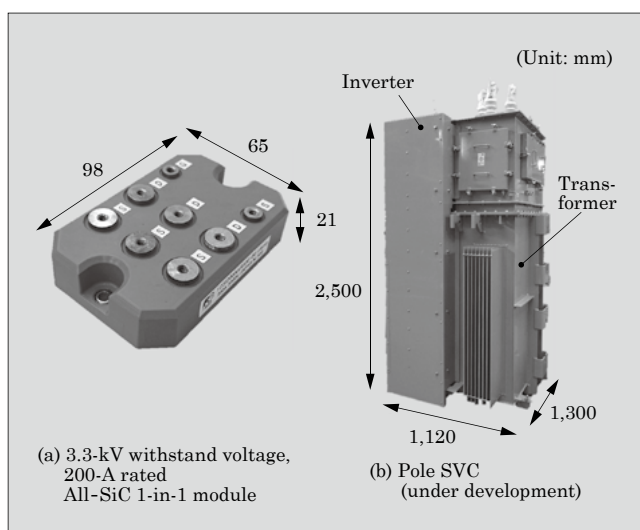


Fig.2 3.3-kV All-SiC module and pole-mount SVC

on-resistance per unit area increases in proportion with increases in withstand voltage, insulated gate bipolar transistor (IGBT) mostly utilized for voltages of 600 V and higher in Si devices. IGBTs reduce on-resistance through conduction modulation that minority carrier holes are injected into the drift layer. However, this also becomes a cause of large switching loss, because tail current occurs during switching due to an accumulation of minority carriers. In contrast, SiC devices exhibit lower drift layer resistance than Si devices, and as a result, are characterized by low on-resistance even without conduction modulation. SiC MOSFETs thereby establish both high withstand voltage and low loss.

3. Module Structure

Figure 3 shows a comparison of the schematic structures of the cross-section of conventional and new modules. The structure of the 3.3-kV All-SiC module follows the design principles for the structure of the 1.2-kV All-SiC module for mass-produced power conditioning systems (PCSs), and thus has a structure that is vastly different from conventional Si-IGBT modules.^{(2),(3)} The structure of the All-SiC module utilizes copper pin wiring on the power board instead of the conventional aluminum bonding wire. This enables large current flow and facilitates high-density mounting of SiC devices. The insulating substrate on which the chips are mounted utilizes a high-strength silicon nitride (Si_3N_4) insulating substrate bonded with thick copper plates instead of conventional aluminum nitride (AlN) as a design feature for improving resistance to epoxy resin sealing stress. Furthermore, by adopting epoxy resin

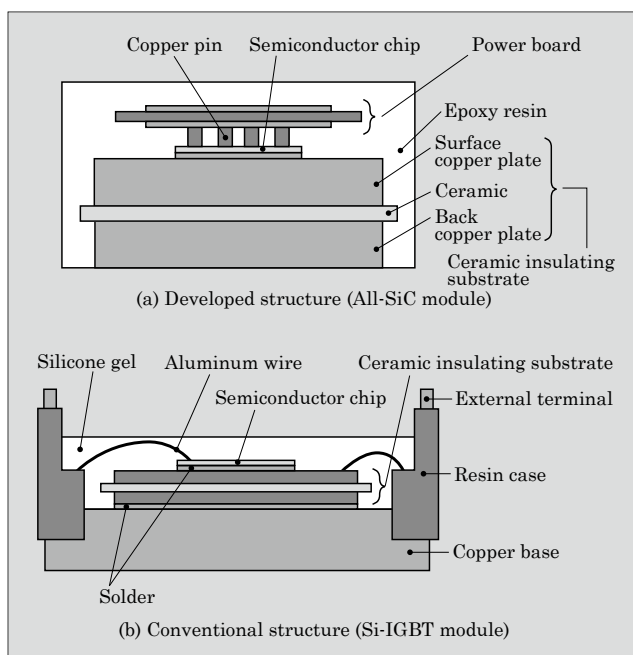


Fig.3 Comparison of modules' cross-sectional schematic structures

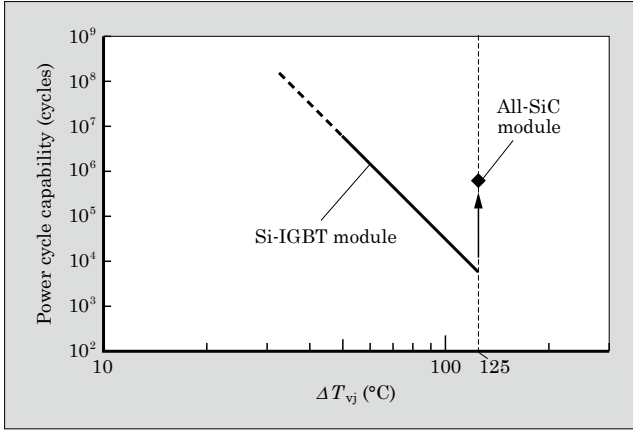


Fig.4 ΔT_{vj} power cycle test results at room temperatures

instead of the conventional silicone gel as the sealing material for the inside of the module, we were able to suppress solder degradation and insulation performance reduction during high-temperature operation while also securing high reliability and achieving weight savings without using a metal base nor case.

Figure 4 shows the results of a ΔT_{vj} power cycle test for the All-SiC module and conventional 3.3-kV Si-IGBT module at room temperature. The All-SiC module exhibited a power cycle capability of at least 120 times greater than that of the Si-IGBT module at $\Delta T_{vj} = 125^\circ\text{C}$. Electric distribution equipment is required to have a service life of at least 20 years, which is twice that of general industrial machines, which is 10 years. In this respect, the product has a sufficient power cycle capability to support this requirement.

4. Characteristics

The newly developed 3.3-kV All-SiC 1-in-1 module has a rated current of 200 A. We compared its characteristics with that of a same rated 200-A Si-IGBT 1-in-1 module that we made by replacing the SiC-MOSFETs with Si-IGBTs and the SiC-SBDs with Si free wheeling diodes (Si-FWDs).

4.1 I - V characteristics during conduction

The I - V characteristics determine the amount of steady-state loss, the loss generated at the time of conduction in the module. Figure 5 shows the I - V characteristics of an All-SiC module and Si-IGBT module at $T_{vj} = 25^\circ\text{C}$ and $T_{vj} = 150^\circ\text{C}$. Compared with the Si-IGBT module, the All-SiC module had a smaller drain voltage by 48% at 25°C and 20% at 150°C at a rated current of 200 A. The SiC-MOSFET has lower steady-state loss than Si-IGBT due to the lower on-resistance.

4.2 Switching characteristics

Switching loss can be classified into three different types: turn-on loss generated during turn on, turn-off loss generated during turn off and reverse recovery loss generated during reverse recovery. Figure 6 shows

turn-on loss, Figure 7, turn-off loss, and Figure 8, reverse recovery loss at $T_{vj} = 150^\circ\text{C}$. Similarly, Fig. 9 shows total switching loss.

Compared with the Si-IGBT module, the All-SiC module reduces turn-on loss by 80%, turn-off loss by 78% and reverse recovery loss by 85% when gate resistance is $4.7\ \Omega$. As a result, total switching loss was

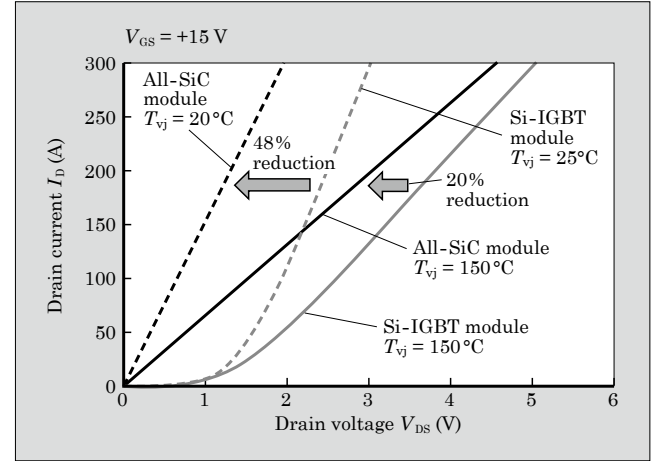


Fig.5 I - V characteristics

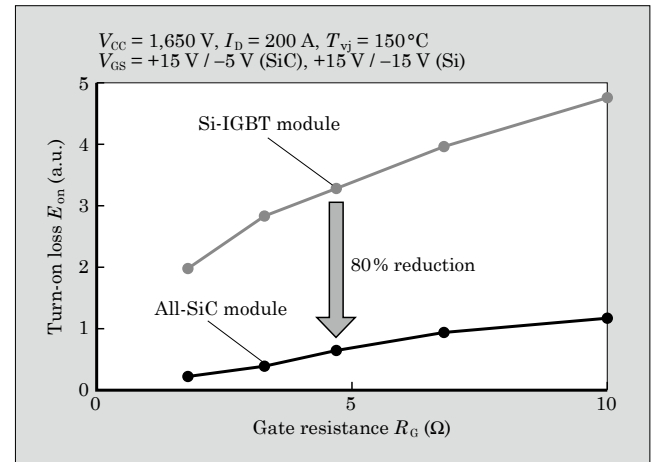


Fig.6 Turn-on loss

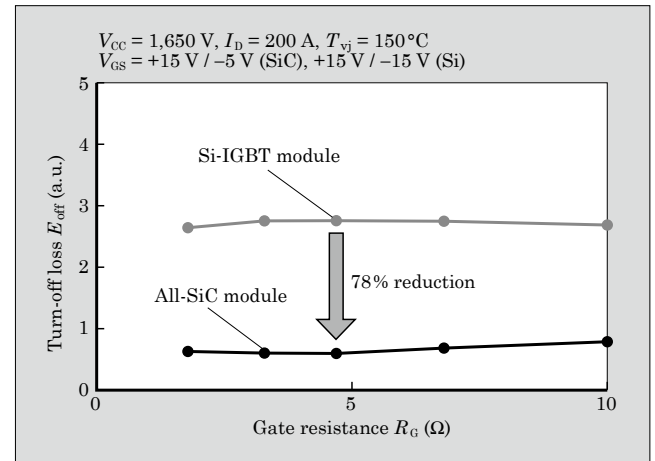


Fig.7 Turn-off loss

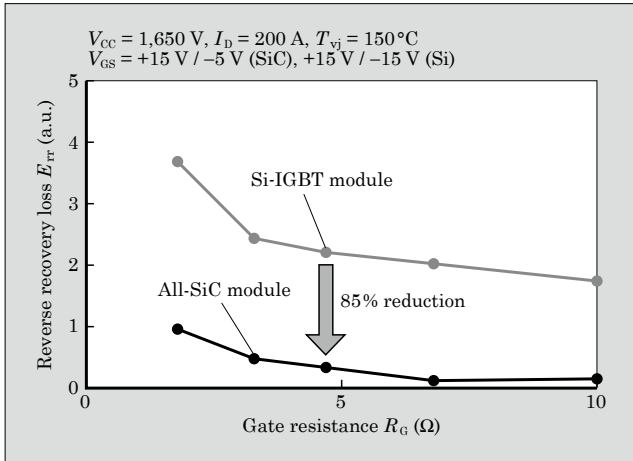


Fig.8 Reverse recovery loss

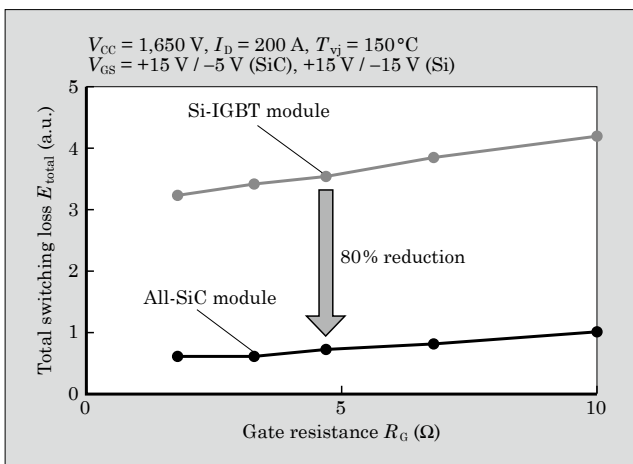


Fig.9 Total switching loss

reduced by 80%.

4.3 Loss simulation of Inverter generated

Figure 10 shows the circuit configuration of the 3-level inverter in the SVC of electric distribution equipment under development. Figure 11 shows simulation results of the inverter generated loss for the All-SiC module and Si-IGBT module under the operating condition of the 3-level inverter for SVC. As the operating conditions of 3-level inverters for SVC, a carrier frequency was set at 13 kHz, which is higher than that generally used for Si-IGBT modules, and thus a steady-state loss occupied only several percent. The inverter generated loss was almost entirely dependent on switching loss. The simulation result showed that inverter generated loss for the All-SiC module was lower by 64% comparing with the Si-IGBT module. This low generated loss resulted in a simplified product design that adopts a self-cooling system for the cooling structure for the SVC inverter while also facilitating size reduction and weight savings and enabling single pole mounting of the distribution system.

Figure 12 shows the carrier frequency dependence for the generated loss of the inverter. Under condi-

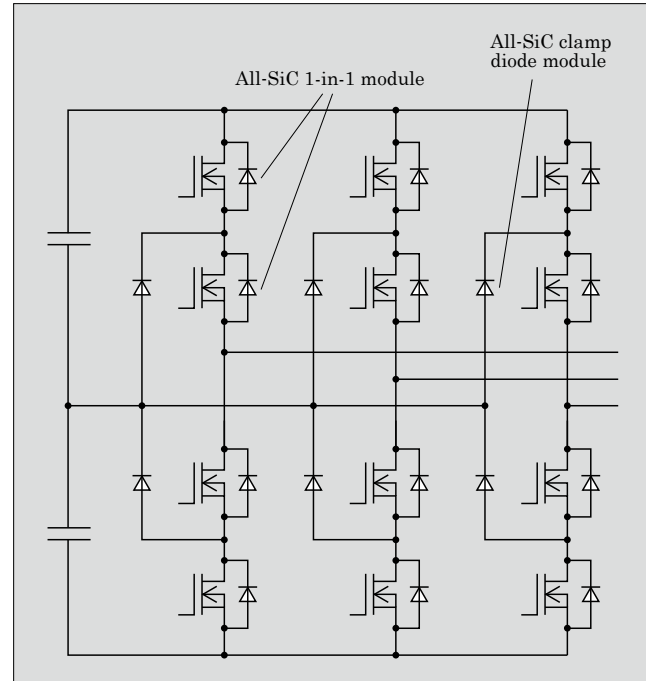


Fig.10 SVC 3-level inverter circuit

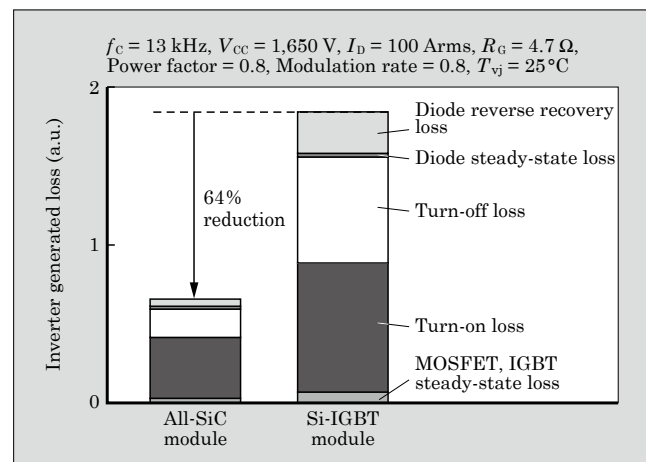


Fig.11 Inverter generated loss simulation

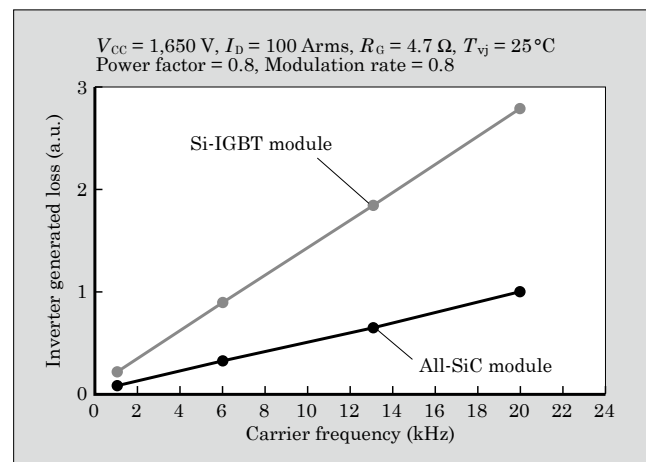


Fig.12 Carrier frequency dependence of inverter generated loss

tions of 3-level inverter operation for SVC, the difference in generated loss between the All-SiC module and the Si-IGBT module grew in proportion with carrier frequency. Based also on this result, it can be said that the All-SiC module is superior when operated at high frequency.

5. Postscript

This paper introduced the 3.3-kV All-SiC modules for electric distribution equipment. This module has high reliability, which follows the design principles of the structure of the 1.2-kV All-SiC module for power conditioning systems. It is characterized by its low loss and high-frequency operation, and those characteristics contribute to the development of smaller and lighter SVC, the electric distribution equipment that can be mounted on a single pole.

We plan to accelerate the development of All-SiC 2-in-1 modules and large-capacity All-SiC modules for rolling stock and achieve even greater size reduction and weight savings in electric distribution equipment so that we can further contribute to the development of

power electronics technology and help realize of a low-carbon society.

The content of this paper is based on the results obtained from the “Demonstration Project for Constructing a Distributed Energy Next-Generation Electric Power Network” implemented by the New Energy and Industrial Technology Development Organization (NEDO). We would like to conclude by expressing our appreciation to all those involved in this project.

References

- (1) Kojima, T. et al. Distribution Static Var Compensators and Static Synchronous Compensators for Suppressing Voltage Fluctuation. FUJI ELECTRIC REVIEW. 2017, vol.63, no.1, p.36-40.
- (2) Nashida, N. et al. All-SiC Module for Mega-Solar Power Conditioner. FUJI ELECTRIC REVIEW. 2014, vol.60, no.4, p.214-218.
- (3) Nakamura, H. et al. All-SiC Module Packaging Technology. FUJI ELECTRIC REVIEW. 2015, vol.61, no.4, p.224-227.



“PrimePACK™” of 7th-Generation “X Series” 1,700-V IGBT Modules

YAMAMOTO, Takuya* YOSHIWATARI, Shinichi* OKAMOTO, Yujin*

ABSTRACT

The demand for large-capacity IGBT modules has been expanding for power conversion systems used in various sectors such as industrial, consumer, automotive and renewable energy. Fuji Electric has developed the “PrimePACK™” as the 7th-generation “X Series” IGBT modules. The module reduces power dissipation through characteristic enhancement of semiconductor chip and significantly reduces thermal resistance by using a newly developed high thermal conductive insulating substrate. Furthermore, by improving the capacity of ΔT_{vj} power cycle and the heat resistance of insulating silicone gel, the module has increased the guaranteed continuous operating temperature from 150 °C to 175 °C. With these technical development, Fuji Electric has achieved a product with a maximum rated current of 1,800 A using newly developed technologies.

1. Introduction

These days, reduction of CO₂ emission is as world-wide trend to prevent global warming. Because of the background and expectation for power electronics technology, power conversion systems with power semiconductors are expanding in various application fields such as consumer and industrial, automotive applications. Especially, the demand for insulated gate bipolar transistors (IGBTs) has been expanding as a key device of power conversion systems for renewable energy, such as photovoltaic power generation or wind power generation, which have been introduced rapidly.

By many technological innovations, Fuji Electric has achieved downsizing, improvement of power dissipation and higher reliability of IGBT modules which contribute to higher efficiency or downsizing of power conversion systems in the past. In order to satisfy further market demands as more downsizing and higher efficiency, Fuji Electric has developed the 7th-generation “X series PrimePACK™*1”.

2. Features of X Series PrimePACK™

Figure 1 shows the outline appearance of the X Series PrimePACK™. The X Series PrimePACK™ has 2 kind of packages named “M271” and “M272,” as same shape as those of conventional “V Series” IGBT modules. Table 1 shows the X Series PrimePACK™ family. Maximum current rating of the X Series PrimePACK™ is 1,800 A for both 1,200 V and 1,700 V ratings. The maximum current rating is about 29% expansion compared with 1,400 A of conventional product. Furthermore, continuous operation junction temperature of $T_{vjop} = 175^{\circ}\text{C}$ has been achieved by advanced charac-

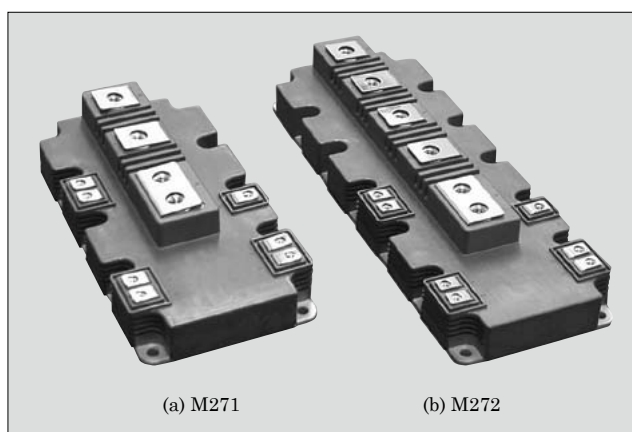


Fig.1 X Series PrimePACK™

teristics of semiconductor chips and package technologies with long-term reliability performance.

3. Electrical Characteristics

In order to improve energy conversion efficiency, it is important to reduce power dissipation of IGBT module. The power dissipation is caused and affected by electrical characteristics of installed semiconductor chips, such as IGBT and free wheeling diode (FWD). The X Series PrimePACK™ enables significant reduction of power dissipation compared with conventional product by adopting the X series chips with latest fine cell technology and thin wafer technology.⁽¹⁾ Moreover, high temperature operating $T_{vjop} = 175^{\circ}\text{C}$, 25 °C higher than conventional has been realized by improving reliability and withstand capability during higher tempera-

*1: PrimePACK™ is a trademark or registered trade mark of Infineon Technologies AG.

* Electronic Devices Business Group, Fuji Electric Co., Ltd.

Table 1 X Series PrimePACK™ family

Package	Rating		Type	Insulating substrate	Insulation withstand voltage	CTI*	T_{vjop}
	Voltage	Current					
M271	1,200 V	900 A	2MBI900XXA120P-50	Al ₂ O ₃	4.0 kV AC	>600	175 °C
		1,200 A	2MBI1200XXE120P-50	AlN			
	1,700 V	900 A	2MBI900XXA170-50	Al ₂ O ₃			
		1,200 A	2MBI1200XXE170-50	AlN			
M272	1,200 V	1,400 A	2MBI1400XXB120P-50	Al ₂ O ₃			
		1,800 A	2MBI1800XXF120P-50	AlN			
	1,700 V	1,000 A	2MBI1000XXB170-50	Al ₂ O ₃			
		1,400 A	2MBI1400XXB170-50	Al ₂ O ₃			
		1,800 A	2MBI1800XXF170-50	AlN			

* Comparative tracking index

ture operation.

3.1 IGBT characteristics

Trade-off relationship between saturation voltage and turn-off energy has been dramatically improved by the X series IGBT with newly developed fine cell technology and thinner wafer technologies. Figure 2 shows comparison of the trade-off characteristic for the X Series PrimePACK™ and a conventional product. The characteristics of the X Series are improved about 0.7 V of saturation voltage and about 11% of turn-off energy compared with conventional product. Moreover, optimized field stop layer has realized suppression of voltage oscillation during turn off and enough breakdown withstand voltage, even adapting thinner wafer.

3.2 FWD characteristics

Forward voltage of the X series FWD has been improved by thinner drift layer as well as X Series IGBT chip. Furthermore, both of soft recovery waveforms and improvement of reverse recovery energy have been realized by lifetime control optimization. Figure 3 shows trade-off relationship between forward voltage and reverse recovery energy. The characteristics of the

X Series are improved about 0.15 V of forward voltage and about 16% of reverse recovery energy. In generally, thinner drift layer causes voltage oscillation and higher voltage spike during reverse recovery. However, the X Series has equal or better performances than the conventional product by optimization of back side voltage termination structure in FWD.

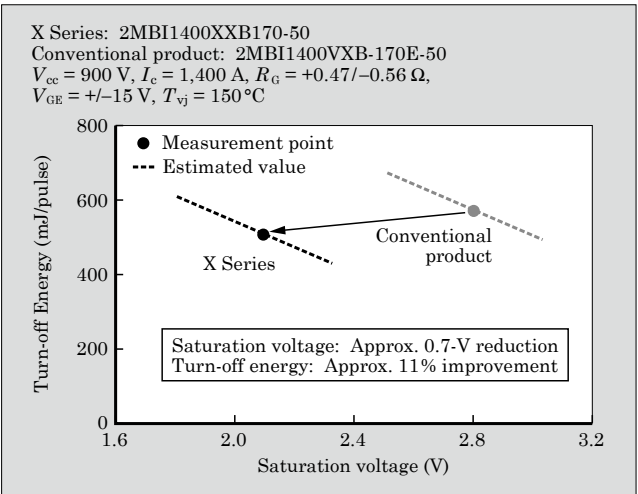


Fig.2 $V_{CE(sat)} - E_{off}$ trade-off relationship (IGBT)

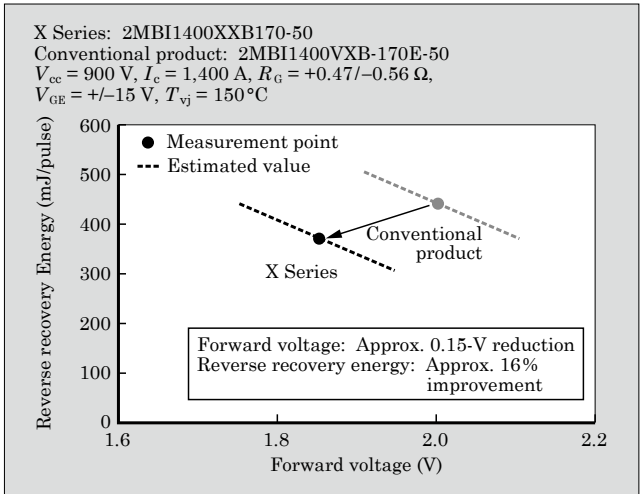


Fig.3 $V_F - E_{rr}$ trade-off relationship (FWD)

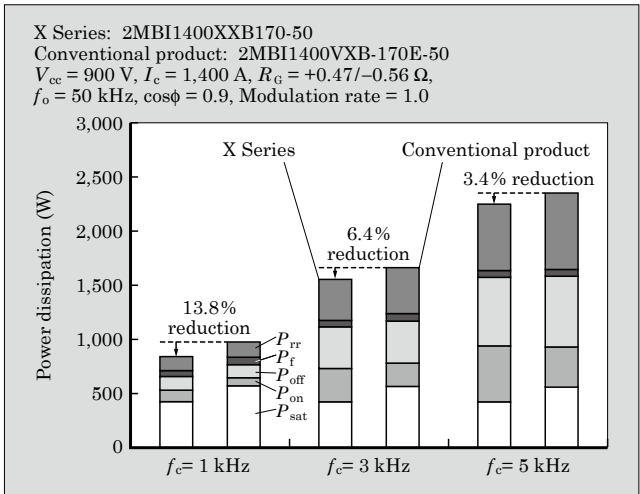


Fig.4 Power dissipation

3.3 Power dissipation

Figure 4 shows calculated results of power dissipation. According to the results, the X Series PrimePACK™ can reduce its power dissipation about 13.8% at a carrier frequency 1 kHz compared with conventional product, and enables to contribute higher efficiency of power conversion systems.

4. Packaging Technology

Table 2 shows a comparison of the X Series and conventional PrimePACK™. The X Series PrimePACK™ is designed to increase output current of power conversion systems with same package size as conventional product. In order to achieve the higher output current, it is necessary to consider countermeasures for higher temperature raising of semiconductor chips and degradation of long-term reliability performance. Reduction of semiconductor chips temperature rising is realized by newly developed packaging technologies. Additionally, continuous operation temperature upgrading also has been achieved from 150°C to 175°C as shown in Table 2. Long-term reliability has been also improved to realize high temperature operation in application field.^{(2),(3)}

4.1 Newly developed high thermal conductive insulating substrate

Improvement of junction-to-case thermal resistance is important to realize effective cooling for heat from semiconductor chips and main terminals. Highest current rating of the X Series PrimePACK™ has newly developed high thermal conductive insulating aluminum nitride (AlN) substrate for higher cooling performance. As a results, thermal resistance of junction-to-case has been improved by about 45% compared with conventional alumina (Al₂O₃) substrate in case of same chip size. Figure 5 shows experimental results for temperature raise in package. The results show that about 11°C temperature reduction of IGBT part has been achieved by the new AlN substrate compared with conventional. Main terminals temperature has also been improved by about 7°C.

Table 2 Comparison of X Series and conventional PrimePACK™

	X Series PrimePACK™	Conventional product
Rated voltage	1,200 V, 1,700 V	1,200 V, 1,700 V
Max. rated current	1,800 A	1,400 A
Insulating substrate	AlN	Al ₂ O ₃
Continuous operation junction temperature T_{vjop}	175°C	150°C
Silicone gel heat resistance	175°C	150°C

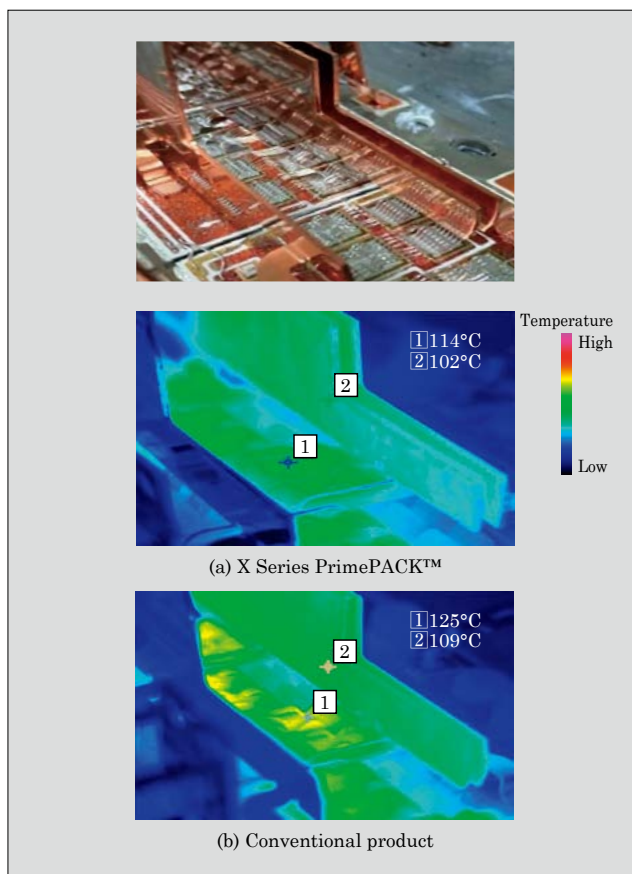


Fig.5 Experimental results of temperature rise

4.2 Expansion of continuous operation junction temperature T_{vjop}

In order to realize more higher output current, operation junction temperature T_{vjop} has been expanded from 150°C to 175°C compared with conventional product. For the expansion, capability improvement against repetitive thermal stress (ΔT_{vj} power cycle capability) is necessary.

Figure 6 shows the ΔT_{vj} power cycle capability. The ΔT_{vj} power cycle capability is degraded by high

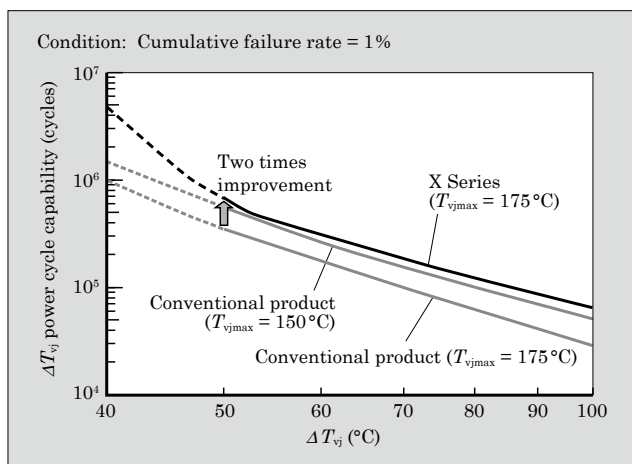


Fig.6 ΔT_{vj} power cycle capability

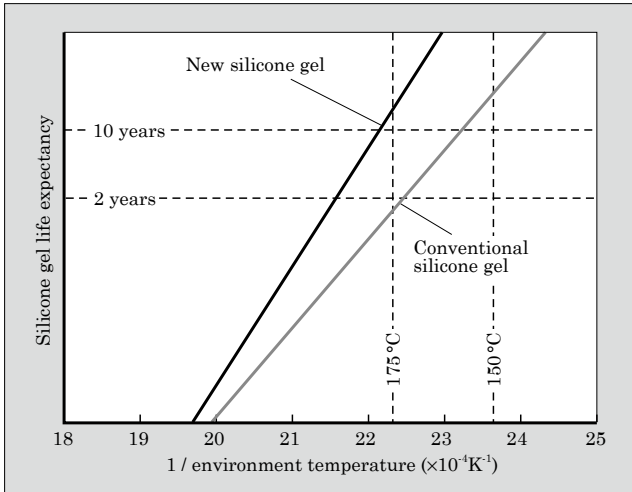


Fig.7 Relationship between temperature and estimated silicone gel life time

temperature operation. For example, the capability of conventional product at $T_{vjmax} = 175^{\circ}\text{C}$ is lower than at 150°C . However, the capability of the X Series PrimePACK™ has been improved about 2 times higher than conventional product under conditions of $T_{vjmax} = 175^{\circ}\text{C}$ and $\Delta T_{vj} = 50^{\circ}\text{C}$. The superior capability has been realized by newly developed solder material and new wire bonding technology for semiconductor chips.

According to the results, the X Series PrimePACK™ has realized higher ΔT_{vj} power cycle capability at $T_{vjmax} = 175^{\circ}\text{C}$ than that of conventional product even at $T_{vjmax} = 150^{\circ}\text{C}$.

4.3 Newly developed silicone gel for high temperature operation

IGBT module has silicone gel in its inside to have enough insulation performance. However conventional silicone gel is degraded by high temperature operation such as 175°C .

Figure 7 shows the relationship between temperature and silicone gel life time. According to the data, conventional silicone gel has over 10 years life time at 150°C . However it's only about 2 years at 175°C . The X series products utilize newly developed silicone gel to have enough life time against high temperature operation such as 175°C . The new silicone gel has over 10 years life time at 175°C , it is almost same life time as convention one at 150°C .

5. Summary

Operation temperature upgrading to $T_{vjop} = 175^{\circ}\text{C}$ by the X Series PrimePACK™ family has been realized by several advanced new technologies such as power dissipation reduction by semiconductor chips improvement, extra cooling by new AlN substrate, ΔT_{vj} power cycle

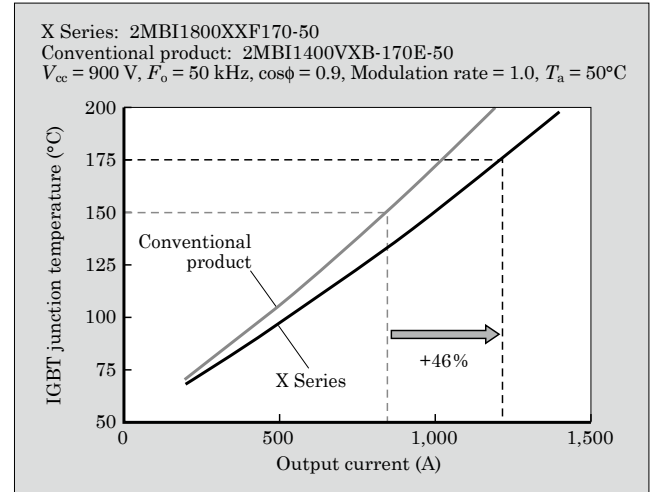


Fig.8 Output current and IGBT junction temperature

capability reinforce and high temperature operating capability by new silicone gel. As a result of these Fuji Electric efforts, higher energy conversion efficiency and more output power of power conversion systems can be realized.

Figure 8 shows relationship between output current of the system and IGBT junction temperature as an example of improvements. As the result, 1.46 times output current can be achieved with the X Series PrimePACK™ compared with the conventional product.

6. Postscript

The 7th-generation "X Series" IGBT module "PrimePACK™" has achieved top class performance in the power semiconductor market by dramatic improvement of semiconductor chip characteristic and new packaging technology. Further downsizing and higher efficiency of power conversion systems will be achieved by the X series families. It will contribute to safe, secure and sustainable society. Fuji Electric will continuously offer superior products with advanced technologies and will contribute to achieving many benefits such as downsizing, higher efficiency and reliable performance of power conversion systems.

References

- (1) Onozawa, Y. et al. "Development of the 1200 V FZ-Diode with soft Recovery Characteristics by the New Local Lifetime Control Technique". Proceeding of ISPSD 2008, p.80-83.
- (2) Momose, F. et al. "The New High Power Density Package Technology for the 7th Generation IGBT Module", PCIM Europe 2015.
- (3) Yoshida, K. et al. 7th-Generation "X Series" IGBT Module "Dual XT". FUJI ELECTRIC REVIEW. 2016, vol.62, no.4, p.236-240.

“HPnC” High-Current SiC Hybrid Module

SEKINO, Yusuke* MITSUMOTO, Takahiro* MORIYA, Tomohiro*

ABSTRACT

Fuji Electric has been developing the “HPnC” high-current power module to be used with electric railcars and photovoltaic and wind power generation facilities. The chip uses 7th-generation “X Series” technology, enabling it to achieve lower power loss. The package employs an aluminum nitride (AlN) insulating substrate that utilizes a high heat-dissipating member, as well as base materials consisting of magnesium and silicon carbide composite materials (MgSiC). Adopting a laminated structure for the enclosure of the terminal makes the internal inductance decrease to 10 nH. Furthermore, Ultrasonic terminal welding is used to comply with the RoHS directive. With these technologies, the module achieves a high current density, which is 12% greater than the conventional HPM.

1. Introduction

In recent years, there has been increasing demand to improve energy efficiency and reduce CO₂ emissions as measures for preventing global warming. As a result, the use of power conversion equipment that employs power semiconductors has been spreading to a wide variety of fields. In particular, there has been advancements in equipment capacity and miniaturization in the fields of electric railcars, photovoltaic power

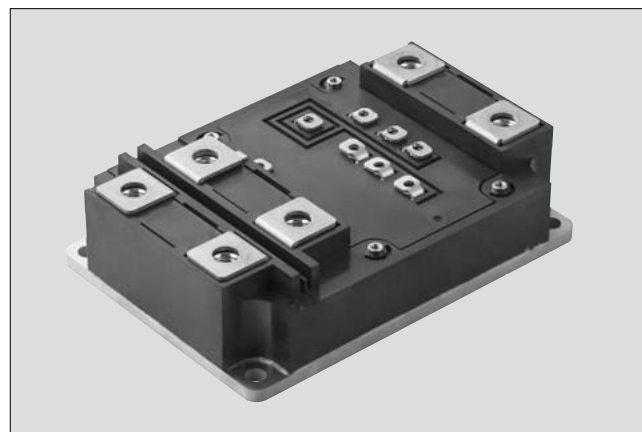


Fig.1 “HPnC” high-current SiC hybrid module

generation and wind power generation. In this respect, the high-current insulated gate bipolar transistor (IGBT) modules used for these types of equipment have been required to be compact by increasing current density.

In order to meet this demand, Fuji Electric has been developing the “HPnC” (High Power next Core) high-current power module. It uses a new package equipped with 7th-generation “X Series” IGBT chips⁽¹⁾ and SiC Schottky barrier diode (SiC-SBD) chips⁽²⁾ (see Fig. 1).

2. Product Line-Up Considerations

Table 1 shows the HPnC product line-up and features. Fuji Electric has been considering two series for the HPnC line-up, namely, a 3,300-V/450-A series and 1,700-V/1,000-A series. The HPnC line-up uses the X Series IGBT. As for FWD, it uses Si based X Series PiN diodes and SiC-SBDs that have enhanced characteristics. In this paper, Fuji Electric will introduce the 3,300-V/450-A HPnC that comes equipped with a 3.3-kV X Series IGBT and SiC-SBD.

Circuit configuration is 2 in 1 with a thermistor for detecting temperature rise inside the module. For the insulating substrate, an aluminum nitride (AlN)

Table 1 Product line-up

Product type	Rated voltage (V)	Rated current (A)	IGBT	FWD	Package type	Circuit configuration	Thermistor	Insulating substrate	Base
2MBI450XUF330-50	3,300	450	X Series	SiC-SBD	M288	2 in 1	Built-in	AlN	MgSiC
2MSI450XUF330-50				X Series					
2MBI1000XUF170-50	1,700	1,000		SiC-SBD					
2MSI1000XUF170-50				X Series					

* Electronic Devices Business Group, Fuji Electric Co., Ltd.

ceramic is used to ensure high heat dissipation and high reliability. As for the base plate, a magnesium and silicon carbide (MgSiC) material is used, which is the same coefficient of thermal expansion as the aluminum and silicon carbide composite material (AlSiC) of conventional products. It secures the high reliability needed for electric railcars. Moreover, MgSiC base plate is higher thermal conductivity than AlSiC base plate. Figure 1 shows the external appearance of the module. The package has mounting compatibility with the modules of other manufacturers.

3. “HPnC” Features

Table 2 shows a comparison of characteristics with the conventional for electric railcar module “HPM” (High Power Module). Compared with the HPM, this new module reduces surge voltage by improving parasitic inductance (internal inductance for the module), increases current density, improves assembly during parallel connections and complies with the RoHS Directive^{*1}.

3.1 Low inductance package

The internal inductance for the HPnC module achieves 10 nH, a 76% improvement compared with the HPM’s value of 42 nH. Figure 2 shows the cross-sectional structure of HPnC. A laminate structure is used between the collector terminal and the emitter terminal to reduce internal inductance. Figure 3 shows a comparison of waveforms during turn off for the HPnC and HPM. When both modules are evaluated at same di/dt 5-kA/ μ s, surge voltage for the HPnC during turn off is about 150 V lower than that of the HPM as a result of reducing inductance. This means that the

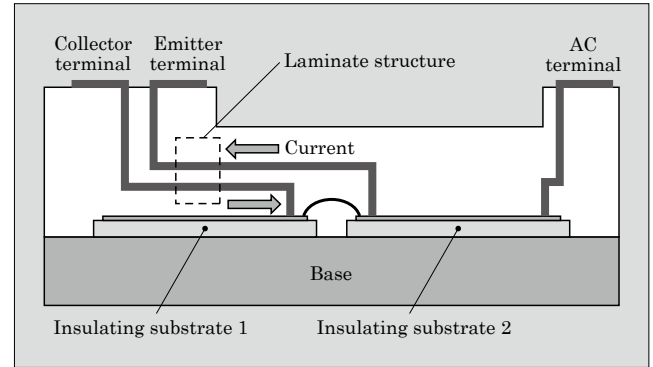


Fig.2 HPnC cross-sectional structure

HPnC can be faster di/dt than the HPM during turn off, in order to reduce switching loss.



3.2 Higher current density

The HPnC achieves a footprint-based current density of 6.43 A/cm², which is about 12% higher than that of the 3.3-kV breakdown voltage HPM, which is 5.76 A/cm². This is the result of reducing thermal resistance $R_{th(j-c)}$ using a low-loss 7th-generation IGBT chip and utilizing an MgSiC base, which has 1.5 times the heat conductivity of the HPM’s AlSiC base.

3.3 Easy parallel connection assembly and superior inductance

High-current IGBT modules are often paralleled to use for high current circuits. Table 3 shows a comparison of inductance and assembly during parallel connection for the HPM and HPnC. Total rated current for the HPM was 2,000 A, with a pair of two 1,000-A 1-in-1 configuration modules connected in series, that are made to be in a 2-in-1 configuration, connected in par-

Table 2 Package characteristics

Package	HPnC	HPM (conventional product)	Improvement rate (%)
External appearance/dimensions (mm)	W : 100 D : 140 H : 38 	W : 130 D : 140 H : 38 	–
Circuit	2 in 1	1 in 1	–
Rating (typical)	3,300 V/450 A + 450 A	3,300 V/1,000 A	–
Module internal inductance (L_P)	10 nH	42 nH (for 2-in-1 configuration)	76.2
Surge voltage (V)	401	548	26.8
Footprint (cm ²)	140	173.7	19.4
Current density (A/cm ²)	6.43	5.76	11.6
Parallel connectivity	Excellent	Poor	–
Inductance during 2 in parallel connection (L_P)	2.5 nH	21 nH	89.0
RoHS Directive	Compliant	Not compliant	–

*1: RoHS Directive: Directive issued by the European Union (EU) concerning restrictions of the use of certain hazardous substances in electrical and electronic equipment.

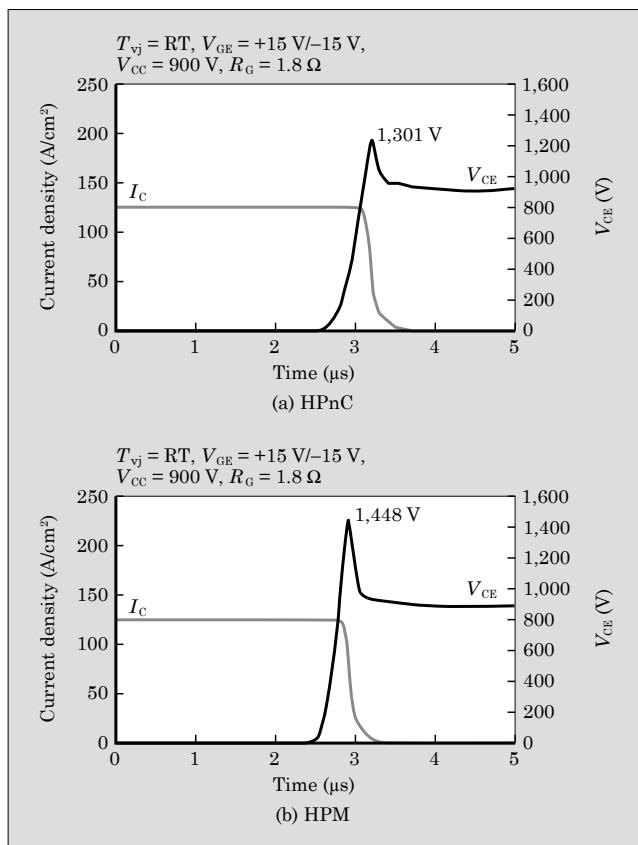


Fig.3 Turn-off comparison

allel. In contrast to this, rated current for the HPnC is 1,800 A, with four 450-A 2-in-1 configuration modules connected in parallel.

Assembly of parallel connections for the HPM is not easy when assembling bus bars to the main circuit

since it involves 3 overlapping layers depending on the terminal position, which include the collector bus bar, AC bus bar and emitter bus bar. Assembly has improved with use of the HPnC since it avoids this 3 layer overlap by positioning the AC terminal by itself on the opposite side of the collector terminal and emitter terminal.

Furthermore, the position of the emitter terminal is far from the capacitor in the HPM, and thus the emitter bus bar needs to be lengthened, which causes an increase in main circuit inductance. As for HPnC, the positions of the collector terminal and emitter terminal are close to the capacitor, which shortens the length of the bus bar and reduces the inductance of the main circuit. Module internal inductance for the 2 HPM modules connected in parallel was 21 nH, while 4 HPnC modules connected in parallel was 2.5 nH, equating to about a 90% reduction. Inductance is determined by the internal inductance of the module and the main circuit. Therefore, by reducing both of these values, it is possible to achieve even faster switching.

3.4 RoHS compliance

In order to comply with the RoHS Directive, the HPnC uses ultrasonic bonding instead of solder bonding to join the terminals and insulating substrate. Fuji Electric achieves higher reliability than the conventional product by matching the coefficients of linear thermal expansion of the materials to be joined.

4. Improvement of Chip Characteristics

Improving generated dissipation for the IGBT module, which is important in miniaturizing the mod-

Table 3 Comparison of parallel connections for HPM and HPnC

	Four 2-in-1 HPnC modules connected in parallel (total of 3,300 V/1,800 A)	Two 1-in-1 HPM modules connected in parallel (total of 3,300 V/2,000 A)
Comparison of assembly during module parallel connections		
Comparison of module inductance during parallel connections	<p>Total inductance: $10/4 = 2.5 \text{ nH}$</p>	<p>Total inductance: $(21 + 21)/2 = 21 \text{ nH}$</p>

*: In order to make the structure easier to understand, it was represented using a spacer.

ule (increasing current density), is greatly dependent on IGBT chip and FWD chip characteristics.

4.1 Improvement of IGBT chip characteristics

Figure 4 shows the improvement in characteristics compared with conventional IGBT chips at $T_{vj} = 150^\circ\text{C}$. Turn-off loss E_{off} has remained the same as before, but collector-emitter voltage $V_{\text{CE(sat)}}$ for the X Series IGBT chip is 2.5 V, which is an improvement of 1.2 V compared with the 3.7 V of conventional IGBT chips. The X Series IGBT has been able to improve the trade off between $V_{\text{CE(sat)}}$ and E_{off} by expanding the active area through edge structure optimization and thinner the drift layer.

4.2 Reduction of switching loss through use of SiC-SBD

Figures 5 and 6 show comparisons of waveforms for the conventional 3.3-kV Si-IGBT module (HPM) and 3.3-kV X Series SiC hybrid modules (HPnCs). In this comparison, 2 HPnCs are connected in parallel to match the rated current to the HPM. The SiC hybrid significantly reduces turn-on loss E_{on} , and recovery loss E_{rr} does not occur through reduction of peak current I_{rr} during reverse recovery. This is due to the fact that the

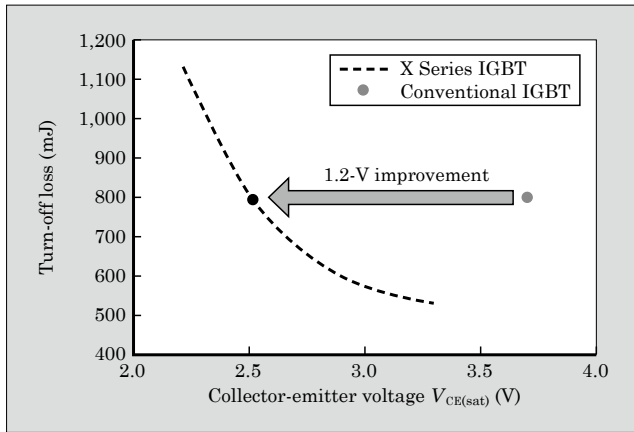


Fig.4 Improvement of 3.3-kV "X Series" IGBT chip characteristics

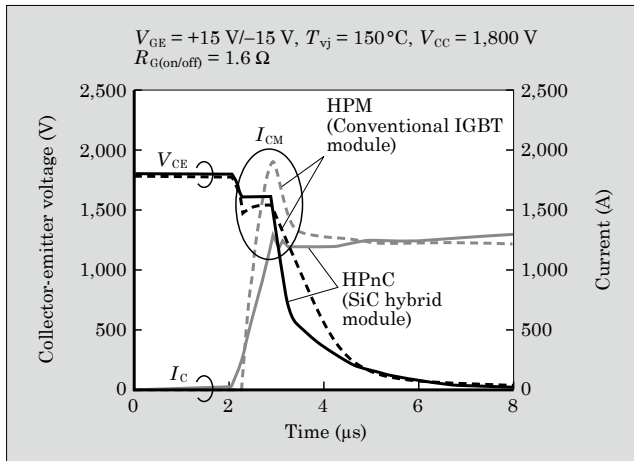


Fig.5 Comparison of turn-on waveforms

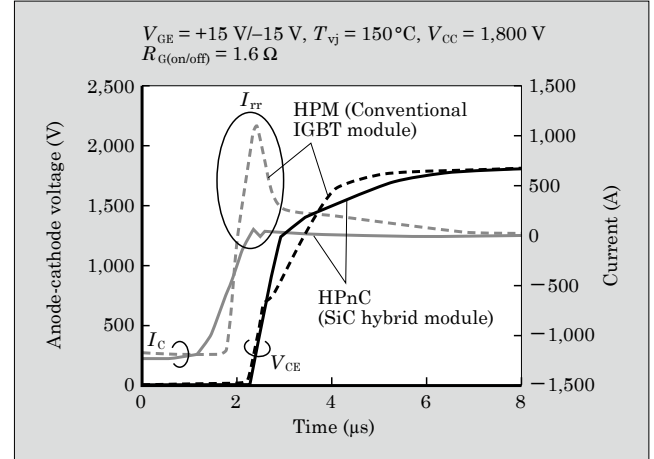


Fig.6 Comparison of recovery waveforms

Table 4 Comparison of switching loss (unit: mJ)

	Turn-on loss E_{on}	Turn-off loss E_{off}	Recovery loss E_{rr}	Total loss E_{total}
HPM (conventional product)	3,493	2,417	903	6,813
HPnC (SiC hybrid)	2,374	2,294	2	4,670
Improvement rate (%)	32	5	99.8	31

SiC-SBD is a unipolar device, and this means that there is no I_{rr} because no carrier occurs. As shown in Table 4, E_{on} is greatly improved by 32% and E_{rr} by 99.8%.

4.3 Inverter generated loss

A comparison of the results of inverter generated dissipation simulations for a 3,300-V/1,000-A HPM and two 3,300-V/450-A HPnC modules connected in parallel is shown in Fig. 7.

Total loss is improved by about 40% compared with the HPM at a carrier frequency f_c of 5 kHz and an output current of 450 A. Furthermore, at the same output current, the f_c value for the HPnC can be achieved to 9 kHz, which was 1.8 times higher than the 5 kHz value for the HPM. Moreover, when f_c for both

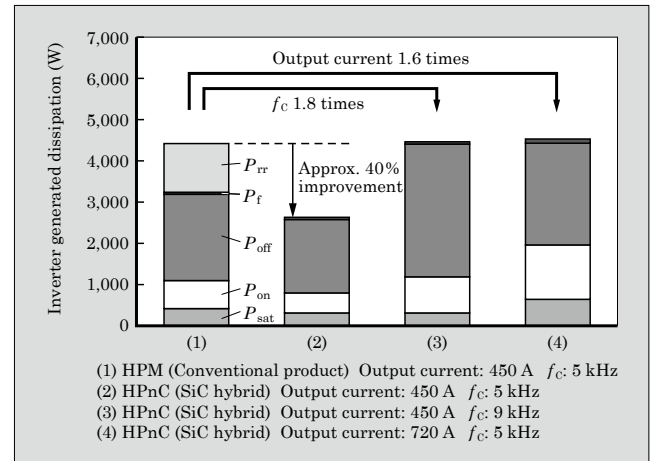


Fig.7 Results of inverter generated dissipation simulation

modules was 5 kHz, output current could be increased 1.6 times from 450 A to 720 A. The expansion in current density and output current increasing contributes to the miniaturization of the filter through expansion of f_c contributes to miniaturization and lower loss in inverters.

5. Postscript

In this paper, Fuji Electric introduced the “HPnC” high-current SiC hybrid module. The 3.3-kV breakdown voltage SiC hybrid module HPnC is capable of suppressing surge voltage, improving high-speed switching and supporting high current applications through parallel connections as a result of employing a laminate structure and reducing inductance through optimization of the main terminal position in the module’s package structure. Moreover, the utilization of ultrasonic terminal welding technology secured a reliability just as high as conventional products while also fulfilling compliance with the RoHS Directive.

In addition, the improvement in characteristics through use of the X Series IGBT and SiC-SBD for the chip enabled the module to reduce inverter generated dissipation, increase current density, expand f_c and achieve miniaturization. In the future, Fuji Electric will work to further improve our packages and our chip technology in order to contribute to the development of power electronics technology.

Some of our research was carried out as part of a project of the joint research body Tsukuba Power Electronics Constellations (TPEC). We would like to conclude by expressing our appreciation to all those involved in the project.

References

- (1) Kawabata, J. et al. 7th-Generation “X Series” IGBT Module. FUJI ELECTRIC REVIEW. 2015, vol.61, no.4, p.237-241.
- (2) Onezawa, T. et al. 1,700-V Withstand Voltage SiC Hybrid Module. FUJI ELECTRIC REVIEW. 2015, vol.61, no.4, p.228-231.



7th-Generation “X Series” RC-IGBT Module Line-Up for Industrial Applications

YAMANO, Akio* TAKASAKI, Aiko* ICHIKAWA, Hiroaki*

ABSTRACT

In order to meet the market demand of the smaller size, lower power dissipation and higher reliability for IGBT modules, Fuji Electric has developed a reverse conduction insulated gate bipolar transistor (RC-IGBT) that integrates an IGBT and a FWD on a single chip. We have also developed the “Dual XT” to expand the line-up of the 7th-generation “X Series” RC-IGBT module for industrial applications that has a rated voltage of 1,200 V. While the “Dual XT” 6th-generation “V Series” IGBT module for industrial applications had a maximum rated current of 600 A, the new module has an expanded rated current of 1,000 A. Compared with the conventional product, which uses the same package, the new product greatly improves the junction temperature and junction temperature rise of the chip during actual operation. This module will contribute to further increase of the output and extension of service life of the power converters.

1. Introduction

In recent years, there has been increasing expectations for power electronics technologies that can efficiently utilize energy and contribute to energy conservation in order to prevent global warming and realize a safe, secure and sustainable society. In particular, the demand for power semiconductors has been expanding as a key device of power conversion systems in various fields such as industry, consumer, automobile and renewable energy.

Since Fuji Electric commercialized an insulated gate bipolar transistor (IGBT) module in 1988, we have contributed to miniaturization, cost reduction and performance improvement of power conversion systems through many IGBT module technology innovations especially to miniaturize the size, reduce the loss and improve the reliability. However, further miniaturization of IGBT modules increases the power density, and it would lead to create the risk of lower reliability due to increasing the operating temperatures of IGBTs and free wheeling diodes (FWDs). For this reason, technological innovations for chips and packages are essential in order to maintain high reliability and increase the power density of the IGBT modules.

To achieve this, we have innovated chip and packaging technology and has developed 7th-generation “X Series” IGBT module, which has facilitated increased power density through its low loss and high reliability characteristics.^{(1),(2)} In addition, we have also developed a reverse-conducting IGBT (RC-IGBT) that integrates an IGBT and FWD into a single chip.^{(3),(4)} We have reduced the number of chips and total chip area while reducing generation loss. We have also achieved further increase in power density through our 1,200-V

7th-generation “X Series” RC-IGBT (X Series RC-IGBT) module for industrial applications by combining this chip and packaging technology. Currently, we are proceeding with the series of X Series RC-IGBT modules, and this time, we have developed the “Dual XT” with RC-IGBT.

2. Characteristics of 7th-Generation “X Series” RC-IGBT Module for Industrial Applications

Figure 1 shows the schematic diagram and equivalent circuit of the X Series RC-IGBT. Inverters that are widely used as power conversion systems require antiparallel connection of an IGBT and a FWD chip. In contrast to this, the RC-IGBT integrates an IGBT and FWD into a single chip.

Compared with the 6th-generation “V Series” IGBT, the X Series RC-IGBTs have also applied finer pattern design rules of X Series chip technology and achieved significant reduction in collector-emitter saturation voltage $V_{CE(sat)}$. Moreover, the latest thin wafer

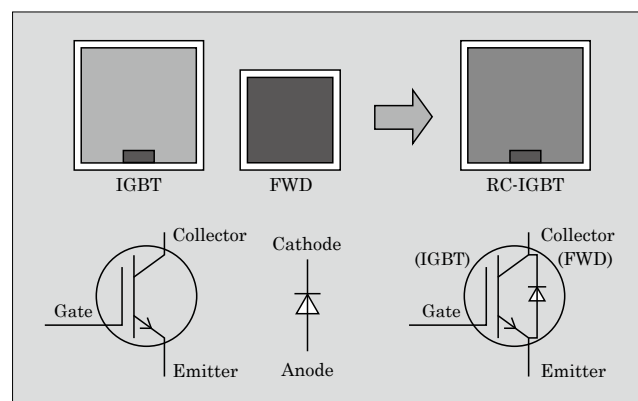


Fig.1 Schematic diagram and equivalent circuit for 7th-generation “X Series” RC-IGBT for industrial applications

* Electronic Devices Business Group, Fuji Electric Co., Ltd.

processing technology has also been applied to improve the trade-off relationship between the saturation voltage and turn-off switching loss. In general, there is the risk of voltage oscillation and breakdown voltage reduction during turn off when utilizing thin wafers. However, the X Series RC-IGBT suppresses them through optimization of each structure for the chip.

Thermal resistance has also been greatly reduced through applying a heat high-dissipating insulating substrate, which is one of the packaging technologies of the X Series. In addition, the module guarantees operating virtual junction temperature under switching conditions T_{vjop} at 175°C and secures high reliability through optimization of wire bonding, utilization of high-strength solder and highly heat-resistant silicone gel.

By employing these technologies, X Series RC-IGBT module achieves a higher rated current in the same package size as previous products that are composed of both conventional IGBT chip and FWD chip.⁽⁵⁾

3. Product Line-Up

Figure 2 shows the external appearance of the newly developed X Series RC-IGBT Dual XT module, Table 1 shows the line-up and Table 2 shows the char-

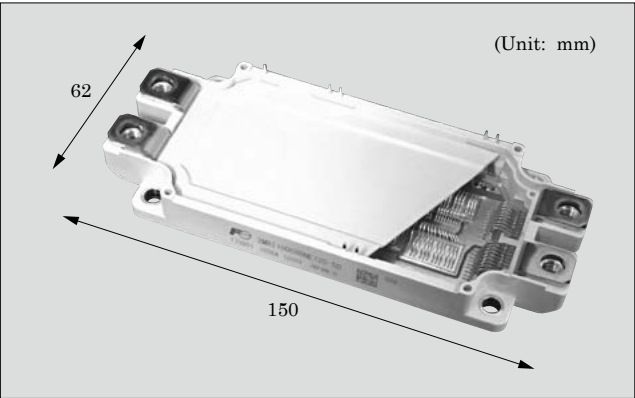


Fig.2 7th-generation “X Series” RC-IGBT “Dual XT” module for industrial applications

Table 1 “Dual XT” line-up

Rated voltage 1,200 V	Rated current (A)						
	225	300	450	600	800	900	1,000
Dual XT	V Series IGBT + V Series FWD						
	X Series IGBT + X Series FWD						X Series RC-IGBT

Table 2 “Dual XT” characteristics

Rated voltage	1,200 V		
Representative type	2MBI600 VN-120-50	2MBI800XNE120-50	2MBI1000XRNE120-50
Series name	6th-generation V Series IGBT module	7th-generation X Series IGBT module	7th-generation X Series RC-IGBT module
Chip	V Series IGBT + V Series FWD	X Series IGBT + X Series FWD	X Series RC-IGBT
Thermal resistance: $R_{th(j-c)}$ (a.u.)	1/1.5 (IGBT/FWD)	0.85/1.1 (IGBT/FWD)	0.55/0.55 (IGBT/FWD)

acteristics. The 7th-generation X Series RC-IGBT Dual XT module has expanded maximum rated current to 1,000 A, whereas the 6th-generation “V Series” IGBT Dual XT module for industrial applications has a maximum rated current of 600 A.

4. Characteristics of 7th-Generation “X Series” RC-IGBT “Dual XT” Module for Industrial Applications

Figure 3 shows the output characteristics of the X Series RC-IGBT Dual XT module with a rated current of 1,000 A compared with the V Series IGBT Dual XT module with a rated current of 600 A in the same package size. The X Series RC-IGBT allows an electric current to flow in both the forward (IGBT) and reverse (FWD) directions by a single chip. In the RC-IGBT, conductivity modulation of IGBT can become difficult to occur when a gate voltage is applied and the IGBT flows the current. In particular, the snapback phenomenon can occur in a low saturation voltage case.^{(6),(7)} In contrast to this, the X Series RC-IGBT has solved the snapback phenomenon through optimization of each structure for the chip.

Figure 4 shows the turn off waveform of the X Series RC-IGBT Dual XT module. Compared with the V Series IGBT Dual XT module, surge voltage has been decreased by about 100 V during turn off under the same switching conditions. Furthermore, there was no observation of abnormal waveforms such as voltage oscillation or reach-through waveforms.

Figure 5 shows the IGBT trade-off relationship of

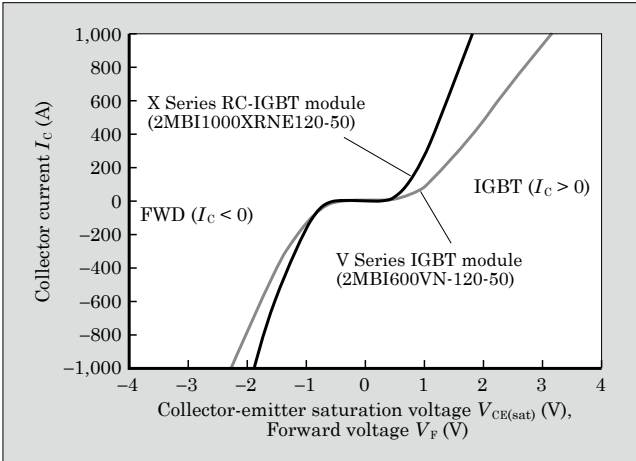


Fig.3 Output characteristics

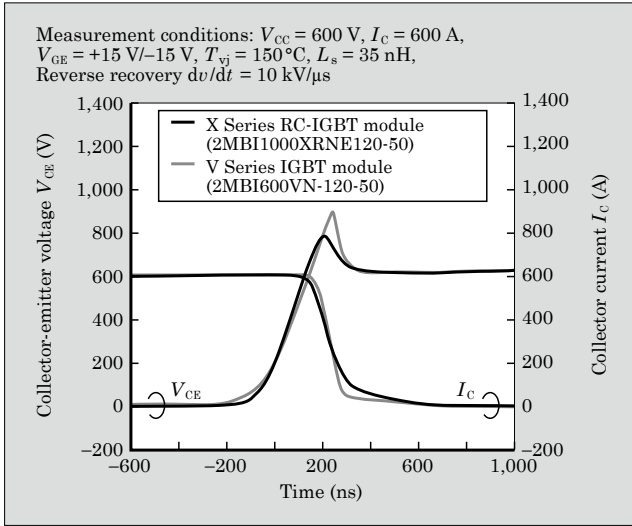


Fig. 4 Turn-off waveforms

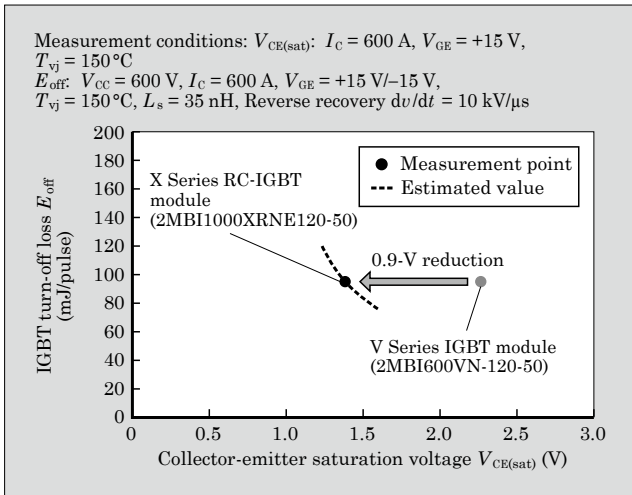


Fig. 5 IGBT trade-off relationship

the X Series RC-IGBT Dual XT module. The dotted line in the figure represents the adjustment of trade-off through structural parameter control. In case of the same switching loss, the X Series RC-IGBT Dual XT module reduces saturation voltage by 0.9 V compared with the V Series IGBT Dual XT module.

Figure 6 shows the inverter power dissipation, virtual junction temperature T_{vj} and delta virtual junction-to-case temperature ΔT_{vj-c} of the X Series RC-IGBT Dual XT module. By combining X Series chip technology with RC-IGBT technology, the module has been able to expand maximum rated current and reduce power loss by 11% compared with the V Series IGBT Dual XT module under the same inverter power dissipation conditions. Furthermore, by combining X Series packaging technology with RC-IGBT technology, the module has been able to greatly reduce thermal resistance and also reduce virtual junction temperature T_{vj} by 34°C and ΔT_{vj-c} by 41%.

Figure 7 shows the variation of T_{vj} during low-frequency operation. The X Series RC-IGBT Dual XT

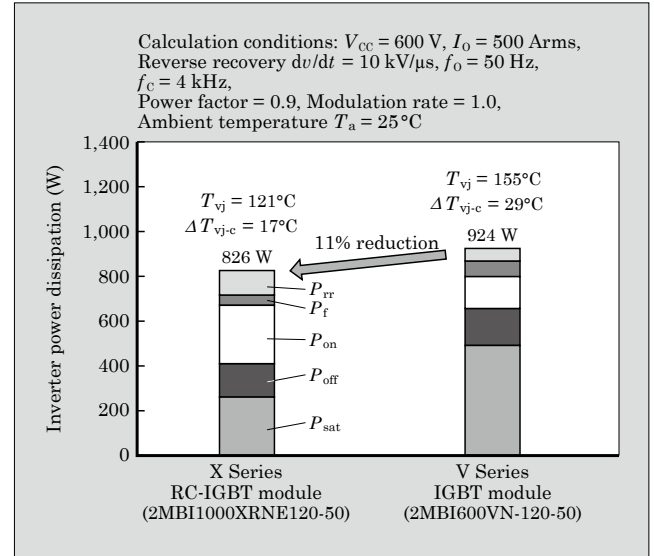


Fig. 6 Inverter power dissipation and virtual junction temperature

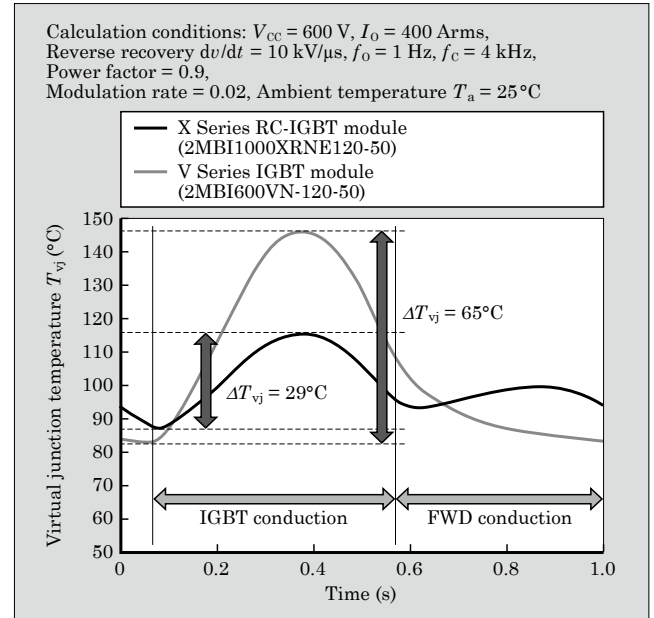


Fig. 7 Time variation for virtual junction temperature T_{vj} during low-frequency operation

module significantly reduces $T_{vj\max}$ through reduction in generated loss and thermal resistance. Furthermore, since the RC-IGBT can flow the current through both IGBT and FWD in the same chip, the thermal ripple is smaller than conventional chips.

Therefore, compared with the V Series IGBT Dual XT module, the X Series RC-IGBT Dual XT module greatly reduces the delta virtual junction temperature ΔT_{vj} . This makes it possible to relax the thermal stress at aluminum wire junctions and solder junctions under the silicon chip. Figure 8 shows the results of calculating ΔT_{vj} power cycle capability and temperature rise during low-frequency operation. The X Series RC-IGBT Dual XT module has dramatically improved

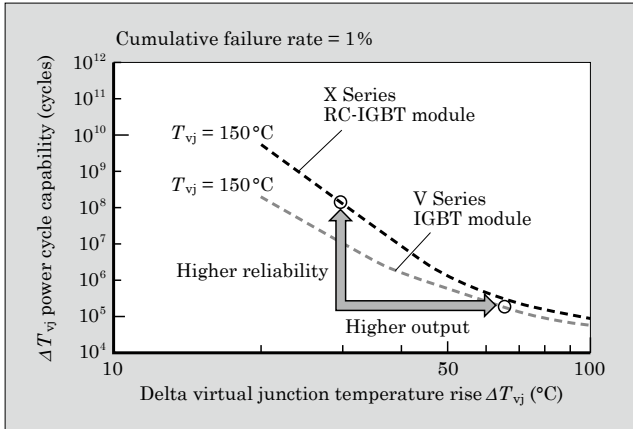


Fig.8 ΔT_{vj} power cycle capability

ΔT_{vj} power cycle capability during low-frequency operation by great reduction ΔT_{vj} . As a result, higher output power can be expected in the case of same power cycle capability, and higher reliability can be expected in the case of same ΔT_{vj} .

Figure 9 shows the inverter operation pattern during continuous operation and overload operation. Fig.

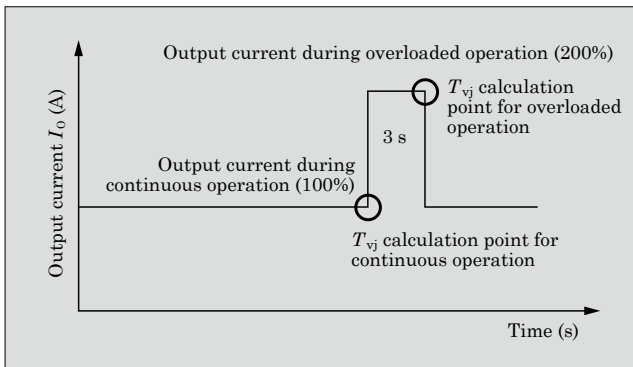


Fig.9 Operation pattern of inverter during continuous operation and overload

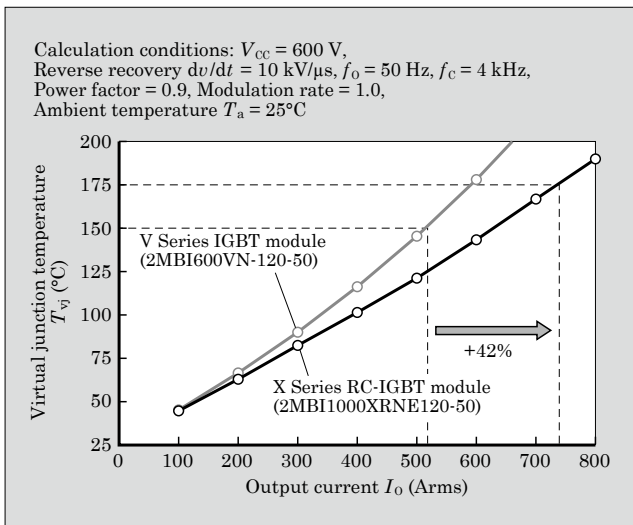


Fig.10 Virtual junction temperature during continuous operation

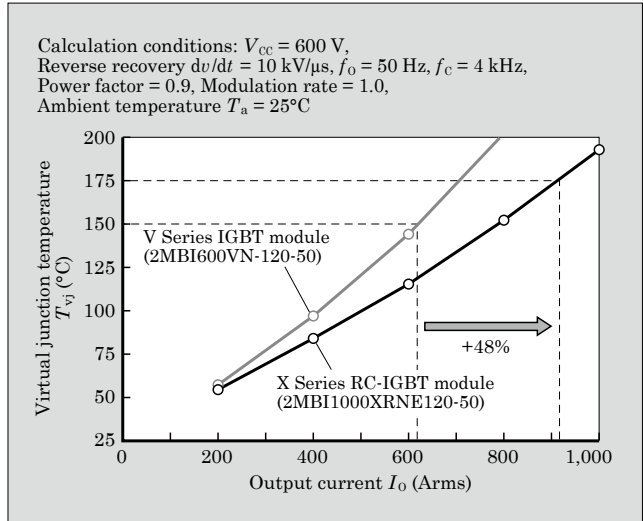


Fig.11 Virtual junction temperature during overloaded operation

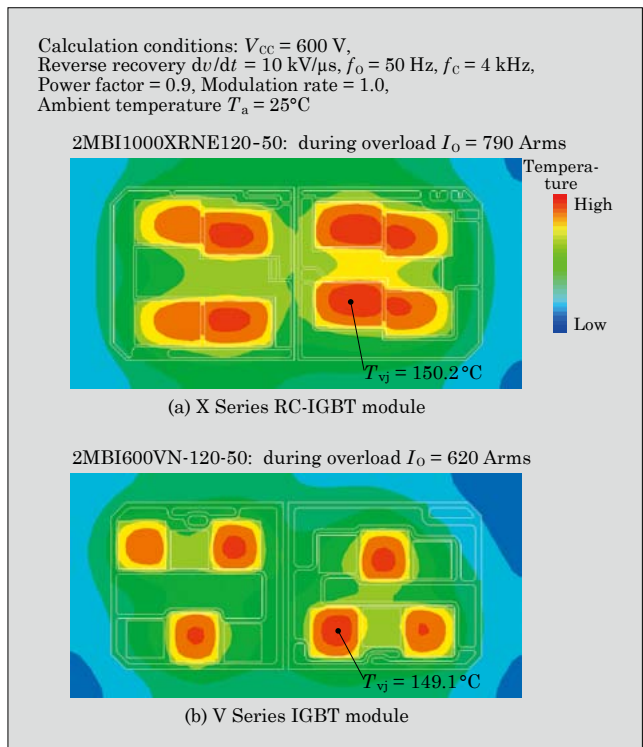


Fig.12 Contour figure created by FEM analysis during overloaded operation

Figure 10 shows the results of calculating output current I_o and T_{vj} when each I_o is 100% (rated current) under the continuous conditions. Figure 11 shows the results of calculating I_o and T_{vj} when each I_o is 200% in 3 seconds under the overload conditions. Figure 12 shows a contour figure created by finite element method (FEM) analysis at a T_{vj} of 150°C during overloaded operation. As shown in Fig. 10, since reducing power dissipation and thermal resistance, moreover raising the T_{vjop} from 150°C of the V Series IGBT module to 175°C of the X Series IGBT module, the X Series RC-IGBT Dual

XT module can expand the output current by 42% in the same package during continuous operation. As shown in Fig. 11, the X Series RC-IGBT Dual XT module can expand the output current by 48% even during overloaded operation. Furthermore, as shown in Fig. 12, the contour figure created by FEM analysis has confirmed that the X Series RC-IGBT Dual XT module is capable of achieving the same T_{vj} of 150°C even when expanding output current by 27% compared with the V Series IGBT Dual XT module. Moreover, a more uniform temperature distribution was also observed as a result of optimizing the chip size and internal layout. Therefore, it can be expected that the module will achieve higher reliability through relaxing the thermal stress for all materials.

5. Postscript

In this paper, we introduced the 7th-generation “X Series” RC-IGBT module line-up for industrial applications. The module achieves a rated current expansion that is inconceivable through utilizing conventional IGBT and FWD. Thus we believe that the module will contribute further to the size and cost reduction of power conversion systems. In the future, we will continue to work for innovating IGBT module technolo-

gies so that we can realize a safe, secure and sustainable society.

References

- (1) Kawabata, J. et al. “The New High Power Density 7th Generation IGBT Module for Compact Power Conversion Systems”, Proceeding of PCIM Europe 2015.
- (2) Kawabata, J. et al. 7th-Generation “X Series” IGBT Module. FUJI ELECTRIC REVIEW. 2015, vol.61, no.4, p.237-241.
- (3) Takahashi, M. et al. “Extended Power Rating of 1200 V IGBT Module with 7 G RC-IGBT Chip Technologies, Proceeding of PCIM Europe 2016.
- (4) Takahashi, K. et al. “1200 V Class Reverse Conducting IGBT Optimized for Hard Switching Inverter”, Proceeding of PCIM Europe 2014.
- (5) Yamano, A. et al. 7th-Generation “X Series” RC-IGBT Module for Industrial Applications. FUJI ELECTRIC REVIEW. 2016, vol.61, no.4, p.241-245.
- (6) Takahashi, H. et al. “1200 V Reverse Conducting IGBT”, Proceeding of ISPSD 2004. p.133-136.
- (7) M, Rahimo. et al. “The Bi-mode Insulated Gate Transistor (BIGT) A Potential Technology for Higher power Applications”, Proceeding of ISPSD 2009. p.283-286.



“M660” High-Power IGBT Module for Automotive Applications

OSAWA, Akihiro* HIGUCHI, Keiichi* NAKANO, Hayato*

ABSTRACT

IGBT modules for automotive applications need to have low power loss to efficiently use battery power. They are also required to achieve small size and lighter weight while having high power. In response to these market demands, Fuji Electric has developed the “M660” direct water-cooled power module. This module adopts a lead frame structure, instead of wire bonding, which was conventionally used for internal wiring. It also employs the cooling structure that integrates a water jacket with reverse-conducting insulated gate bipolar transistors (RC-IGBTs) that have improved characteristics. With these structures, the M660 achieves the rated capacity of 750 V/1,200 A, which is the world’s highest power as a general-purpose 6-in-1 IGBT module.

1. Introduction

Efforts around the world to reduce CO₂ emissions and achieve energy savings have been rapidly increasing. Against this backdrop, automobile manufacturers have been actively promoting the use of electrically powered vehicles such as hybrid electric vehicles (HEV) and electric vehicles (EV) instead of vehicles powered by internal combustion engines that use conventional gasoline and diesel fuel. Insulated gate bipolar transistor (IGBT) modules are used in HEV and EV as one of the key components of the power electronics technology employed in the operation of electric motors. IGBT modules are being required to achieve size reductions and weight savings, as well as realize low power loss in order to facilitate better use of battery power. In addition, they are also required to be larger capacity.

In order to meet these demands, Fuji Electric has developed a direct water-cooled power module. In this paper, we will introduce the features and performance characteristics of the “M660” high-power IGBT module for automotive applications.

2. “M660” Characteristics

Figure 1 shows the external view of the M660, and Table 1, its characteristics.

As can be seen from Table 1, compared with the conventional product, the M660 has reduced collector-emitter saturation voltage $V_{CE(sat)}$ by 22% and thermal resistance $R_{th(j-w)}$ by 31%, while improving power density by 58%. The definitions for power density and motor output used in Table 1 are as follows:

(a) Power density = Used DC voltage × Output current / Module volume

(b) Motor output = Used DC voltage × Output current × Motor efficiency

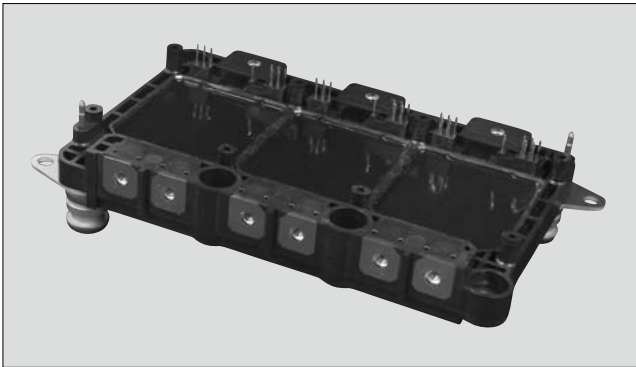


Fig.1 “M660” high-power IGBT module for automotive applications

Table 1 “M660” characteristics

Item	M660	Conventional product
Internal wiring	Lead frame	Wire bonding
Chip	RC-IGBT	RC-IGBT
Collector-emitter voltage	750 V	750 V
Rated current	1,200 A	800 A
Collector-emitter saturation voltage	1.54 V	1.98 V
Thermal resistance	0.09 °C/W	0.13 °C/W
Dimensions (mm)	W178 × D116 × H24	W162 × D116 × H24
Power density	684 kVA/L	433 kVA/L
Motor output	200 kW	150 kW

* Electronic Devices Business Group, Fuji Electric Co., Ltd.

3. Technologies Applied to “M660”

3.1 Application of lead frame technology

Fuji Electric has utilized a lead frame for the main circuit wiring of the direct water-cooled power module. In contrast to wire bonding connections, the use of a lead frame structure has the following 2 advantages:

- By reducing the size of the direct copper bonding (DCB) substrate, making the product size smaller. Wire bonding connections require larger size of the DCB substrate than lead frame structure because it needs the bonding area of multiple wires.
- The lead frame structure has larger contact area with the chip, and this creates more heat dissipation, thus reducing the maximum temperature of the chip.

In addition to the advantages mentioned in (a) and (b), the use of resin as the sealing material has made it possible to reduce stress generated in the solder under the lead frame, thus improves the power cycle capability. Furthermore, in wire bonding connections, it is necessary to make multiple bonding processes for wires. In contrast to this connection, by the lead frame structure, a single lead sheet is laid and connected to DCB substrate, thus providing the IGBT module with excellent productivity.

Figure 2 shows the internal layout of the half bridge circuit of an IGBT module that utilizes wire bonding connections, as well as one that utilizes a lead frame structure.

By employing lead frame technology for the M660, the size of the IGBT module has been reduced by 23% compared with modules that utilize a wire structure.

3.2 RC-IGBT utilization and characteristic improvement

In order to reduce the size of the module, the M660 makes use of a reverse-conducting IGBT (RC-IGBT). The RC-IGBT uses an IGBT with a field stop (FS) structure as the base, while using a structure that arranges stripe-shaped IGBT units and free wheeling diode (FWD) units alternately placed on a single chip. Figure 3 shows the schematic structure of the RC-IGBT.

The use of the single chip made it possible to re-

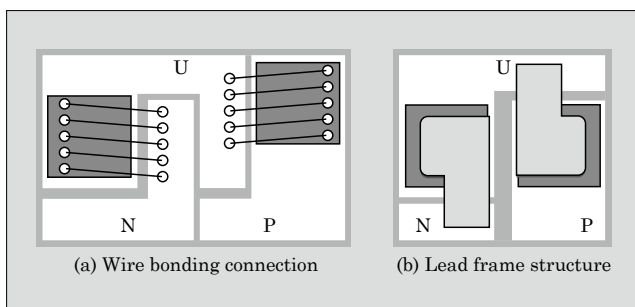


Fig.2 Internal layouts of half bridge circuits

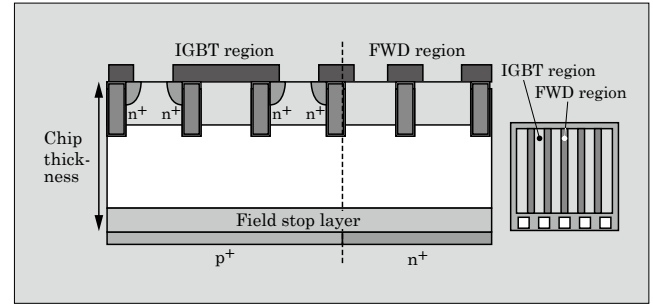


Fig.3 Schematic structure of RC-IGBT

duce the size of the region referred to as the guard ring (a region for securing breakdown voltage for the periphery of the chip), thus enabling a smaller chip area than conventional products that employed a structure composed of separate chips for the IGBT and FWD. Moreover, heat is dissipated from the region of the FWD when the IGBT operates, and conversely, from the region of the IGBT when the FWD operates, reducing thermal resistance when either the IGBT or FWD operate.⁽¹⁾

Fuji Electric has been releasing modules for automotive applications that come equipped with an RC-IGBT.⁽²⁾ This time, we have undertaken to reduce loss even further for the IGBT module. Reduction of steady-state loss through chip thinning is one method for reducing loss in mounted RC-IGBT chips. Therefore, we developed a cutting-edge thin wafer processing technology that has reduced steady-state loss for the RC-IGBT by thinning the wafer to a thickness sufficient for a breakdown voltage of 750 V. In addition, the surface structures such as trench pitch, channel density and contact were all optimized. Figure 4 shows the $V_{CE(sat)}$ -collector current I_{CRM} characteristics for the M660 and a module with the conventional RC-IGBT, and Figure 5 shows the diode forward voltage V_F -diode forward current I_{FRM} characteristics.

Compared with the conventional product, the M660 has reduced $V_{CE(sat)}$ by 22% and V_F by 4.2% at a rated current of 1,200 A by optimizing the cell design of the IGBT.

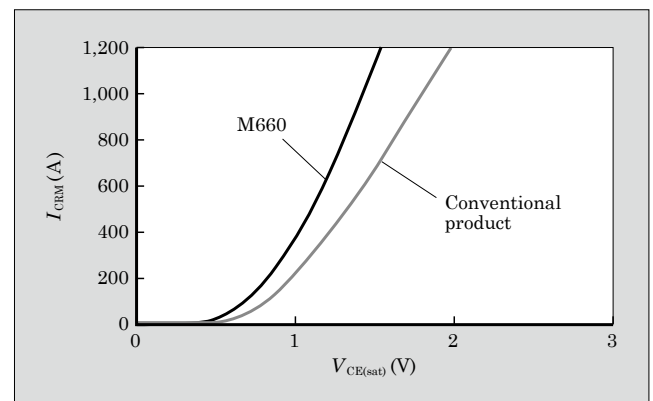


Fig.4 $V_{CE(sat)}$ - I_{CRM} characteristics

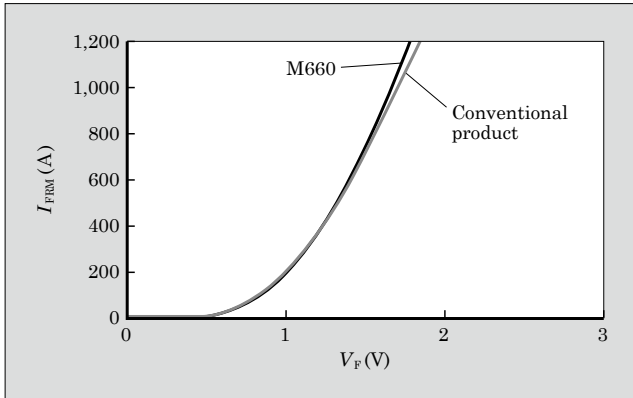


Fig.5 V_F - I_{FRM} characteristics

3.3 I_t^2 capability

Current squared time I_t^2 is an indicator that represents the overcurrent withstand capability for the FWD built into the IGBT module. A current from the inverter in its regenerative operation flows through FWD and charges a capacitor. The FWD needs to withstand the regenerative current I_t^2 without breaking down (see Fig. 6). The main failure modes of the FWD during regeneration relate to device destruction due to large current flow or generated heat destruction of the wire due to heat being generated in the wire.⁽³⁾

Figure 7 shows the I_t^2 capabilities for the M660 and an IGBT module with wire bonded separate

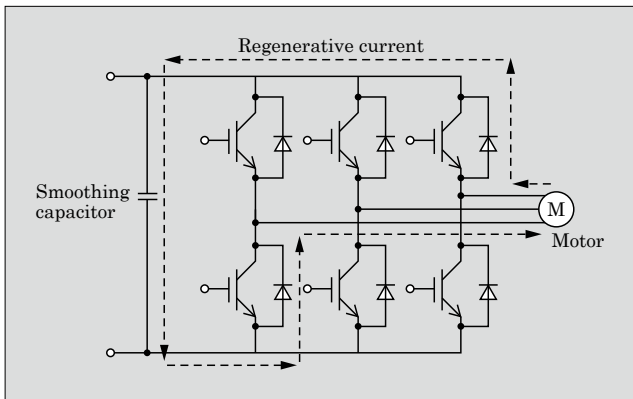


Fig.6 Inverter regenerative operation

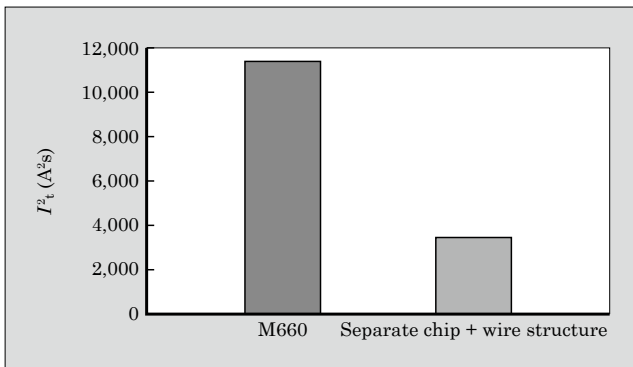


Fig.7 I_t^2 capability

chips. It can be seen that the M660 has an I_t^2 capability of at least 3 times that of the IGBT module with wire bonded separate chips. Temperature rise in the FWD region is suppressed in the RC-IGBT because heat spreads to the IGBT region when current flows through the FWD region. Furthermore, the lead frame structure employed by the M660 widens the contact region for the chip compared with wire bonding connection. Therefore, heat is transferred to the surface of the lead frame and local temperature rise is mitigated.

3.4 Utilization of efficient heat dissipating cooling unit

Fuji Electric has elucidated the fact that space yielded between the water-cooled fins and water jacket causes degradation in thermal resistance, and it has been developing a high-efficiency cooling structure that integrates the heat sinks and water jacket.⁽⁴⁾

To further improve the cooling efficiency brought about by the water jacket integrated cooling structure, the internal structure improvement for the cooling unit is made in the M660.

As a result, the M660 reduced thermal resistance $R_{th(j-w)}$ to 0.1 °C/W, which is a 23% improvement over the $R_{th(j-w)}$ value of 0.13 °C/W for the conventional product. However, when implementing a thermal design, it is necessary to use the maximum $R_{th(j-w)}$ value in the module. Therefore, it was believed that thermal resistance could be reduced even further by reducing in-plane fluctuations for cooling performance. Figure 8 shows the positional relationship for the operation phases of the M660, as well as the in-plane fluctuation for $R_{th(j-w)}$ before and after optimizing the internal structure for the cooling unit.

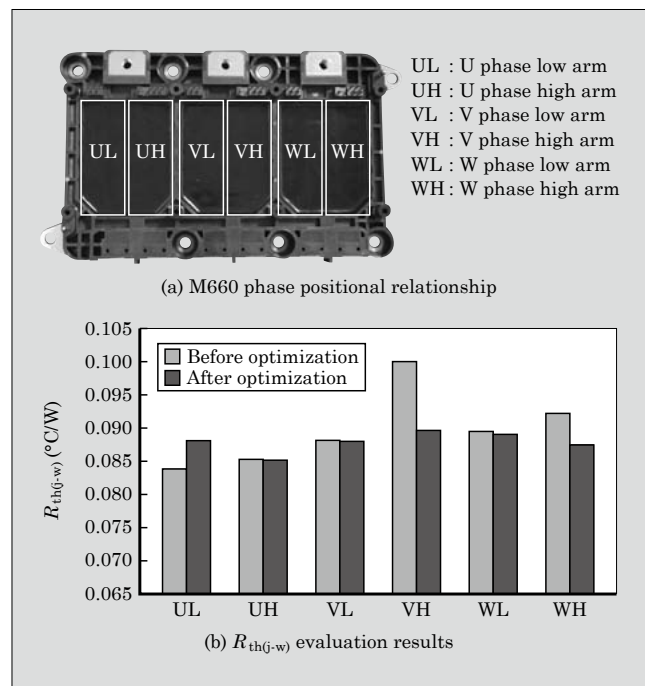


Fig.8 Thermal resistance $R_{th(j-w)}$ evaluation results before and after cooling unit improvement

As is clear from Fig. 8(b), it was possible to further improve $R_{th(j-w)}$ another 10% to achieve a value of $0.09^{\circ}\text{C}/\text{W}$ by improving the in-plane distribution for VH phase cooling performance.

4. Operable Current

In order to estimate maximum allowable current, a simulation was implemented with respect to chip temperature T_{vjop} with output current as a parameter in both the M660 and the conventional product (equipped with RC-IGBT with wire bonding).

The simulation conditions included battery voltage $V_{DC} = 450\text{ V}$, PWM switching frequency $f_c = 5, 8$ and 10 kHz , refrigerant temperature $T_w = 65^{\circ}\text{C}$ and refrigerant flow rate $= 10\text{ L/min}$. Figure 9 shows the results of the T_{vjop} simulation for the M660, and Figure 10 shows the results of the T_{vjop} simulation for the conventional product.

Please note that Figs. 9 and 10 do not taken into

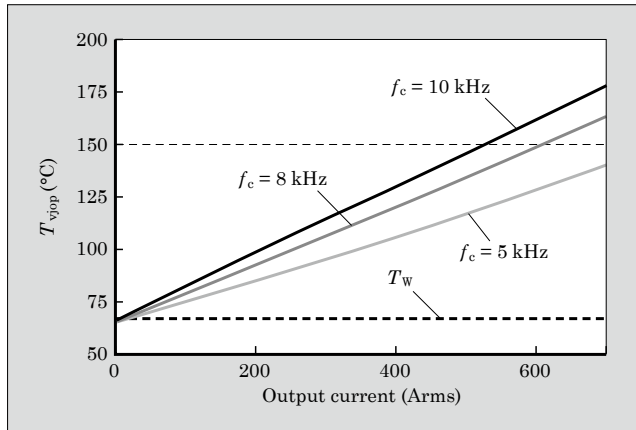


Fig.9 M660's T_{vjop} simulation results

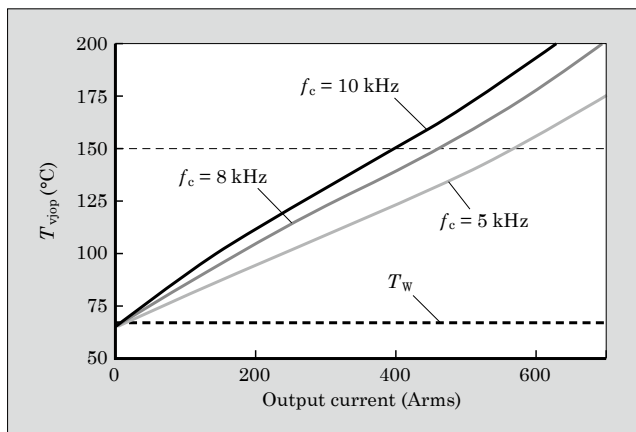


Fig.10 Conventional product's T_{vjop} simulation results

consideration RC-IGBT characteristic fluctuations or changes in thermal resistance due to solder cracking while simulating actual use. At $f_c = 10\text{ kHz}$, the maximum output current for which T_{vjop} remains below 150°C was improved to 525 Arms for the M660, which is 1.35 times better than the conventional product's value of 390 Arms.

Actual products should have some margin in the characteristics in consideration of characteristic fluctuations in the mounted chip and solder cracking during actual operation. The guaranteed temperature for the RC-IGBT mounted to the M660 is 175°C . In a worst case scenario that includes margin at $f_c = 10\text{ kHz}$, the M660 will be able to output current up to about 600 Arms.

The M660 reduces loss for the chip and achieves excellent heat dissipation performance through the use of lead frame technology, improved characteristics of RC-IGBT chip and cooling structure that integrates an optimized water jacket. As a result, the M660 is capable of operating in a larger current than conventional products.

5. Postscript

In this paper, we introduced the “M660” high-power IGBT module for automotive applications. The M660 is a general purpose 6-in-1 IGBT module that has achieved the world's largest rated capacity of $750\text{ V}/1,200\text{ A}$ through the utilization of a lead frame, characteristic enhanced RC-IGBT and cooling structure that integrates an optimized direct water-cooled water jacket.

We will continue to work to meet the growing demands of the electric vehicle industry so that we can help alleviate global warming.

References

- (1) Sato, K. et al. Functionality Enhancement of 3rd-Generation Direct Liquid Cooling Power Module for Automotive Applications Equipped with RC-IGBT. FUJI ELECTRIC REVIEW. 2016, vol.62, no.4, p.256-260.
- (2) Enomoto, K. et al. 3rd-Generation Direct Liquid Cooling Power Module for Automotive Applications. FUJI ELECTRIC REVIEW. 2017, vol.63, no.1, 61-62.
- (3) Osawa, A. et al. “700 kVA/L power density IGBT module for xEV power density”, PCIM Asia 2017, p.137-143.
- (4) Gohara, H. et al. “Next-gen IGBT module structure for hybrid vehicle with high cooling performance and high temperature operation”, PCIM Europe 2014, p.1187-1194.

6.5th-Generation Automotive Pressure Sensors

UZAWA, Ryohei* NISHIKAWA, Mutsuo* TANAKA, Takahide*

ABSTRACT

There is increasing demand for reducing the environmental load of automobiles. Automotive pressure sensors, which are indispensable for control systems for high efficient engines and cleaner exhaust gas, are required to achieve high-temperature operation, corrosion resistance, electrification resistance, and miniaturization. In order to meet these demands, the 6.5th-generation automotive pressure sensors have been developed. They inherit from the 6th-generation series while providing several enhancements, such as improved electrification resistance and corrosion resistance to exhaust gas and vaporized fuel, as well as a smaller size and improved reliability of sensor accuracy. They optimize temperature characteristic to guarantee operation at 150 °C and add a clamp function to prevent erroneous detection by separating the diagnostic voltage range from the normal output voltage range.

1. Introduction

Currently, automobiles are strongly required to reduce their environmental impact as seen in the imposition of air pollutant and CO₂ emissions regulations, as well as to improve safety and comfort. To meet these regulations, development of control systems for electrically driven vehicles such as hybrid electric vehicles, electric vehicles and fuel cell vehicles is accelerating. Meanwhile, fuel efficiency of gasoline- and diesel-fueled vehicles have improved by precisely controlling the air-to-fuel ratio. Further, technologies to make exhaust gas cleaner by recirculating the gas after combustion so as to reduce air pollutants are becoming widespread at an increasing speed. Pressure sensors are used as one essential device in engine control and their uses include improving engine efficiency and purifying exhaust gas. They are becoming more important year by year.

Fuji Electric started mass producing automotive pressure sensors in 1984. Since then, we have been proposing high-reliability technology, circuit technology and sophisticated micro-electro-mechanical systems (MEMS) technology to meet the requirement of reliability to withstand a severe operating environment and improved detection accuracy. Our pressure sensors are adopted in automobiles in Japan and overseas. Starting in 2010, we have been mass-producing the 6th-generation automotive pressure sensors with digital trimming based on the complementary metal-oxide-semiconductor (CMOS) process.⁽¹⁾

This paper presents the 6.5th-generation automotive pressure sensor. It is based on the conventional 6th-generation automotive pressure sensor while inheriting the basic “all-in-one chip” concept. It is pro-

vided with corrosion resistance and electrification resistance and is guaranteed to operate at 150 °C with a smaller sensor cell size.

2. Overview of Pressure Sensor

2.1 Examples of use of automotive pressure sensors

Figure 1 shows examples of use of automotive pressure sensors. To improve the fuel efficiency of vehicles, most fuel injection systems are now electronically controlled. These electronically-controlled fuel injection systems use a manifold absolute pressure (MAP) sensor for measuring the intake pressure or have a temperature manifold absolute pressure (TMAP) sensor equipped with a temperature sensing function. In addition, many pressure sensors are used to improve fuel efficiency and control engine systems so as to suppress the emission of air pollutants. Such sensors include atmospheric pressure sensors for highland correction intended for preventing any decrease in fuel efficiency when vehicles are travelling at high altitudes, pressure sensors for detecting any clogging of the air intake system air filter box, exhaust pressure sensors for exhaust gas recirculation (EGR) systems to reuse exhaust gas and boost pressure sensors mounted on turbo engines.

Another type of automotive pressure sensor to be mentioned is a pressure sensor for detecting any clogging of diesel particulate filters (DPFs). It is used to deal with stricter exhaust gas regulations represented by the 2016 tightening of emissions regulations of Japan and European Euro 6 in 2014.

Additionally, sensors for meeting safety regulations include fuel tank pressure sensors (FTPSs) for detecting tank leaks, and they are used in Europe and the U.S.

Demand for pressure sensors is also increasing for controlling air conditioner coolant pressure, the pres-

* Electronic Devices Business Group, Fuji Electric Co., Ltd.

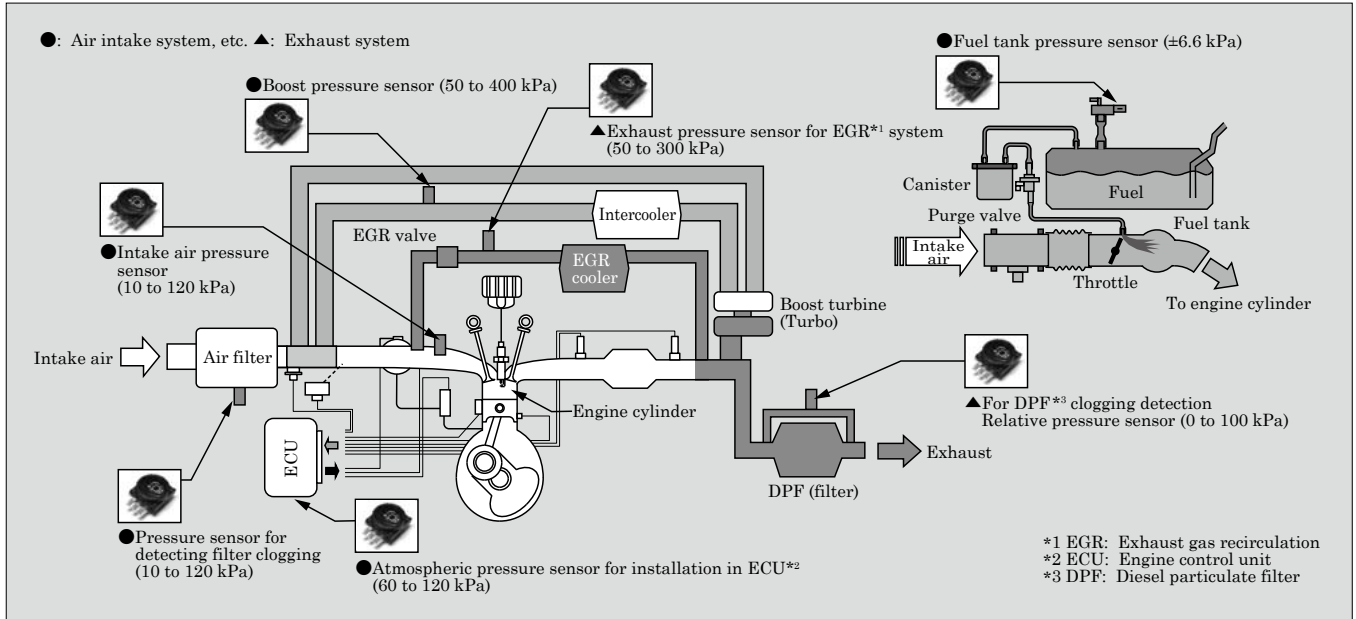


Fig.1 Examples of use of automotive pressure sensors

sure of heat pumps used in electric vehicles and the hydraulic pressure of transmissions. In this way, the scope in which automotive pressure sensors are applied is rapidly expanding and their demand increasing.

2.2 Installation environment of automotive pressure sensors

Conventionally, the medium (target) to be measured by intake or boost pressure sensors was mostly air. However, the scope of application of pressure sensors is expanding as described earlier, and the media to be measured have become severe such as those containing exhaust gas and vaporized fuel including gasoline and diesel oil. Accordingly, sensors need to have corrosion resistance against these media to be measured and electrification resistance against charged vaporized fuels.

In addition, engine rooms are being made smaller and mounting density increased for the purpose of increasing the cabin space intended for improving fuel efficiency and comfort. This has caused a temperature increase in the ambient environment for pressure sensors and exposure to electromagnetic noise generated from various electronic devices. This is why increase in the guaranteed operating temperature and strengthened electromagnetic compatibility (EMC) are required.

3. Features of 6.5th-Generation Pressure Sensor

3.1 Product overview

Figure 2 shows the appearance of the 6.5th-generation automotive pressure sensor and the previous 6th-generation automotive pressure sensor. Table 1 shows the specifications of the 6.5th-generation automotive pressure sensor.

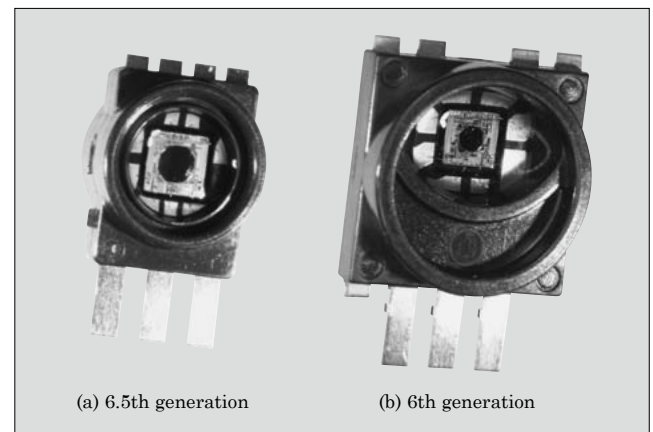


Fig.2 Automotive pressure sensor

The 6.5th-generation automotive pressure sensor is equipped with corrosion resistance and electrification resistance. Its maximum guaranteed operating temperature has been increased from 125 °C of the conventional product to 150 °C. For detecting failures, a clamp function has been added for separating the wire harness disconnection detection range (diagnostic voltage range) from the normal use range. The size of the sensor cell has been reduced to approximately 48% of that of the 6th-generation automotive pressure sensor in terms of the volume.

3.2 Corrosion resistance

Figure 3 shows the cross-section structure of the sensor cell of a pressure sensor. Against incoming foreign objects such as soot, the sensor chip and wire are protected by using gelled protection material capable of transmitting pressure. With this product, there is a need to prevent exhaust gas and vaporized fuel such as gasoline and diesel oil from passing through the pro-

Table 1 Specifications of 6.5th-generation automotive pressure sensor

Item	Specification
Product size (resin part)	W7.5 × H10 × D5.6 (mm)
Operating temperature range	−40 °C to +150 °C
Operating pressure range (in-take pressure sensor)	20 to 120 kPa
Rated pressure	Pressure range × 3
Power supply voltage	5 ± 0.25 V
Output voltage (at power supply voltage of 5 V)	0.5 to 4.5 V
Sink and source capacities	Sink: 1 mA, Source: 0.1 mA
Clamp function	Clamp voltage 0.3 V/4.7 V (typ.)
Corrosion resistance	In accordance with JASO M 611-92/B Method (Gasoline/diesel component)
ESD (external interface terminals)	
MM (0 Ω, 200 pF)	±1 kV or more
HBM (1.5 Ω, 100 pF)	±8 kV or more
Transient voltage surge	ISO 7637 (2011) standard Pulse 1, 2, 3a, 3b LEVEL-III cleared
Impulse	±1 kV or more
Latch-up (current injection method)	±500 mA or more
EMS (G-TEM) (100 V/m)	Variation: 1% FS or less
Overvoltage (between Vcc and GND)	16.5 V (max.)
Reverse connection (between Vcc and GND)	0.3 A (max.)

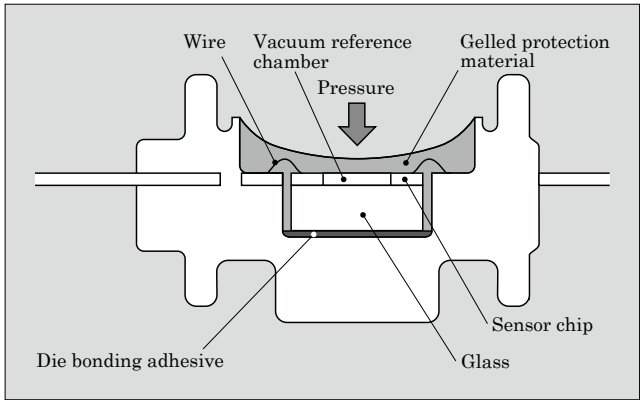


Fig.3 Cross-section structure of sensor cell

tection material since it would corrode the wire bonding pad on the chip surface. Hence, corrosion prevention areas have been provided on the wire bonding pad and test pad as shown in Fig. 4.

3.3 Electrification resistance

Figure 5 outlines the pressure sensing unit integrated in the pressure sensor. Fuji Electric's proprietary etching technology is used to process part of the silicon into a thin film to form a diaphragm. The 4 piezoresistors composed of the diffusion wiring provided on the diaphragm constitute a Wheatstone

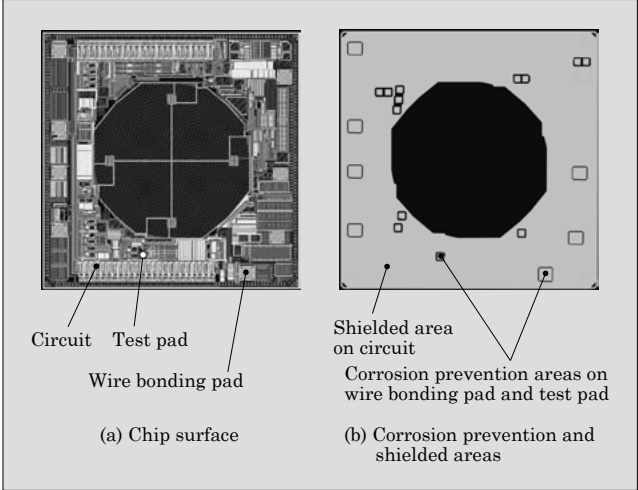


Fig.4 Corrosion prevention and shielded areas

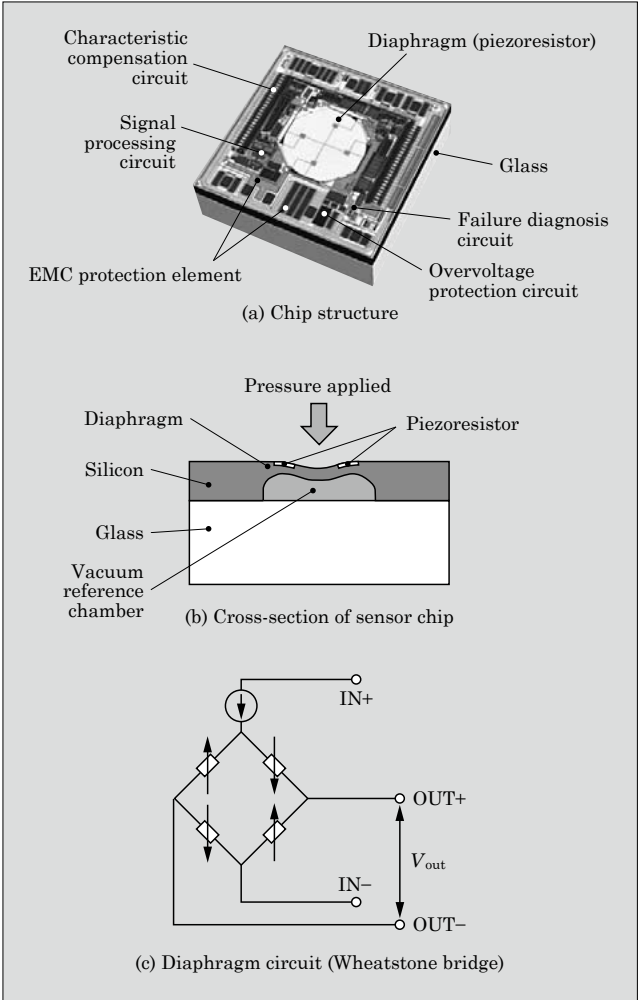


Fig.5 Overview of pressure sensing unit

bridge. When the diaphragm is deformed by the pressure applied, the respective piezoresistance values change, generating a potential difference in the output of the Wheatstone bridge. The pressure sensing unit amplifies this potential difference to convert the pressure into an electric signal.

There is a need to prevent electrically charged vaporized fuel from attaching to the gelled protection material and causing a variation of the piezoresistance values since this would affect the sensor characteristics. Hence, this product employs a shielded structure with polysilicon used for the flexible part (diaphragm) of the MEMS. As shown in Fig. 4, the same layer as that of the corrosion prevention areas is used to form a shielded area. The intention is to improve the resistance to electrostatic charging of the circuit except for the diaphragm.

To optimize the structure, we have used device simulation for analysis. Figure 6 shows an example of changes in the chip surface charge and piezoresistor area. With an unshielded structure, the resistance value of the piezoresistor changes as the quantity of electric charge on the chip surface increases [see Fig. 6(a)]. To deal with this phenomenon, a shield has been provided in an appropriate location on the piezoresistor. This has made the piezoresistance constant regardless of the electric charge density on the chip surface [see Fig. 6(b)]. Figure 7 shows the result of actually applying electric charge to the product with this structure to obtain output characteristic changes. It has been confirmed that output is stabilized by appropriately locating the shield and the shielded area of the

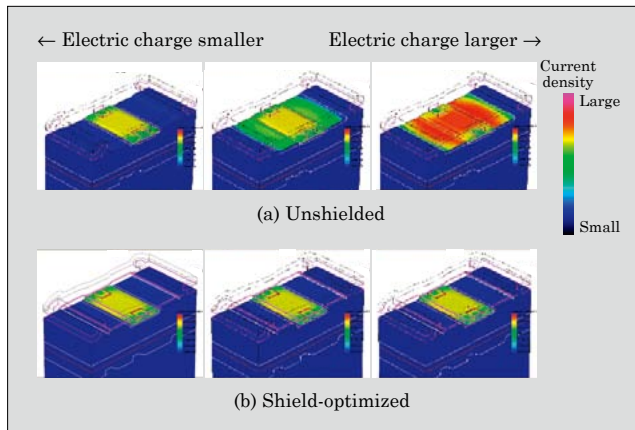


Fig.6 Example of changes in chip surface charge and piezoresistor area

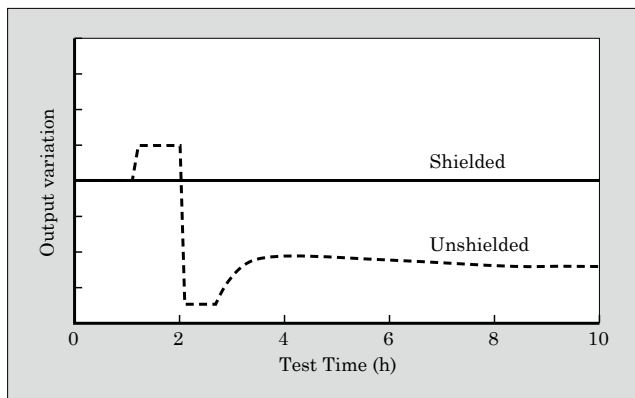


Fig.7 Result of electrification resistance test

circuit shown in Fig. 4.

3.4 High-temperature operation guarantee and clamp function

Figure 8 shows a circuit block diagram of this product. Deterioration of characteristics in the high-temperature operation range has been restrained by optimizing the temperature characteristics of the individual circuit blocks. This results in guaranteeing that the device will work at 150 °C.

Figure 9 shows a pressure-output characteristic diagram of this product. The sensor output is brought into the diagnostic voltage range when the wire harness is disconnected, which causes the upper-level system to detect a failure. Meanwhile, when overpressure or underpressure is applied the output is brought into the diagnostic voltage range, which may cause the upper-level to erroneously detect disconnection. This product is equipped with a clamp function, where a circuit is provided to clamp the output voltage and reliably separate the diagnostic voltage range from the normal output voltage range, thereby preventing erroneous detection.

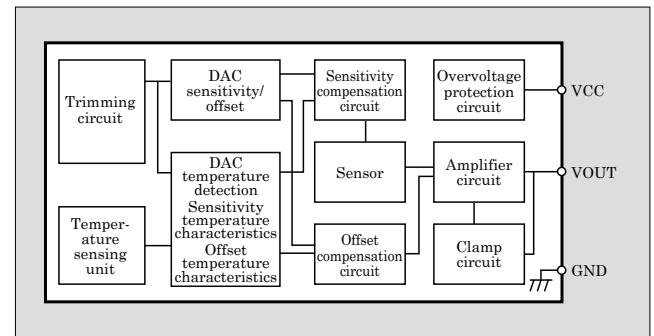


Fig.8 Block diagram of 6.5th-generation automotive pressure sensor

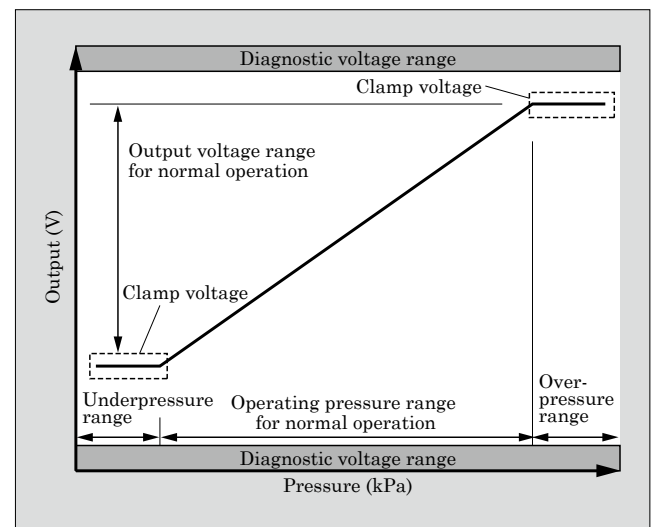


Fig.9 Pressure-output characteristic diagram of 6.5th-generation pressure sensor

4. Postscript

This paper has presented the 6.5th-generation automotive pressure sensor. Increasingly stringent requirements are expected for pressure sensors to see a widespread rollout in Japan and overseas. They will need to offer better product performance from the perspective of improved fuel efficiency and compliance

with environmental and safety regulations. Fuji Electric intends to continue meeting market needs in and work on developing the products required by the market.

References

- (1) Mutsuo, N. et al. 6th Generation Small Pressure Sensor. FUJI ELECTRIC REVIEW. 2011, vol.57, no.3, p.103-107.



“FA8A80 Series” 650-V PWM Power Supply Control ICs

HIASA, Nobuyuki* ENDO, Yuta* KARINO, Taichi*

ABSTRACT

Switching power supplies for electronic devices, which are increasingly being required to save energy and reduce the number of parts usage, need to achieve high efficiency, low standby power, and reduction in the number of parts. Fuji Electric has developed the “FA8A80 Series” 650-V PWM power supply control ICs, which allows power supplies to achieve compact size and improve safety, as well as high efficiency and low stand-by power, which are inherited from the “FA8A60 Series.” The maximum applied voltage for the high-voltage input terminals has increased to 650 V from the previous withstand voltage of 500 V. Furthermore, the series has also achieved greater surge resistance. Their protection functions have the same characteristics as conventional products, facilitating to use existing design resources to promote labor savings in power supply design.

1. Introduction

In order to prevent global warming, which is posing a serious problem, there is an increasing need to save on the energy used by electronic devices themselves and reduce the parts and materials used for them. Accordingly, switching power supplies, which function as power converters of electronic devices, need to offer higher efficiency and lower standby power and have fewer parts. In developing countries, electronic devices are becoming widespread as their economies develop. Meanwhile, slow infrastructure development has caused frequent instantaneous power failures and voltage fluctuations of commercial power supplies (AC power supplies). During recovery from an instantaneous power failure, in particular, excessively high voltage generated in the AC power supply poses problems. These include damage to the power supply due to the AC power voltage exceeding the input voltage range of the power supply or high surge voltage applied. Accordingly, power supplies increasingly need to support high input voltage and ensure safety and reliability such as by having a high surge resistance.

In order to meet the needs of the switching power supply market described earlier, Fuji Electric has commercialized the “FA8A60 Series.” The series are current mode pulse width modulation (PWM) ICs in a small package (SOP-8). The products offer high efficiency and are equipped with a low stand-by power function. They are intended for controlling switching power supplies.

We have now developed the “FA8A80 Series” 650-V PWM power supply control ICs. They inherit the features of the “FA8A60 Series” and allow power supplies to come in a compact size and have improved safety.

2. Overview of “FA8A80 Series”

Figure 1 shows the external appearance of the FA8A80 Series. The FA8A80 Series is based on the

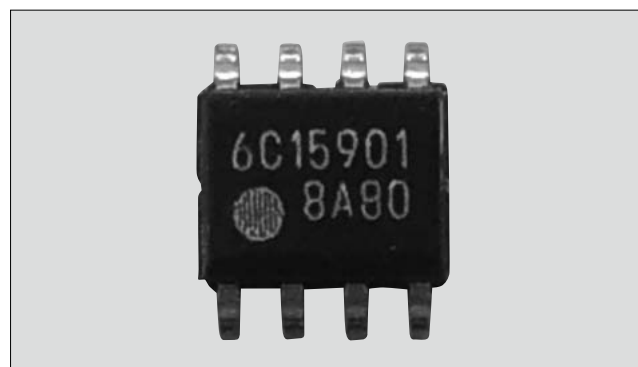


Fig.1 “FA8A80 Series” 650-V PWM power supply control IC

Table 1 Function overview of “FA8A80 Series”

Item	FA8A80 Series	Conventional product
Start-up device	Integrated	
Maximum applied voltage for high-voltage input terminal	650 V	500 V
ESD resistance of high-voltage input terminal (HBM)	±2 kV	+1 kV/ -2 kV
Maximum sink current of LAT terminal	500 μA	100 μA
External latch function	Integrated	
Function to reduce switching frequency	Integrated	
Function to set frequency reduction state	Integrated	
Function to adjust burst operation	Integrated	
Function to correct overload protection level for AC input voltage	Integrated	
Power-off mode	Integrated	
Standby power (with no load)	30 mW or less	

* Electronic Devices Business Group, Fuji Electric Co., Ltd.

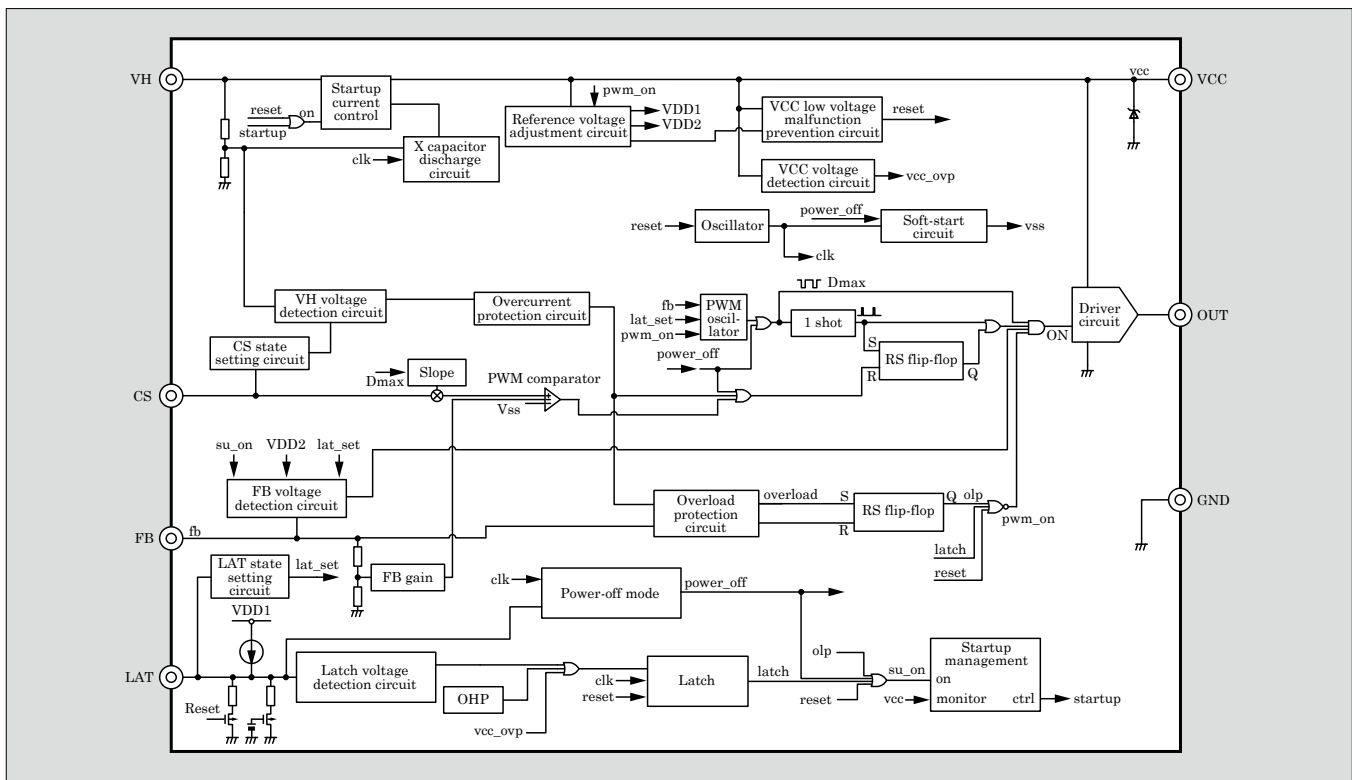


Fig.2 “FA8A80 Series” block diagram (FA8A90N)

conventional FA8A60 Series. It has increased the maximum applied voltage for the high-voltage input terminals connected to the AC power supply to 650 V from the previous 500 V. Further, it has been given greater surge resistance by improving the electrostatic discharge (ESD) resistance of the VH terminal to 2 kV.

In addition, the sink current characteristic of the fault detection signal input (LAT) terminal for stopping power supply in the event of an abnormality has been improved. This improvement eliminates the use of a Zener diode (ZD) that has to be added depending on the protection specifications of a power supply to protect the IC.

Furthermore, we have employed the same basic functions, characteristics and terminal layout as those of conventional products. This makes it possible to utilize the existing power supply design resources, leading to reduced design periods. Table 1 shows an overview of the features of the FA8A80 Series, and Fig. 2, a block diagram.

3. Features of “FA8A80 Series”

3.1 Support for high-voltage input by providing 650 V start-up device

Figure 3 shows a schematic diagram of the VH terminal and internal circuit. The VH terminal connected to the AC power supply unit has a function of supplying current when the VCC terminal voltage is low and stopping the current supply at a certain voltage or higher.

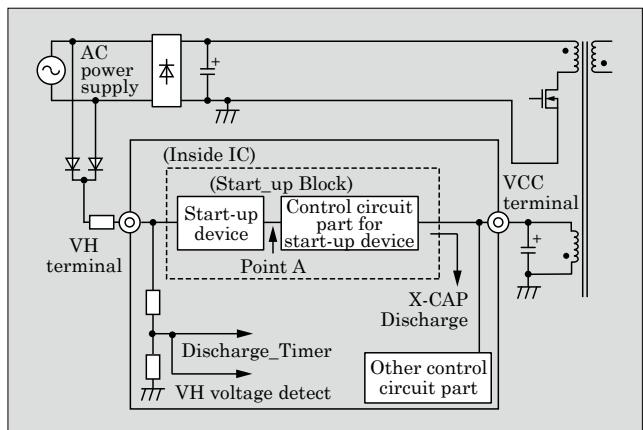


Fig.3 Schematic diagram of VH terminal and internal circuit

As shown in Fig. 4, the output voltage of the start-up device (at Point A in Fig. 3) depends on the VH terminal voltage. For that reason, with a conventional start-up device, increasing the applied voltage causes the voltage at Point A in Fig. 3 to exceed the allowable applied voltage of the start-up device control circuit to which the current is input.

Accordingly, we have improved the dependence of the start-up device on the VH voltage with the FA8A80 Series. We have achieved a characteristic in which the rated voltage of the start-up device control circuit is not exceeded even if the maximum applied voltage to the VH terminal is increased. This has permitted a high-voltage input of 650 V.

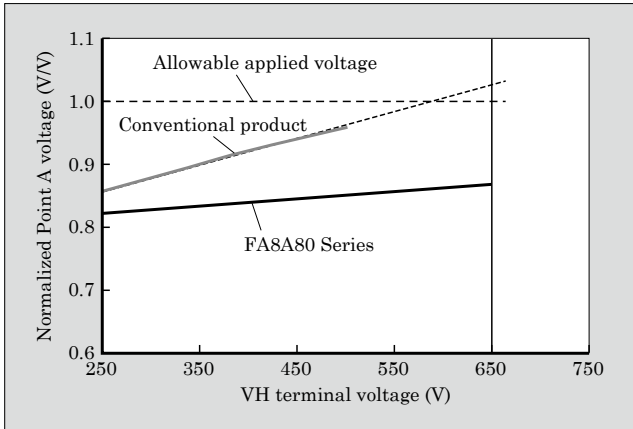


Fig.4 Relationship between VH terminal voltage and internal voltage

3.2 Improved ESD withstand voltage

The human body model (HBM) ESD withstand voltage on the VH terminal of conventional products was +1 kV. With the FA8A80 Series, the breakdown resistance as well as the maximum applied voltage to the VH terminal has been increased. This has led to a guarantee voltage of ± 2 kV with the HBM for all IC terminals.

3.3 Support for various power supplies by frequency reduction and burst operation

To realize high efficiency and low standby power as with conventional products, the FA8A80 Series integrates a function for improving efficiency during light- and no-load operation. This is achieved by reducing the switching frequency during light-load operation and having burst operation (intermittent operation) during no-load operation. In addition, 3 switching frequency reduction characteristics as shown in Fig. 5 are provided in order to support power supplies of various specifications. The LAT terminal is equipped with a function to set the frequency reduction state by selecting one of the 3 characteristics and a burst operation

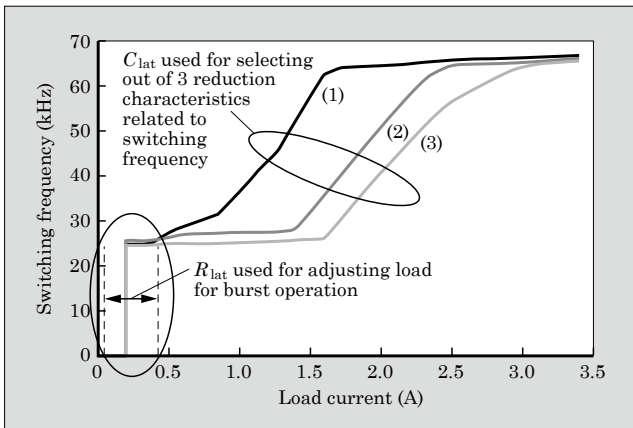


Fig.5 Change of frequency by using function to set frequency reduction state and function to adjust burst operation

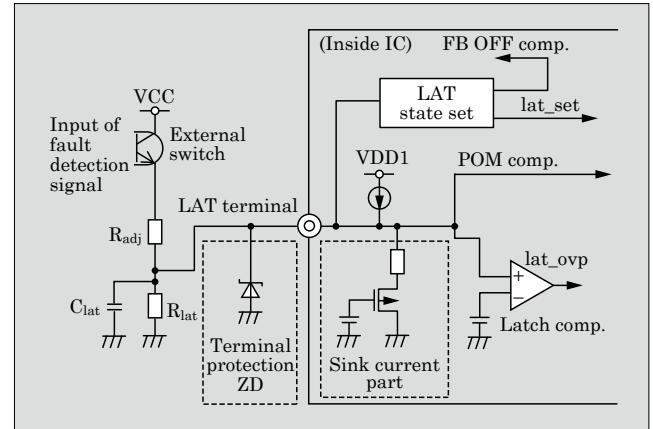


Fig.6 External circuit configuration of LAT terminal

adjustment function.

Figure 6 shows an external circuit configuration of the LAT terminal. The function to set the frequency reduction state can select one of the 3 reduction characteristics by setting the capacity C_{lat} connected between the LAT terminal and GND to a specific value. For a power supply specification in the normal operating conditions with a high load, the characteristic (1) in Fig. 5 is selected. As light-load operation increases, characteristic (2) or (3) in Fig. 5 with a wider load current range for operation at a low frequency is selected to save energy.

The burst operation adjustment function is intended to adjust the load current for burst operation. It does this by setting FB OFF, the threshold voltage for stopping switching output of the FB terminal. The FB OFF voltage is determined by the value of the resistor R_{lat} connected between the LAT terminal and GND shown in Fig. 6 and the constant-current output value of the LAT terminal to set the load current value for burst operation.

By appropriately setting the load current during burst operation, the power supply specifications of the standby power and output voltage ripple can be satisfied without generating any sound. This is very important in designing power supplies. An excessively large set value for the load current for burst operation may cause the power supply output voltage ripple to exceed the specification while the standby power is decreased, or it may cause the burst frequency to increase to an audible range and generate unwanted sound. Meanwhile, an excessively small set value may cause the standby power to exceed the specification. Accordingly, the setting can be adjusted to an optimum value by, for example, selecting a small R_{lat} value that corresponds to the upper limit of the standby power specification and increasing the R_{lat} value within a range that does not cause unwanted sound.

3.4 Size reduction of power supply by improving characteristics of external latch function

The external latch function stops switching op-

eration (to enter a latch state) by bringing the LAT terminal voltage to 2.0 V (max.) or higher, which is the external latch function threshold, using the fault detection signal generated within the power supply in the event of device fault. In this way, it ensures the power supply is safe.

For designing a power supply, the adjustment resistor R_{adj} shown in Fig. 6 is used to set the external circuit constant that achieves both the time between fault detection and protective stop of the power supply specification and the LAT terminal rating of the IC specification.

The VCC terminal, which is a power supply to the external circuit, is generally connected to the auxiliary winding of the transformer as shown in Fig. 3. The voltage may vary by about 20 V (ratio of the maximum voltage to the minimum voltage: approximately 3 times) depending on the size of the load current of the power supply. Accordingly, with an inappropriate R_{adj} value, the time taken before latch protective stop

may increase when the VCC terminal voltage is low. This will result in a failure to satisfy the power supply specification, and the LAT terminal voltage after the protective stop may increase to higher than the rated voltage when the VCC terminal voltage is high. This will result in a failure to satisfy the IC specification. In cases like this, an R_{adj} value satisfying the power supply specification must be selected and a ZD for LAT terminal protection must be added between the LAT terminal and GND. This required expensive external components and board space.

To deal with this issue, the FA8A80 Series has increased the maximum current and improved the current-voltage characteristic of the sink current part of the LAT terminal shown in Fig. 6. The maximum value for the sink current valid at a voltage equal to or higher than the latch protection threshold has been increased from 100 μ A to 500 μ A. This has expanded the selection range available for the adjustment resistor value R_{adj} to include a resistance value one-fifth that of conventional products.

In addition, we have expanded the terminal voltage range generating a sink current by improving the current-voltage characteristic. Together with the increase in the maximum current value described above, this allows a pickup current larger than that of conventional products to be set while ensuring a margin with reference to the rated voltage of the terminal even with a greatly varying VCC terminal voltage (see Fig. 7).

These characteristic improvements can do away with the need for ZD for terminal protection, leading to size and cost reduction for power supplies.

4. Effect of Application to Power Supplies

4.1 Labor saving in power supply design

As characteristics of the start-up device and LAT

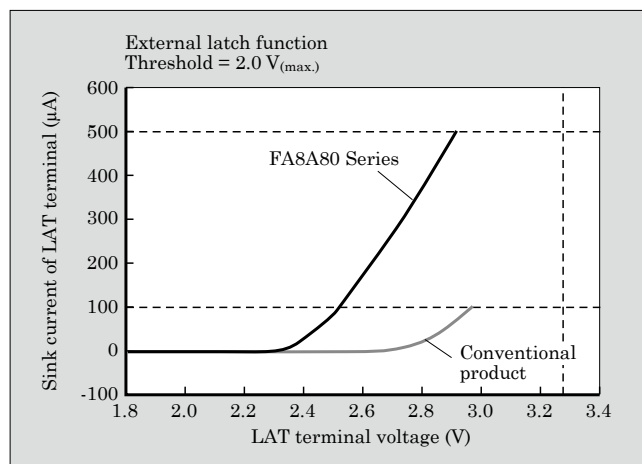


Fig.7 I-V characteristic of LAT terminal

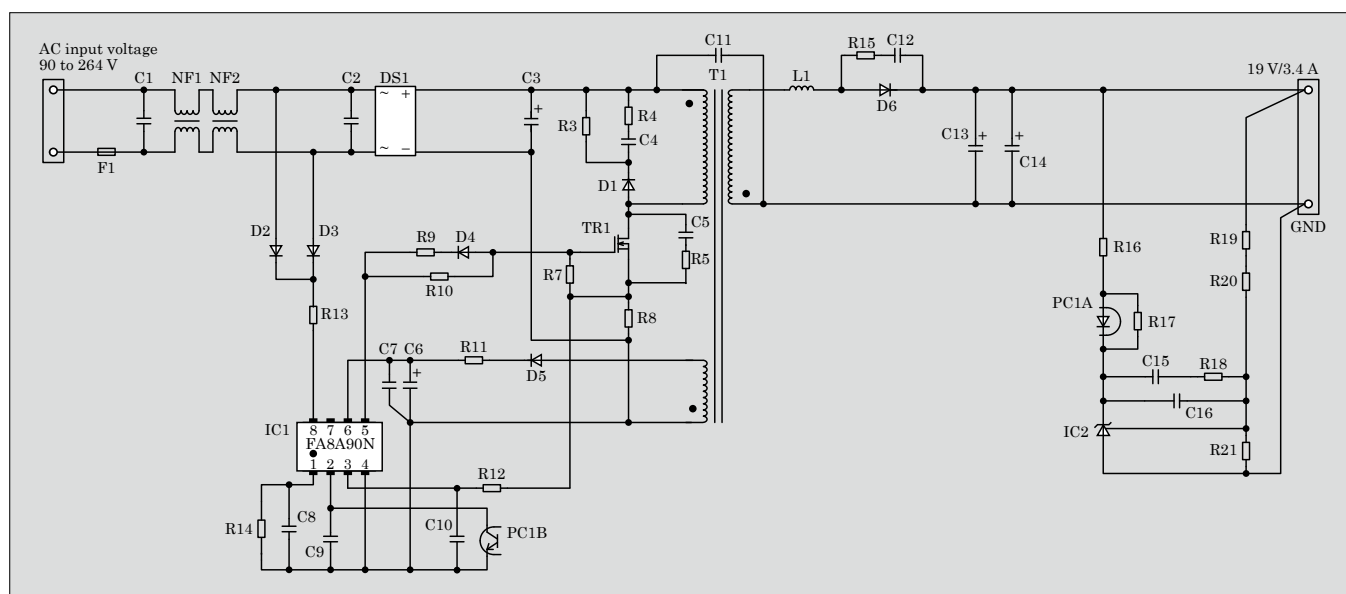


Fig.8 Circuit diagram of "FA8A80 Series" evaluation-use power supply board (19 V/3.4 A, 65 W)

terminal have been changed, we have revised the entire IC chip of conventional products. Meanwhile, we have employed the same terminal layout so that the device can be replaced with conventional products. We have designed the circuit and chip so that characteristics other than those changed are not affected.

We have used the evaluation-use power supply board as shown in Fig. 8 for comparative evaluation. We have confirmed there is a power supply performance equivalent to that of conventional products with the maximum efficiency at approximately 89% as shown in Fig. 9. We have also confirmed that the average efficiency among 4 load factors is 86% or higher with reference to the rated output current as shown in Table 2. The standby power during no-load operation shown in Fig. 10 is less than 30 mW. This characteristic has been confirmed to be equivalent to that of conventional products.

Based on these, it is simple to replace the device with conventional products and the labor for power supply design can be saved by utilizing the existing power supply design resources.

Figure 11 shows the line-up of the FA8A80 Series.

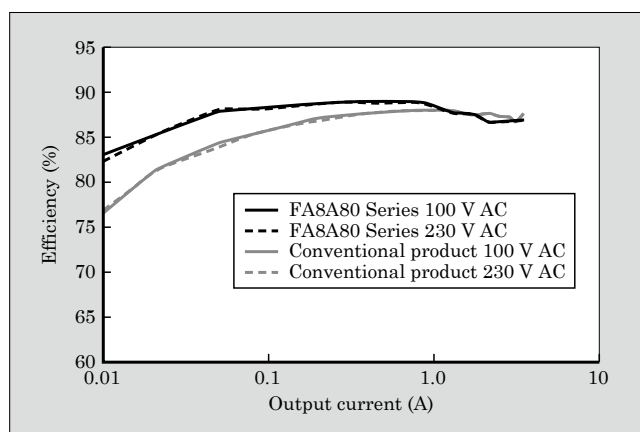


Fig.9 Power conversion efficiency

Table 2 Average efficiency of “FA8A80 Series”

Input voltage		100 V AC	230 V AC
Average efficiency (%)		87.50	87.51
Efficiency by load factor (%)	25%	88.76	88.01
	50%	87.59	87.44
	75%	86.69	86.97
	100%	86.95	87.63

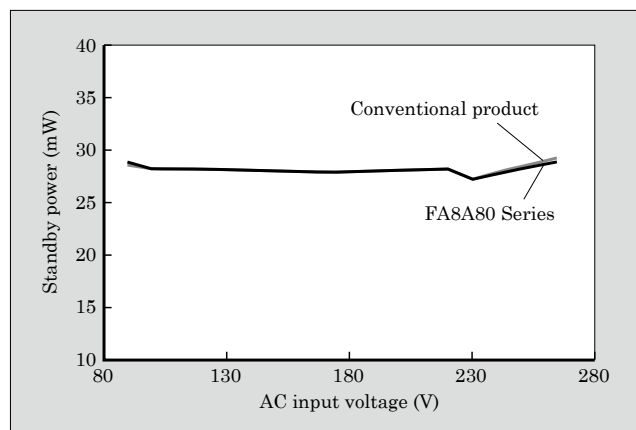


Fig.10 Standby power during no-load operation

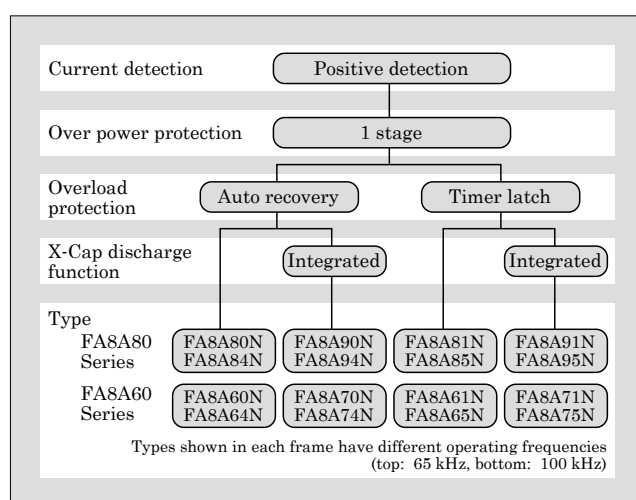


Fig.11 Product line-up of “FA8A80 Series”

Compatibility with conventional products is maintained by providing the same combinations of functions and operating frequencies.

5. Postscript

This paper has described the “FA8A80 Series” 650-V PWM power supply control IC. Current mode PWM control ICs increasingly need to have a greater input voltage range and improved safety while needing to integrate many functions for supporting various power supply specifications. In the future, we intend to continue to offer products that meet market needs.

“Super J MOS S2 Series” and “Super J MOS S2FD Series” for DFN 8 × 8 Packages

SHIMATO, Takayuki* WATANABE, Sota* MATSUMOTO, Kazunori*

ABSTRACT

Fuji Electric has launched the DFN 8 × 8 package line-up of the “Super J MOS S2 Series” and “Super J MOS S2FD Series” 2nd-generation low power loss SJ-MOSFETs having a super-junction structure. This surface mount package is smaller and thinner than the previous D2-PACK package. The DFN 8 × 8 package doesn’t have a lead terminal, but all electrode pads are arranged on its back surface. Compared with the D2-PACK, the mounting area has been reduced by 58% and the package height to 0.85 mm, thus making high-density mounting possible. It also comes equipped with a sub-source terminal for speeding up switching operations.

1. Introduction

Energy consumption has been increasing steadily due to an increase in the global population mainly in emerging countries, economic development in China and other countries, and a greater volume of information being processed as a result of today’s IT innovation. Along with the increased energy consumption, securing the space for power converters has become important, not to mention improving their efficiency. In data centers and other facilities, small, thin and high-output power supplies are required as communication power supplies used in those facilities so that the limited space is effectively used. Recently, various devices including digital consumer electronics, in addition to IT-related devices such as PCs and servers, have come to be connected with the Internet by the Internet of Things (IoT). Due to the addition of various communication functions, the space available for the power supply mounted in those devices has come to be limited.

These circumstances have created increasing demand for smaller and thinner power supplies to be mounted in various devices. To reduce the size and thickness of power supplies, the size and thickness of passive components such as transformers and capacitors and semiconductor switching elements must be reduced. An effective way of achieving this is to increase the frequency at which power supplies operate. For that reason, power metal-oxide-semiconductor field-effect transistors (MOSFETs) capable of high-frequency operation are often used for semiconductor switching elements. This has created a demand for power MOSFETs that can switch at higher speeds and offer lower loss than those of conventional products.

2. Product Line-Up and Major Characteristics

To improve the power dissipation of power MOSFETs, Fuji Electric has launched the “Super J MOS Series” of SJ-MOSFETs, which apply a superjunction structure. We have replaced the conventional planar MOSFETs with them. To meet the demand for smaller and thinner power supplies, Fuji Electric launched the new surface-mount dual flat nonlead (DFN) 8 × 8 package that is smaller and thinner than the conventional D2-PACK package. They are included in the latest series of “Super J MOS S2 Series” (S2 Series) and “Super J MOS S2FD Series” (S2FD Series), which has a parasitic diode faster than that of the S2 Series. Figure 1 shows the external appearance of the DFN 8 × 8 package and Table 1 the product line-up and major characteristics.⁽¹⁾⁻⁽⁷⁾

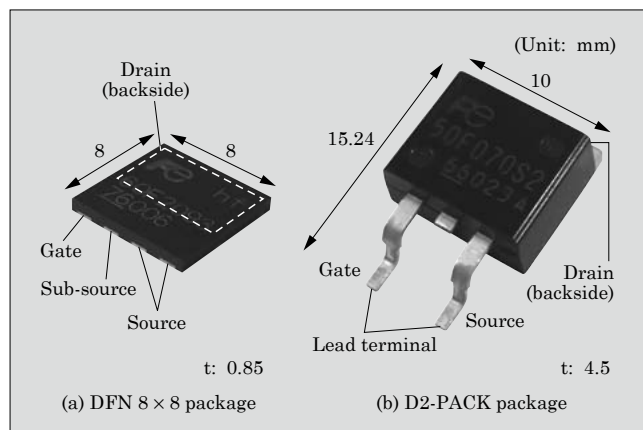


Fig.1 External appearance of package

* Electronic Devices Business Group, Fuji Electric Co., Ltd.

Table 1 Product line-up and major characteristics of DFN 8 × 8 package

Series name	Type	On-state resistance $r_{DS(on)(max.)}$ (mΩ)	Drain-source voltage V_{DS} (V)
Super J MOS S2 Series	FML60N091S2	91	600
	FML60N103S2	103	
	FML60N115S2	115	
	FML60N146S2	146	
	FML60N187S2	187	
	FML60N223S2	223	
Super J MOS S2FD Series	FML60N093S2FD	93	
	FML60N104S2FD	104	
	FML60N118S2FD	118	
	FML60N150S2FD	150	
	FML60N191S2FD	191	

3. Features

3.1 Compact and low height

Figure 2 shows external dimensions of the DFN 8 × 8 package. It is a square of 8 mm × 8 mm with a greatly reduced thickness of 0.85 mm. The structure with all electrode pads arranged on the back surface of the package does not have lead terminals. This allows higher-density mounting on a printed circuit board than packages with lead terminals such as D2-PACK. The electrode pad arrangement includes (1) gate, (2) sub-source, (3) (4) source and (5) drain and one feature is the provision of a sub-source terminal.

The following shows major indicators of the external appearances of the DFN 8 × 8 package as ratios to those of the D2-PACK package, which is a conventional and typical surface mount package:

- (a) Footprint: 58% smaller
- (b) Package height: 81% lower
- (c) Package volume (including lead terminals): 92% smaller

Table 2 shows on-state resistances per unit footprint and per unit mounting volume. DFN 8 × 8 package products have reduced the on-state resistances per

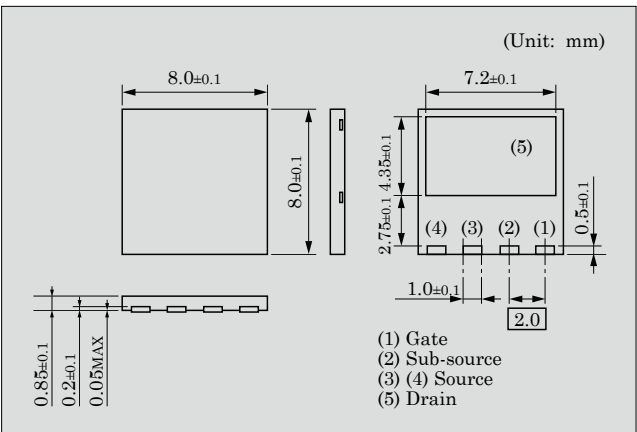


Fig.2 External dimensions of package

Table 2 On-state resistances per unit footprint and per unit mounting volume

Package	Applicable $r_{DS(on)(max.)}$	Per unit footprint $r_{DS(on)(max.)}$	Per unit mounting volume $r_{DS(on)(max.)}$
	Ω	Ω · mm ²	Ω · mm ³
DFN 8 × 8	0.090	5.8	4.90
D2-PACK	0.079	12.0	54.18
Ratio (DFN 8 × 8 / D2-PACK)	113.9%	47.8%	9.0%

unit footprint and per unit mounting volume by 52% and 91% respectively, compared with D2-PACK products. By reducing the package height to 0.85 mm, the package can be mounted on the back side of a double-sided board. This allows power supplies to be smaller and thinner and offer higher power density.

3.2 Low switching loss

Figure 3 shows the gate drive circuits of a DFN 8 × 8 package product and a typical 3-terminal package product, such as TO-220 or D2-PACK. A typical 3-terminal package product has a structure where inductance L_s such as lead inductance L_{s1} and source substrate wiring inductance L_{s2} inside the package is included in the gate drive circuit. Consequently, during MOSFET switching operation, a back electromotive force is generated on L_s by the time derivative of drain current di_D/dt and affects the gate drive voltage. This back electromotive force works to reduce the gate volt-

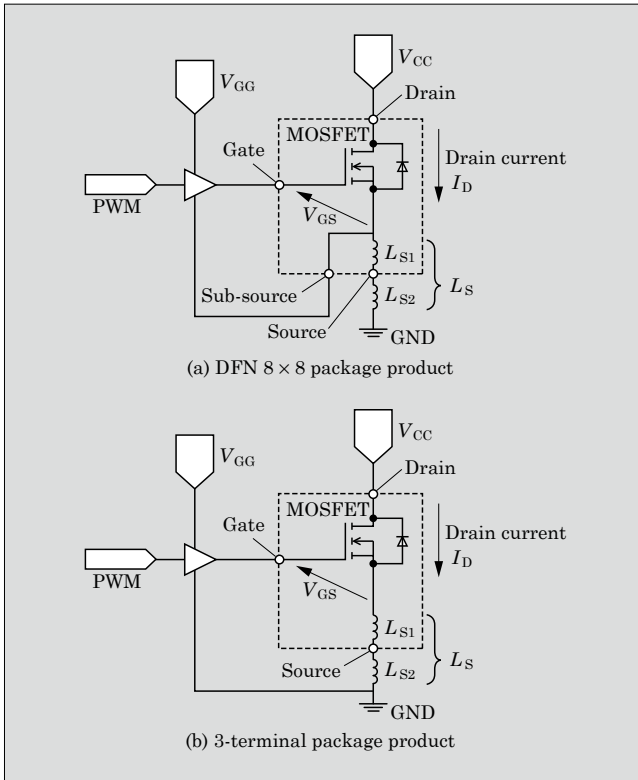


Fig.3 Drive circuits of DFN 8 × 8 package product and 3-terminal package product

age when the MOSFET is turned on, and to increase the gate voltage when the MOSFET is turned off. This causes a delay in the switching time and hinders any attempt to reduce the switching loss and achieve higher frequency.

On the other hand, a sub-source terminal is added to DFN 8 × 8 package products. This allows L_s to be separated from the gate drive circuit and the influence of the back electromotive force generated on L_s can be eliminated. As a result, shortening the switching time reduces the switching loss and achieves higher frequency.

Figure 4 shows a comparison of the gate resistance dependency of turn-on loss between a DFN 8 × 8 package product and a 3-terminal package product when used in a chopper circuit. Figure 5 shows the same with turn-off loss. For the measurement, we used “FML60N150S2FD” (600 V, 150 mΩ) as a DFN 8 × 8 package product and the TO-220 “FMP133S2FD” (600 V, 133 mΩ) as a 3-terminal package product. The measurement conditions were: $V_{CC} = 400$ V, $I_D = 20$ A and $V_{GG} = 10$ V.

The DFN 8 × 8 package product showed a great improvement in both turn-on loss and turn-off loss in the entire range of 0 to 25 Ω of the external gate resistance. When the external gate resistance is 10 Ω, turn-

on loss is reduced by 75% and turn-off loss is reduced by 35%.

4. Effect of Application

For verifying the effect of application of DFN 8 × 8 package products, we used a DFN 8 × 8 package product and TO-220 as a typical 3-terminal package product in a power factor correction (PFC) circuit as shown in Fig. 6 to compare the power supply performance. As the control IC of the PFC circuit, we used “FA5612,” Fuji Electric’s continuous current mode PFC control IC. As the input and output conditions and circuit constant, we set the input voltage at 100 V/50 Hz, output voltage at 390 V DC and MOSFET gate resistance R_G at 22 Ω. For the evaluation, we used “FML60N223S2” (600 V/223 mΩ) as a DFN 8 × 8 package product and the TO-220 “FMP60N190S2” (600 V/190 mΩ).

Figure 7 shows the load dependency of power supply efficiency. The DFN 8 × 8 package product shows a better efficiency compared with TO-220 in the range with a load factor of 50% or higher. In terms of efficiency with 100% load, the result shows an efficiency improvement of 0.2 points.

Figure 8 shows a comparison of switching loss under conditions where the maximum current flows in the MOSFET with 100% load. Both the turn-on loss and turn-off loss are smaller with the DFN 8 × 8 package product and the total switching loss has been reduced by 30%. In this way, power loss has been re-

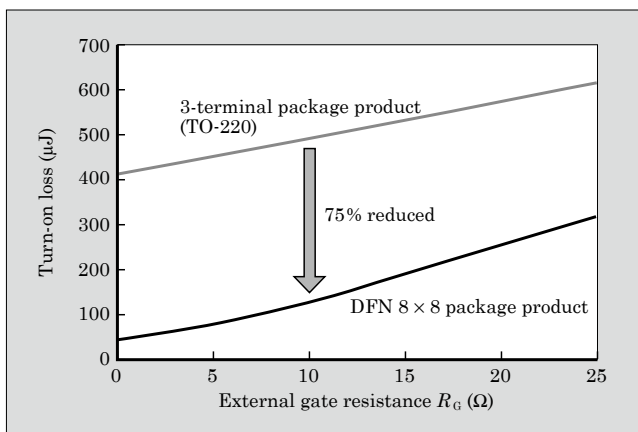


Fig.4 Comparison of turn-on loss

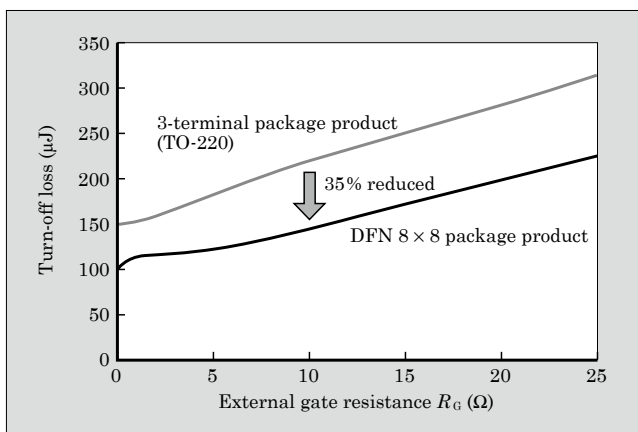


Fig.5 Comparison of turn-off loss

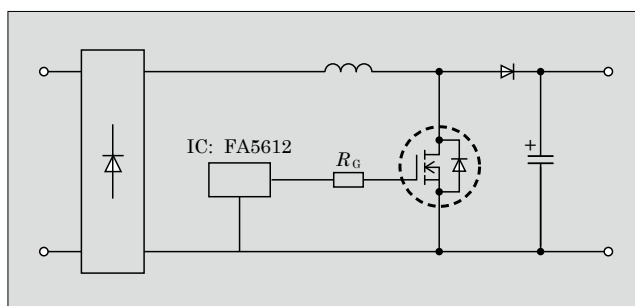


Fig.6 Circuit diagram of PFC demonstration board

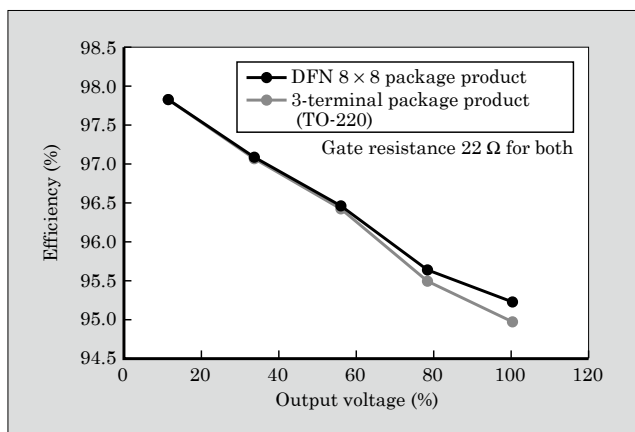


Fig.7 Efficiency characteristic of power supply

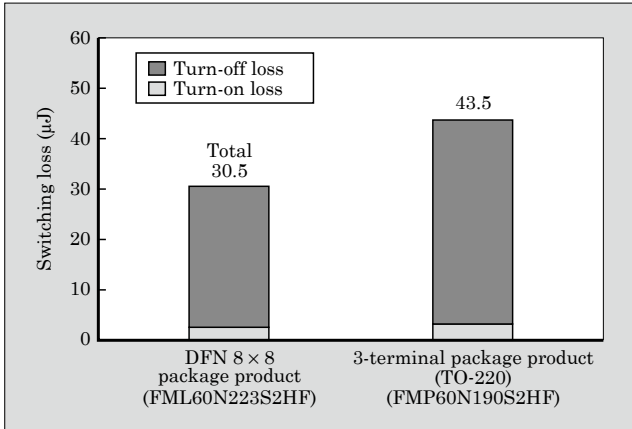


Fig.8 Switching loss comparison

duced and efficiency improved.

Figures 9 and 10 show turn-on and turn-off waveforms respectively under conditions where the maximum current flows in the MOSFET with 100% load. The solid lines show waveforms for the DFN 8 × 8 package product and the broken lines waveforms for

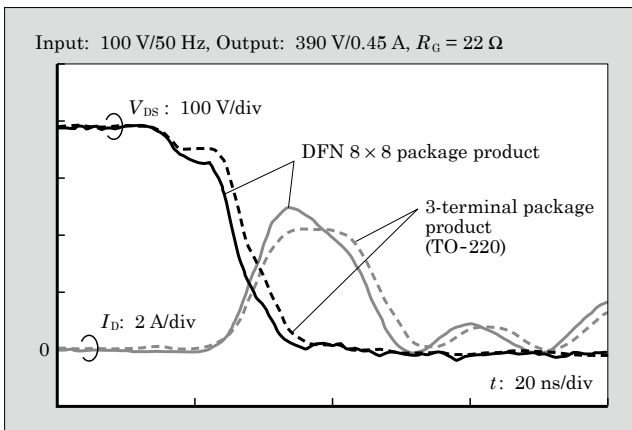


Fig.9 Turn-on waveforms

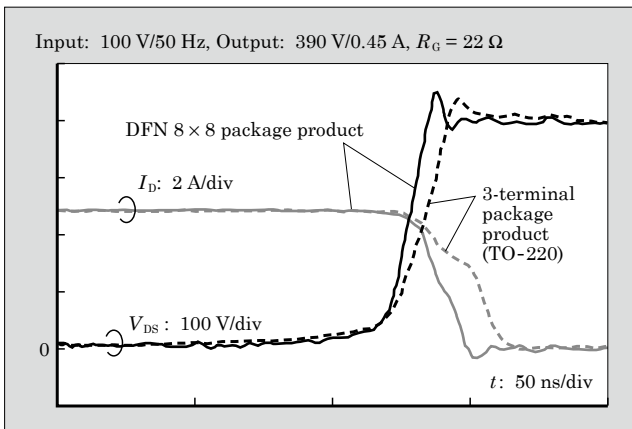


Fig.10 Turn-off waveforms

TO-220. The switching speed is faster with the DFN 8 × 8 package product for both turn-on and turn-off. The period of crossover of drain voltage V_{DS} waveform and drain current I_D waveform at the time of switching is shorter, which indicates a smaller switching loss. This is an effect of separating L_s from the gate drive circuit by using the sub-source terminal as shown in Fig. 3.

This leads to the conclusion that DFN 8 × 8 package products contribute to high-speed switching operation and improved power supply efficiency.

5. Postscript

This paper has presented a line-up of DFN 8 × 8 packages integrating the “Super J MOS S2 Series” and “Super J MOS S2FD Series,” which achieve both low on-state resistance and low switching loss. The product line-up is capable of high-speed switching operation by utilizing the package effect in addition to having characteristics of low on-state resistance and low switching loss. This allows higher-frequency operation of power supplies than with conventional package products and raises expectations for contributions to size reduction and power density increase for power supplies.

In the future, to keep up with changes in market needs, we intend to continue to work on providing comprehensive solutions in ways such as expanding the package line-up in addition to improving the $r_{DS(on)}$ performance and providing a wider drain-source voltage selection of power MOSFETs.

References

- (1) Tamura, T. et al. “Super J-MOS” Low Power Loss Superjunction MOSFETs. FUJI ELECTRIC REVIEW. 2012, vol.58, no.2, p.79-82.
- (2) Tamura, T. et al. “Reduction of Turn-off Loss in 600 V-class Superjunction MOSFET by Surface Design”. PCIM Asia 2011, p.102-107.
- (3) Watanabe, S. et al. “A Low Switching Loss Superjunction MOSFET “Super J-MOS” by Optimizing Surface Design” PCIM Asia 2012, p.160-165.
- (4) Oonishi, Y. et al. Superjunction MOSFET. FUJI ELECTRIC REVIEW. 2010, vol.56, no.2, p.65-68.
- (5) Watanabe, S. et al. 2nd-Generation Low-Loss SJ-MOSFET “Super J MOS S2 Series”. FUJI ELECTRIC REVIEW. 2015, vol.61, no.4, p.276-279.
- (6) Watanabe, S. et al. 2nd-Generation Low-Loss SJ-MOSFET “Super J MOS S2 Series”. FUJI ELECTRIC REVIEW. 2016, vol.61, no.4, p.276-279.
- (7) Sakata, T. et al. “A Low-Switching Noise and High-Efficiency Superjunction MOSFET, Super J MOS® S2”. PCIM Asia 2015, p.419-426.

“PrimePACK™” of 7th-Generation “X Series” 1,700-V IGBT Modules

YAMAMOTO, Takuya* YOSHIWATARI, Shinichi* OKAMOTO, Yujin*

In recent years, reduction of CO₂ emission is as worldwide trend to prevent global warming. Therefore, renewable energy such as photovoltaic power generation and wind power generation has been introduced rapidly. In such application field, power conversion system is utilized and its capacity is increasing. Demand for high power insulated gate bipolar transistor (IGBT) modules has been also expanding.

Downsizing, lower power dissipation and higher reliability have been increasingly required for these power conversion system. In order to satisfy these requirement, Fuji Electric has developed the “X Series PrimePACK™*1” as additional line-up to the 7th-generation “X Series” IGBT module family.

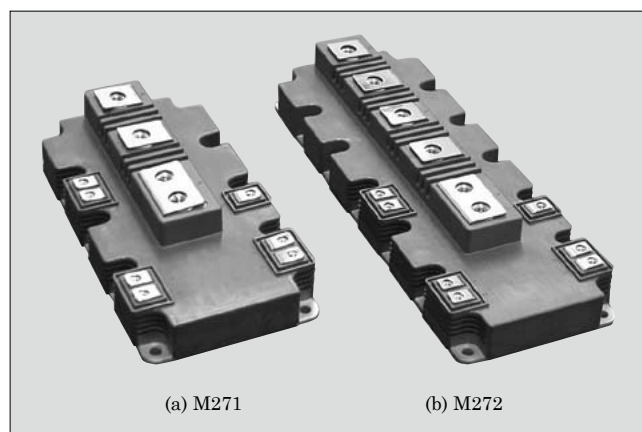


Fig.1 X Series PrimePACK™

Table 1 X Series PrimePACK™ family

Package	Rating		Type	Insulating substrate	Insulation withstand voltage	CTI*	T _{jop}
	Voltage	Current					
M271	1,200 V	900 A	2MBI900XXA120P-50	Al ₂ O ₃	4.0 kV AC	>600	175 °C
		1,200 A	2MBI1200XXE120P-50	AlN			
	1,700 V	900 A	2MBI900XXA170-50	Al ₂ O ₃			
		1,200 A	2MBI1200XXE170-50	AlN			
M272	1,200 V	1,400 A	2MBI1400XXB120P-50	Al ₂ O ₃			
		1,800 A	2MBI1800XXF120P-50	AlN			
	1,700 V	1,000 A	2MBI1000XXB170-50	Al ₂ O ₃			
		1,400 A	2MBI1400XXB170-50	Al ₂ O ₃			
		1,800 A	2MBI1800XXF170-50	AlN			

*Comparative tracking index

* Electronic Devices Business Group, Fuji Electric Co., Ltd.

1. Features

Figure 1 shows the external appearance of the X Series PrimePACK™, and Table 1 shows the product family. The package has 2 types, M271 and M272, which are featured by the following 3 points:

- (1) Upgrading maximum rating current from 1,400 A to 1,800 A
- (2) Expands continuous operating junction temperature T_{jop}
- (3) Higher cooling performance by newly developed high thermal conductivity insulating substrate

2. Electrical Characteristics

The X Series PrimePACK™ enables significant reduction of power dissipation compared with the conventional product by adopting X series chip technologies. Figures 2 and 3 show a comparison of the on-state voltage and switching energy trade-off characteristics for the IGBT and freewheeling diode (FWD).

The X series IGBT utilize newly developed fine cell technology and thinner wafer technologies. As a result, characteristics of the X Series are improved about 0.7 V of saturation voltage and about 11% of turn-off energy compared with conventional product. Forward voltage of the X series FWD has been improved about 0.15 V by thinner drift layer, as well as the X Series IGBT chip. Furthermore, softer reverse recovery has been realized by optimization of lifetime control, and reverse recovery energy has been also improved by

*1: PrimePACK™ is a trademark or registered trade mark of Infineon Technologies AG.

about 16%.

Figure 4 shows calculation results for power dissipation. At carrier frequency of 1 kHz, power dissipa-

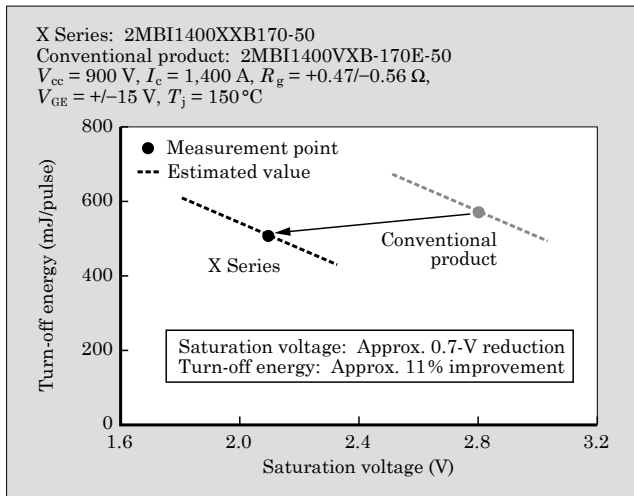


Fig.2 Trade-off characteristics (IGBT)

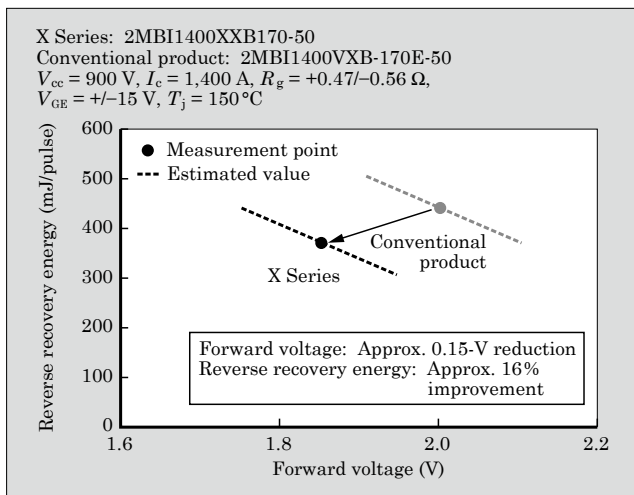


Fig.3 Trade-off characteristics (FWD)

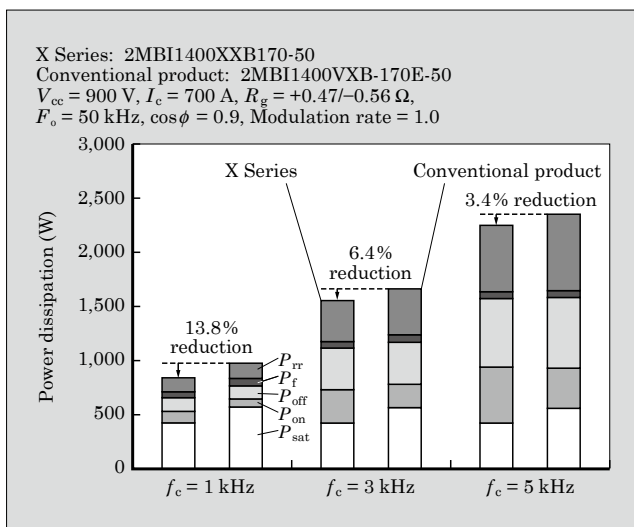


Fig.4 Power dissipation

tion of the X Series PrimePACK™ has been improved by about 13.8% compared with the conventional product.

3. Packaging Technology

The X Series products are designed to increase output current in order to downsize power conversion systems. To achieve this target, the continuous operating junction temperature T_{vjop} was expanded from the previous temperature of 150°C to 175°C . Furthermore, junction-to-case thermal resistance was also improved by newly developed higher thermal conductive insulating substrate.

To expand T_{vjop} , it is necessary to improve capability for repetitive thermal stress (ΔT_{vj} power cycle capability), and degradation of long-term reliability at high temperatures operating. The ΔT_{vj} power cycle capability of conventional product is degraded in higher $T_{vjmax} = 175^\circ\text{C}$ compared with 150°C . To improve the degradation, the X Series utilizes a newly developed solder material and new wire bonding technology for the semiconductor chip. As the results, ΔT_{vj} power cycle capability has been improved to twice of conventional products under conditions of $T_{vjmax} = 175^\circ\text{C}$, $\Delta T_{vj} = 50^\circ\text{C}$. In addition, new silicone gel for the X series has been developed to have enough life time against high temperature operation such as 175°C . The life time is almost same as conventional one in 150°C .

Moreover, the highest current rating product of the X Series PrimePACK™ utilizes newly developed a high thermal conductive insulating aluminum nitride (AlN) substrate for efficient heat irradiation from semiconductor chip. As a result, the thermal resistance of junction-to-case has been improved by about 45% compared with the conventional alumina (Al_2O_3) substrate at the same chip size.

Figure 5 shows the calculation result of the relationship between inverter output current and IGBT

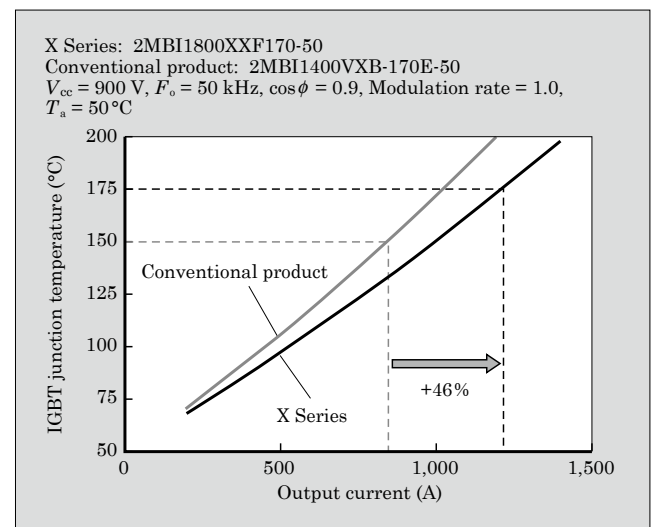


Fig.5 Inverter output current and IGBT junction temperature

junction temperature. Output current has been improved by about 46% for the X Series PrimePACK™ compared with conventional products as a result of greatly enhanced T_{vj} and heat irradiation performance mentioned above. Fuji Electric believes that this product can contribute to achieving a safe and secure sustainable society by enabling the size reduction, lower power dissipation and higher reliability of power conversion systems.

Launch time

Starting in April 2018

Product Inquiries

Industrial Power Semiconductor Module Department,
Business Planning Division, Electronic Devices
Business Group, Fuji Electric Co., Ltd.

Tel: +81 (263) 27-2943



I-Type “PrimePACK™” of 3-Level IGBT Modules

YAMAMOTO, Sayaka*

In recent years, renewable energies have been gathering attention and the markets for photovoltaic and wind power generation have been growing. Developments are continuously being made to meet the high-voltage and large-capacity needs of this field. In addition to improvements in power generation efficiency, improvements in power conversion efficiency are greatly expected.

Fuji Electric has been mass producing insulated gate bipolar transistor (IGBT) modules that integrate a T-type 3-level power conversion circuit on a single-package by utilizing our uniquely developed reverse blocking IGBTs (RB-IGBTs) for the neutral point switch. Furthermore, we have also developed a highly versatile 3-level large-capacity module that utilizes the “PrimePACK™”^{*1} large-capacity package to satisfy large-capacity needs. The module has been highly evaluated by the market.

This time, we have developed the I-type PrimePACK™ of 3-level IGBT module that supports a DC power supply voltage of 1,500 V to meet the higher voltage of photovoltaic power generation.

In this paper, the features and electrical characteristics of this product are described.

1. Features and Electrical Characteristics of Package

Figure 1 shows the external appearance of the “M404 package” used with this product, and Figure 2, the outline drawing.

- (1) Completion of a package capable of large-capacity parallel connections



Fig.1 External appearance of “M404 package”

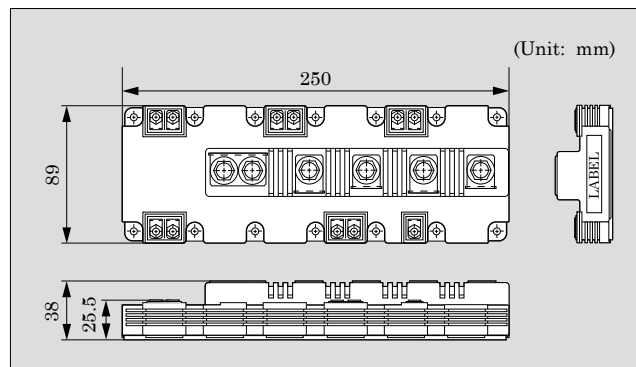


Fig.2 Outline drawing of “M404 package”

The I-type PrimePACK™ uses the same M404 package as the T-type PrimePACK™. Therefore, these packages are easily interchangeable due to the compatible terminals. Furthermore, the IGBT module that uses the M404 package has the following features:

- (a) Internal inductance is small on account of the laminate structure of the main terminal bus bar inside the module.
 - (b) Equipment size reduction is now possible as a result of the space savings achieved through the small footprint of the module and compact cooling fins.
 - (c) The package uses a terminal configuration suitable for parallel connections, thus making it easy to use for even larger capacity applications.
 - (d) It comes equipped with a built-in thermistor for temperature detection.
- (2) I-type power conversion system

Figure 3 shows the equivalent circuits for the I-type and T-type 3-level IGBT modules which are used for power conversion systems. The I-type employs a serial connection for its switching elements, and it thus can be used for equipment with higher voltage than the T-type does.

- (3) Total generated loss and main specifications

Figure 4 shows the total power loss for 2-level and 3-level power conversion systems, and Table 1 shows the main specifications of the I-type PrimePACK™. Efficiency is higher for 3-level system than 2-level system by 0.4%. The T-type circuit uses RB-IGBTs for the AC switching component, allowing it to reduce more loss than the I-type circuit. The I-type circuit however

* Electronic Devices Business Group, Fuji Electric Co., Ltd.

^{*1}: PrimePACK™ is a trademark or registered trade mark of Infineon Technologies AG.

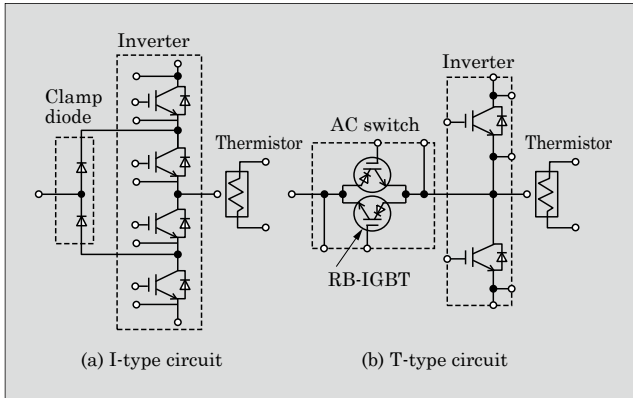


Fig.3 Equivalent circuits for 3-level IGBT module

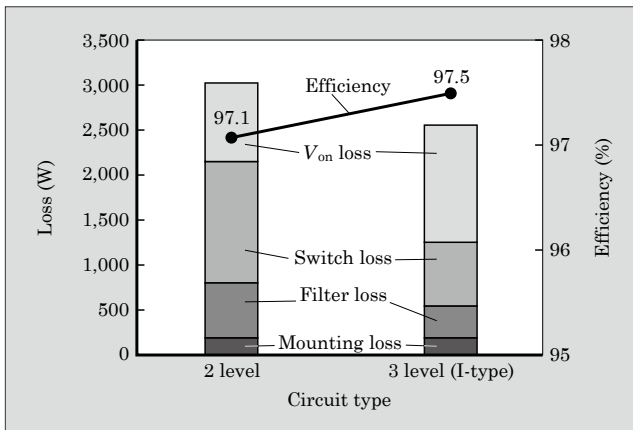


Fig.4 Comparison of total power loss

Table 1 Main specifications of I-type PrimePACK™

Item		Specification
Package type		I-type PrimePACK™
Type		4MBI600VC -120-50 4MBI600VC -120-60
Package dimensions		L250 × W89 × H38 (mm)
Inverter	V_{CES}	1,200 V
	I_c (IGBT)	600 A
	$-I_c$ (FWD)	600 A
	V_{GES}	±20 V
	T_j	175 °C
	T_{jop}	150 °C
	$V_{GE(th)}$ (chip) $V_{GE} = 20$ V	6.0 to 7.0 V ($I_c = 600$ mA)
	$V_{CE(sat)}$ (chip) $V_{GE} = 15$ V $T_j = 25$ °C	typ. 1.85 V ($I_c = 600$ A)
	V_F (chip) $T_j = 25$ °C	typ. 1.70 V ($I_F = 600$ A)
	$R_{th(j-c)}$ IGBT	max. 0.061 °C/W
Clamp diode	$R_{th(j-c)}$ FWD	max. 0.092 °C/W
	V_{iso}	4,000 V AC (AC: 1 min)
Characteristic data display		No Yes

is more suitable for high voltage applications. By creating a 3-level module series that includes the I-type and T-type, flexible support can be done for the various products of users.

2. Characteristics Data Indication

Additionally, products having static characteristic indication on module package are line upped to respond to users' requests. Figure 5 shows the layout and external appearance for the characteristics data indication. This provides users with the following advantages:

- Pairing can now be implemented in-house.
- Individual module data can be checked in-house, thus facilitating replacement maintenance.
- Unfilled pair of modules will not be remained because lot specific pairing is no longer necessary.

These features allow users to flexibly implement the parallel connections of the modules without remaining unfilled pairs and facilitate pairing selection and inventory control.

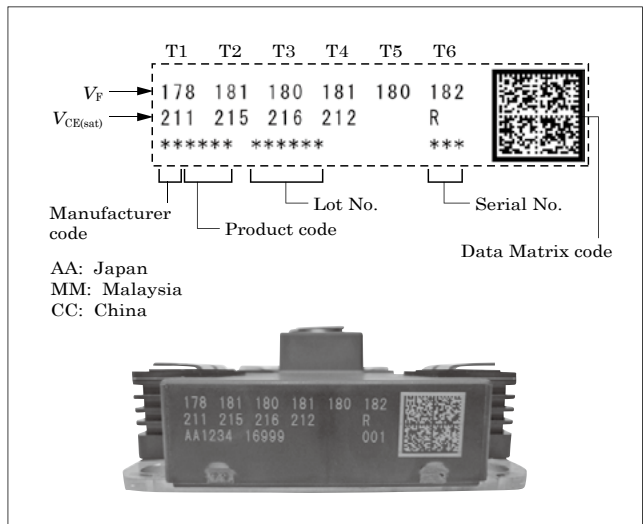


Fig.5 Layout and external appearance of characteristics data indication

Launch time

January 2018

Product Inquiries

Industrial Power Semiconductor Module Department,
Business Planning Division, Electronic Devices
Business Group, Fuji Electric Co., Ltd.
Tel: +81 (263) 27-6958

~~~~~

# “SUPER ECO MOLTRA II” Cast Resin Transformer Achieving Super High Efficiency

MIYATA, Tomokazu\*

A new requirement appeared in FY2014 to replace high-voltage distribution transformers with ones offering significantly better energy saving performance compared with the existing models. This was based on the secondary criteria for Top Runner transformers (Top Runner transformers 2014) under the “Act on the Rational Use of Energy” (Energy Saving Act). In addition, taking the opportunity of the Olympic and Paralympic Games Tokyo 2020, many enterprises are conducting activities to improve environmental friendliness. Further, there is increasing demand for products with a better energy saving performance than that of Top Runner transformers 2014. These things show that the energy saving performance of transformers has entered the next stage.

In 2014, Fuji Electric released the “Top Runner MOLTRA 2014” as a product that satisfies the requirements for Top Runner transformers 2014. In 2015, we adopted an amorphous alloy and released the “Amorphous MOLTRA” with the maximum conversion efficiency improved to significantly reduce the no-load loss, which is referred to as standby power. Furthermore, the “SUPER ECO MOLTRA II,” released in June 2017, has realized an achievement rate of 130% with reference to the standard energy consumption efficiency of Top Runner transformers 2014 with the same footprint as that of Top Runner MOLTRA 2014 (see Fig. 1). This paper presents the features of the SUPER



Fig.1 SUPER ECO MOLTRA II

ECO MOLTRA II and the effect of introducing it.

## 1. Overview of SUPER ECO MOLTRA II

Figure 2 shows efficiency curves of the SUPER ECO MOLTRA II and other transformers.

### 1.1 Features

- (a) Achieved 130% of the standard energy consumption efficiency of Top Runner transformers 2014 in the average of all capacity models.
- (b) Efficiency significantly improved from that of the Top Runner MOLTRA 2014 over the entire load factor range.
- (c) A footprint equivalent to that of the Top Runner MOLTRA 2014 achieved.
- (d) Vacuum casting employed for all capacity mod-

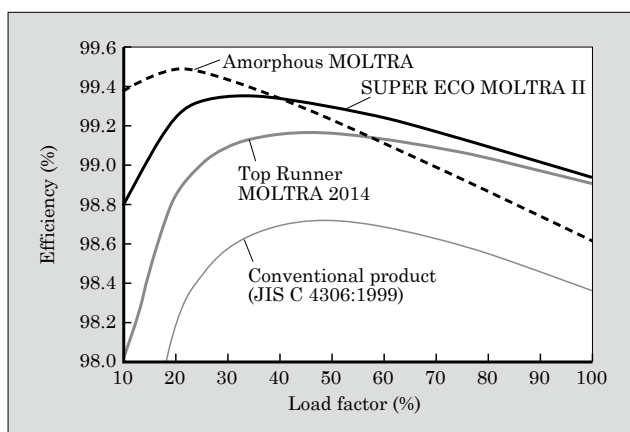


Fig.2 Efficiency curves of various transformers (3-phase 300 kVA)

Table 1 Specifications of SUPER ECO MOLTRA II

| Item                          | Specification                                                               |                             |
|-------------------------------|-----------------------------------------------------------------------------|-----------------------------|
| Number of phases              | Single-phase                                                                | 3-phase                     |
| Frequency (Hz)                | 50/60                                                                       |                             |
| Rated capacity (kVA)          | 50, 75, 100, 150, 200, 300                                                  | 75, 100, 150, 200, 300, 500 |
| Primary voltage (V)           | R6600-F6300-6000 (single-phase 50 kVA only)<br>F6750-R6600-F6450-F6300-6150 |                             |
| Secondary voltage (V)         | 210-105                                                                     | 210, 420, 440               |
| Insulation system temperature | F                                                                           |                             |

\* Power Electronics Systems Business Group, Fuji Electric Co., Ltd.

els to achieve molded windings with high insulation reliability.

- (e) High incombustibility achieved and acquired type test certificate for IEC 60076-11.
- (f) High seismic resistance in compliance with JEM-TR252 achieved.

## 1.2 Specifications

Table 1 shows the specifications of the SUPER ECO MOLTRA II.

## 2. Background Technology

The total loss of a transformer is represented by the sum of a certain no-load loss that does not depend on the load factor and a value resulting from multiplying the load loss by the square of the load factor (see Equation 1). Energy consumption efficiency is represented by the total loss at the reference load factor.

$$\text{Total loss (W)} = \text{No-load loss (W)} + \left[ \frac{m}{100} \right]^2 \times \text{Load loss (W)} \cdots \cdots (1)$$

$m$  : Reference load factor (%)

Transformers with a capacity of 500 kVA or smaller: 40%

Transformers with a capacity of over 500 kVA: 50%

To improve energy consumption efficiency, the no-load loss has been reduced with the Amorphous MOLTRA. With the SUPER ECO MOLTRA II, both the no-load loss and load loss have been reduced so as to improve the efficiency over the entire load factor range.

### 2.1 Technology for reducing no-load loss

We have employed a high magnetic flux density steel strip of sheet metal provided with magnetic domain control as the iron core material. In addition, we have optimized the design magnetic flux density to reduce the no-load loss and miniaturize the iron core.

### 2.2 Technology for reducing load loss

The conventional MOLTRA used aluminum for the conductor of the windings. With the SUPER ECO MOLTRA II, we have employed copper, which is characterized by its high electric conductivity, and optimized the cross-section area of the winding conductor to reduce the load loss and miniaturize the windings.

## 3. Effect of Introducing SUPER ECO MOLTRA II

### 3.1 Selection of transformers

As shown in Fig. 2, the SUPER ECO MOLTRA II features higher efficiency than the Top Runner MOLTRA 2014 over the entire load factor range. In particular, it has excellent efficiency in the high load factor range and high energy saving performance is

brought out in data centers and water treatment facilities which have a high average load factor per day. Meanwhile, the Amorphous MOLTRA shows especially high efficiency in the low load factor range, decreasing power usage in the nighttime, and exhibits high energy saving performance in buildings and hospitals which have a low average load factor per day. However, efficiency decreases as the load factor increases, and care is needed here. Accordingly, it is important to select a transformer suitable for the actual condition of the load so as to produce the energy saving effect expected.

### 3.2 Effect of introduction

Figure 3 shows the effect of replacing a conven-

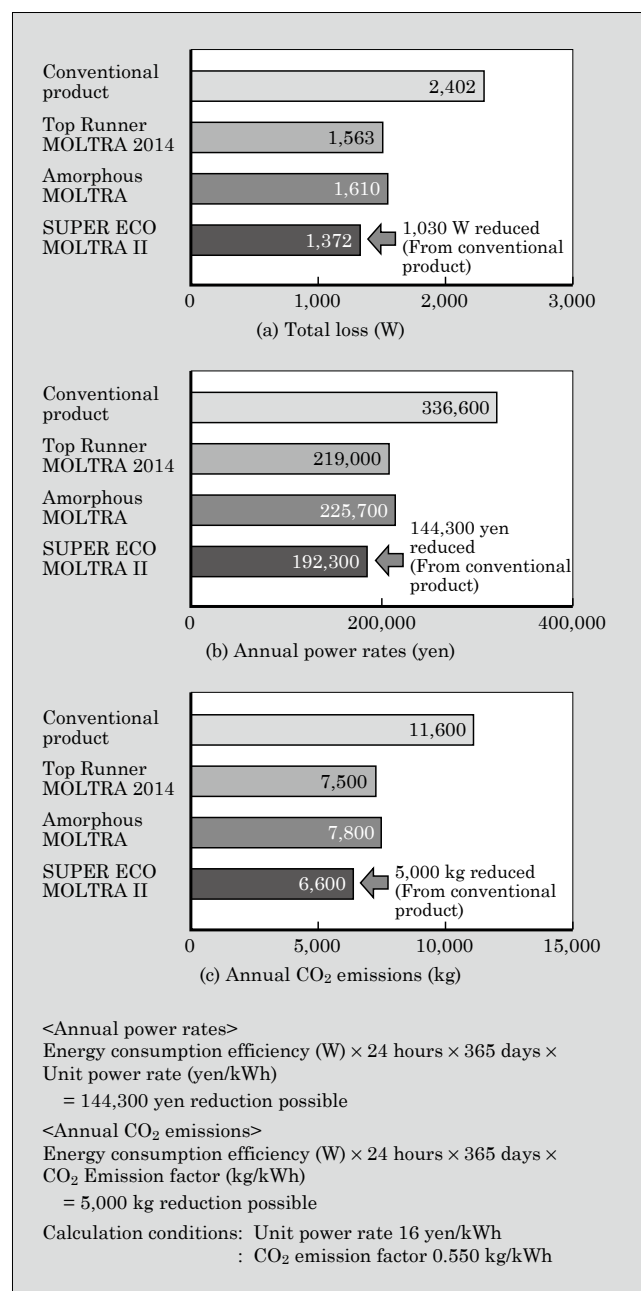


Fig.3 Effect of introducing SUPER ECO MOLTRA II (three-phase 300 kVA, load factor 60%)

tional transformer with the SUPER ECO MOLTRA II. Under the conditions of three-phase 300 kVA and a load factor of 60%, the annual power rates can be reduced by 144,300 yen and CO<sub>2</sub> emissions by 5,000 kg as compared with a conventional transformer.

Power usage for each time period varies. Hence,

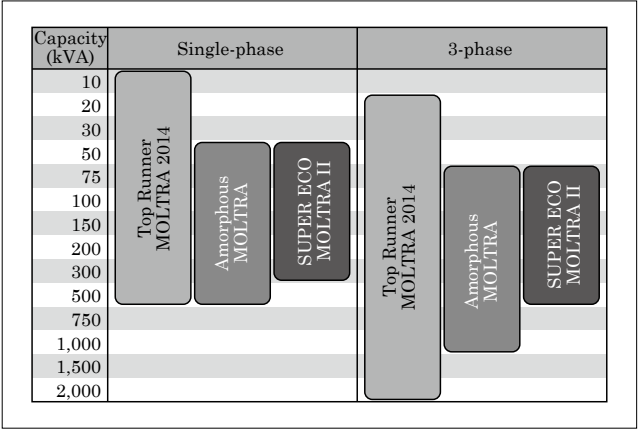


Fig.4 Products conforming to Top Runner transformers 2014

it is preferable to select the optimum transformer that can reduce operation costs by taking into account the time-of-day power rates offered by utility companies so that energy can be saved.

Fuji Electric offers a line-up of products conforming to the energy saving standards of Top Runner transformers 2014 including the SUPER ECO MOLTRA II and the Amorphous MOLTRA as shown in Fig. 4. These allow users to select the optimum transformers.

**Launch time**  
June 2017

**Product Inquiries**  
Facilities Electrical Machinery Engineering  
Department, Transmission & Distribution Systems  
Division, Power Electronics Systems Business  
Group, Fuji Electric Co., Ltd.  
Tel: +81 (3) 5435-7089

# 6.5th-Generation Automotive Pressure Sensors

NISHIKAWA, Mutsuo\*

Currently, there is a strong requirement for automobiles to have a reduced environmental impact as seen in the imposition of air pollutant and CO<sub>2</sub> emission regulations, in addition to having improved safety and comfort. In order to meet these regulations, fuel efficiency is being improved by precisely controlling the air-to-fuel ratio. Further, technology to make exhaust gas cleaner by recirculating the gas after combustion is becoming widespread at an increasing speed. In addition, engine rooms are being made smaller and mounting density increased. The aim is to increase the cabin space so that there is greater fuel efficiency and comfort.

This has caused temperatures to rise in the operating environment of automotive pressure sensors. Moreover, the requirement of having electromagnetic compatibility (EMC) against electromagnetic noise generated from various electronic devices is becoming increasingly rigorous. Furthermore, the scope of application of pressure sensors, which was mostly to measure air in the past, is expanding to a variety of difficult media (targets) to be measured. These include those containing exhaust gas and vaporized fuel such as gasoline and diesel oil.

To meet these requirements, Fuji Electric has developed the higher performance 6.5th-generation automotive pressure sensor based on the 6th-generation pressure sensor<sup>(1)</sup> with digital trimming that started mass production in 2010.

## 1. Features

Figure 1 shows the appearance of the cells of the 6.5th-generation pressure sensor and the previous 6th-generation pressure sensor. Table 1 shows the specifications of the 6.5th-generation pressure sensor. This product uses the conventional technology of integrating the pressure sensing unit and signal processing unit into one chip. It also provides corrosion resistance and resistance to electrostatic charging to raise the maximum guaranteed operating temperature from 125°C of the conventional product to 150°C. To detect failures, a clamp function has been added for separating the wire harness disconnection detection domain (diagnostic voltage domain) from the normal use domain. The size of the sensor cell has been reduced to approximately 48% of that of the 6th-generation pres-

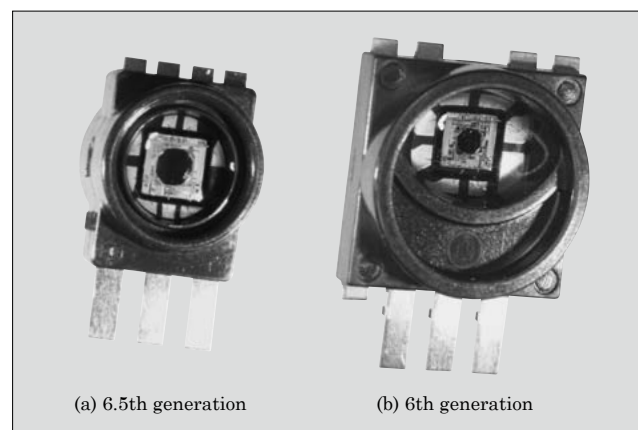


Fig.1 Automotive pressure sensor

Table 1 Specifications of 6.5th-generation pressure sensor

| Item                                              | Specification                                                         |
|---------------------------------------------------|-----------------------------------------------------------------------|
| Product size (resin part)                         | W7.5 × H10 × D5.6 (mm)                                                |
| Operating temperature range                       | −40 °C to +150 °C                                                     |
| Operating pressure range (intake pressure sensor) | 20 to 120 kPa                                                         |
| Rated pressure                                    | Pressure range × 3                                                    |
| Power supply voltage                              | 5 ± 0.25 V                                                            |
| Output voltage (at power supply voltage of 5 V)   | 0.5 to 4.5 V                                                          |
| Sink and source capacities                        | Sink: 1 mA, source: 0.1 mA                                            |
| Clamp function                                    | Clamp voltage 0.3 V/4.7 V (typ.)                                      |
| Corrosion resistance                              | In accordance with JASO M 611-92/B Method (Gasoline/diesel component) |
| ESD (external interface terminals)                |                                                                       |
| MM (0 Ω, 200 pF)                                  | ±1 kV or more                                                         |
| HBM (1.5 Ω, 100 pF)                               | ±8 kV or more                                                         |
| Transient voltage surge                           | ISO 7637 (2011) standard Pulse 1, 2, 3a, 3b LEVEL-III cleared         |
| Impulse                                           | ±1 kV or more                                                         |
| Latch-up (current injection method)               | ±500 mA or more                                                       |
| EMS (G-TEM) (100 V/m)                             | Variation: 1% FS or less                                              |
| Overvoltage (between Vcc and GND)                 | 16.5 V (max.)                                                         |
| Reverse connection (between Vcc and GND)          | 0.3 A (max.)                                                          |

sure sensor in terms of the volume.

\* Electronic Devices Business Group, Fuji Electric Co., Ltd.



2. Background Technology

2.1 Corrosion resistance

Figure 2 shows the cross-section structure of the sensor cell of a pressure sensor. The sensor chip and wire are protected against incoming foreign objects such as soot by using gelled protection material capable of transmitting pressure. With this product, there is a need to prevent exhaust gas and vaporized fuel such as gasoline and diesel oil from passing through the protection material since they would corrode the wire bonding pad on the chip surface. Therefore, corrosion prevention areas have been provided on the bonding pad and test pad as shown in Fig. 3.

2.2 Resistance to electrostatic charging

Figure 4 outlines the pressure sensing unit integrated in the pressure sensor. Fuji Electric’s proprietary etching technology is used to process part of the silicon into a thin film to form a diaphragm. The 4 piezoresistors composed of the diffusion wiring provided on the diaphragm constitute a Wheatstone bridge. When the diaphragm is deformed by the pressure applied, the respective piezoresistance values

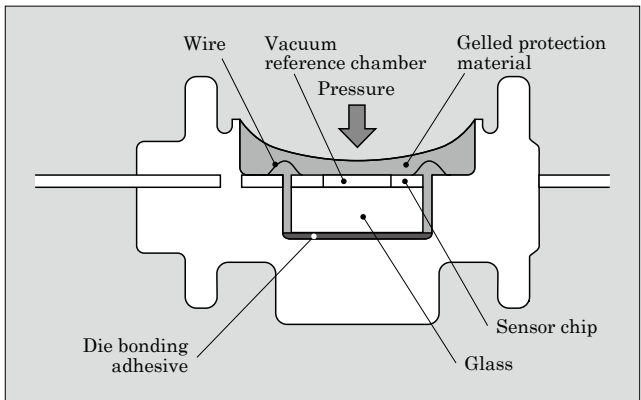


Fig.2 Cross-section structure of sensor cell

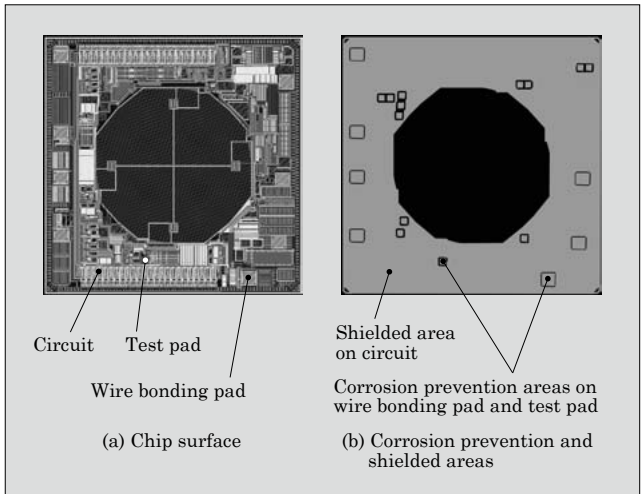


Fig.3 Corrosion prevention and shielded areas

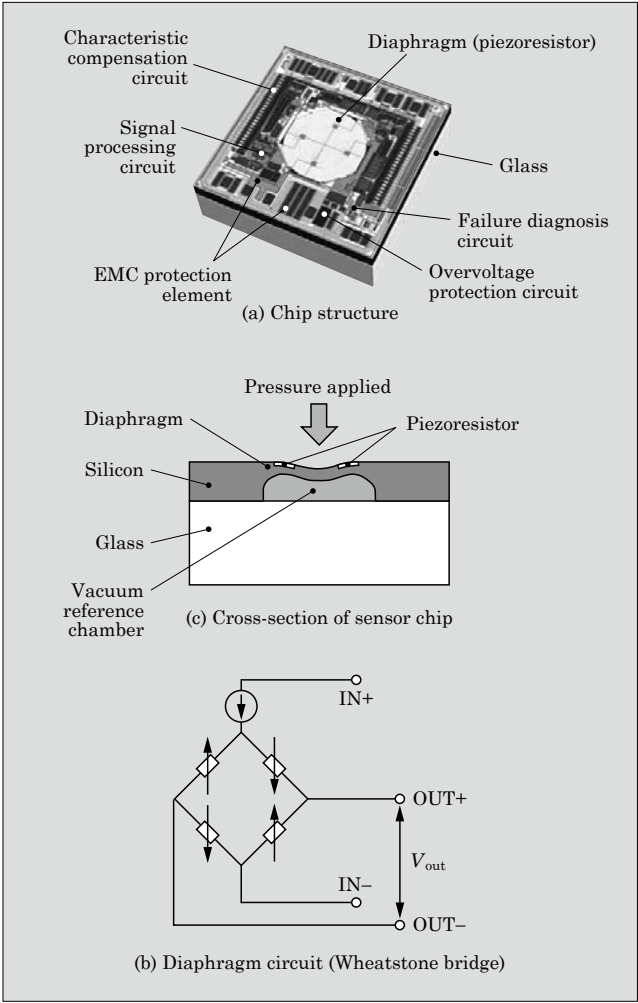


Fig.4 Overview of pressure-sensing unit

change, generating a potential difference in the output of the Wheatstone bridge. This potential difference is amplified to convert the pressure into an electric signal.

Any electrically charged vaporized fuel attached on the gelled protection material would cause the piezo-resistance values to vary and degrade the sensor characteristics. To prevent that, this product employs a shielded structure with polysilicon used for the flexible part (diaphragm) of the micro electro mechanical systems (MEMSs). As shown in Fig. 3, the same layer as that of the corrosion prevention areas is used to form a shielded area. The idea is to improve the resistance to electrostatic charging of the circuit except the diaphragm.

An electric charge that causes the potential on the gel surface to be a few kV was applied to the product with this structure. The resultant output characteristic changes are shown in Fig. 5. With an unshielded structure, the output significantly varies some time after the start of applying the charge. Unlike the unshielded structure, this shielded product does not show any output variation over a long time of application and achieves high resistance to electrostatic charging.

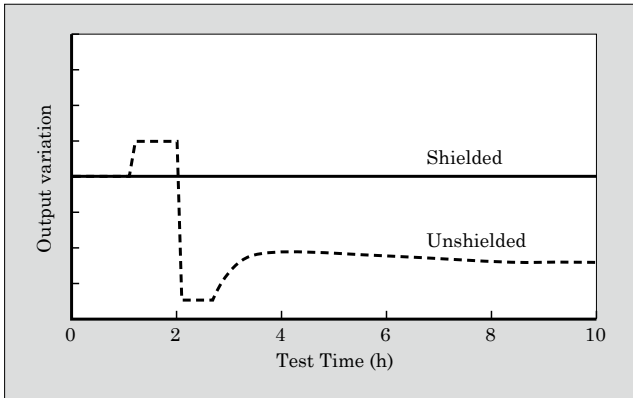


Fig.5 Result of test of resistance to electrostatic charging

#### References

- (1) Mutsuo, N. et al. 6th Generation Small Pressure Sensor. FUJI ELECTRIC REVIEW. 2011, vol.57, no.3, p.103-107.

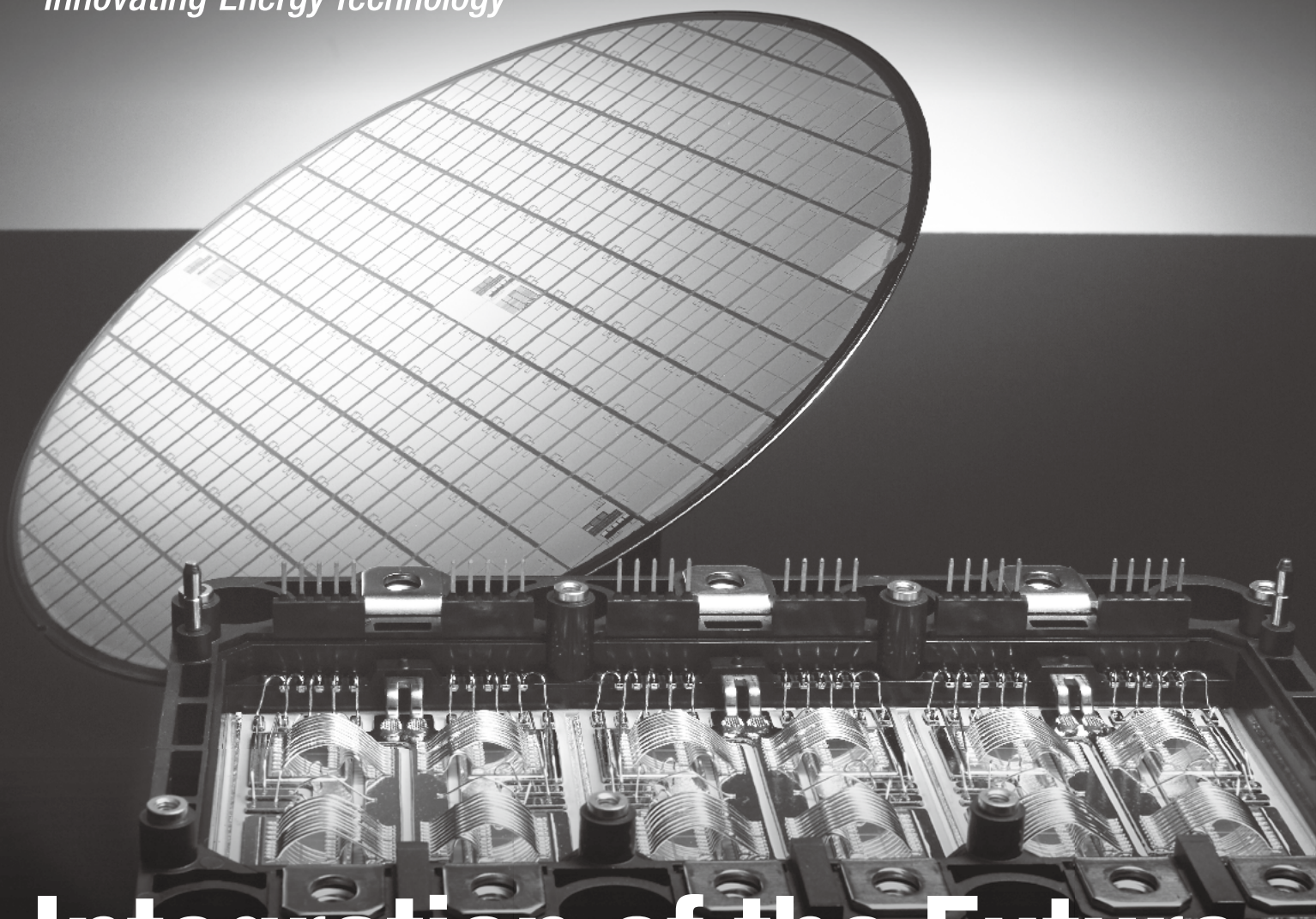
#### Launch time

November 2017

#### Product Inquiries

Automotive Semiconductor Discrete Department,  
Electronic Devices Business Group, Fuji Electric  
Co., Ltd.

Tel: +81 (263) 25-2777



# Integration of the Future

Fuji Electric's power semiconductors densely containing our unique power electronics technology and possibility of application. We have been improving these key devices to have a high withstanding voltage, high capacitance, low power loss, and compact & light-weight package. The key devices have vigorously playing active parts in the clean energy field including photovoltaic and wind power generation, the energy conservation field, demanded in the industry and the home, and the traffic field including hybrid and electric vehicles. Moreover, we have been developing the next generation power semiconductors of higher performance using new material SiC. Fuji Electric will continue to renovate energy technologies and contribute to realize a safe, secure and sustainable society.



---

## Fuji Electric's power semiconductors

---

# Overseas Subsidiaries

\* Non-consolidated subsidiaries

## America

### Fuji Electric Corp. of America

Sales of electrical machinery and equipment, semiconductor devices, drive control equipment, and devices

Tel +1-732-560-9410

URL <http://www.americas.fujielectric.com/>

### Reliable Turbine Services LLC

Repair and maintenance of steam turbines, generators, and peripheral equipment

Tel +1-573-468-4045

### Fuji SEMEC Inc.\*

Manufacture and sales of door opening and closing systems

Tel +1-450-641-4811

## Asia

### Fuji Electric Asia Pacific Pte. Ltd.

Sales of electrical distribution and control equipment, drive control equipment, and semiconductor devices

Tel +65-6533-0014

URL <http://www.sg.fujielectric.com/>

### Fuji SMBE Pte. Ltd. \*

Manufacture, sales, and services relating to low-voltage power distribution board (switchgear, control equipment)

Tel +65-6756-0988

URL <http://smbe.fujielectric.com/>

### Fuji Electric (Thailand) Co., Ltd. \*

Sales and engineering of electric substation equipment, control panels, and other electric equipment

Tel +66-2-210-0615

URL <http://www.th.fujielectric.com/en/>

### Fuji Electric Manufacturing (Thailand) Co., Ltd.

Manufacture and sales of inverters (LV/MV), power systems (UPS, PCS, switching power supply systems), electric substation equipment (GIS) and vending machines

Tel +66-2-5292178

### Fuji Tusco Co., Ltd. \*

Manufacture and sales of Power Transformers, Distribution Transformers and Cast Resin Transformers

Tel +66-2324-0100

URL <http://www.ftu.fujielectric.com/>

### Fuji Electric Vietnam Co., Ltd. \*

Sales of electrical distribution and control equipment and drive control equipment

Tel +84-24-3935-1593

URL <http://www.vn.fujielectric.com/en/>

### Fuji Furukawa E&C (Vietnam) Co., Ltd. \*

Engineering and construction of mechanics and electrical works

Tel +84-4-3755-5067

### Fuji CAC Joint Stock Company \*

Provide the Solution for Electrical and Process Control System

Tel +84-28-3742-0959

URL [www.fujicac.com](http://www.fujicac.com)

### PT. Fuji Electric Indonesia \*

Sales of inverters, servos, UPS, tools, and other component products

Tel +62 21 574-4571

URL <http://www.id.fujielectric.com/>

### Fuji Electric India Pvt. Ltd. \*

Sales of drive control equipment and semiconductor devices

Tel +91-22-4010 4870

URL <http://www.fujielectric.co.in>

### Fuji Electric Philippines, Inc.

Manufacture of semiconductor devices

Tel +63-2-844-6183

### Fuji Electric (Malaysia) Sdn. Bhd.

Manufacture of magnetic disk and aluminum substrate for magnetic disk

Tel +60-4-403-1111

URL <http://www.fujielectric.com.my/>

### Fuji Furukawa E&C (Malaysia) Sdn. Bhd. \*

Engineering and construction of mechanics and electrical works

Tel +60-3-4297-5322

### Fuji Electric Taiwan Co., Ltd.

Sales of semiconductor devices, electrical distribution and control equipment, and drive control equipment

Tel +886-2-2511-1820

### Fuji Electric Korea Co., Ltd.

Sales of power distribution and control equipment, drive control equipment, rotators, high-voltage inverters, electronic control panels, medium- and large-sized UPS, and measurement equipment

Tel +82-2-780-5011

URL <http://www.fujielectric.co.kr/>

### Fuji Electric Co., Ltd. (Middle East Branch Office)

Promotion of electrical products for the electrical utilities and the industrial plants

Tel +973-17 564 569

### Fuji Electric Co., Ltd. (Myanmar Branch Office)

Providing research, feasibility studies, Liaison services

Tel +95-1-382714

### Representative office of Fuji Electric Co., Ltd. (Cambodia)

Providing research, feasibility studies, Liaison services

Tel +855-(0)23-964-070

## Europe

### Fuji Electric Europe GmbH

Sales of electrical/electronic machinery and components

Tel +49-69-6690290

URL <http://www.fujielectric-europe.com/>

### Fuji Electric France S.A.S

Manufacture and sales of measurement and control devices

Tel +33-4-73-98-26-98

URL <http://www.fujielectric.fr/>

### Fuji N2telligence GmbH \*

Sales and engineering of fuel cells and peripheral equipment

Tel +49 (0) 3841 758 4500

## China

### Fuji Electric (China) Co., Ltd.

Sales of locally manufactured or imported products in China, and export of locally manufactured products

Tel +86-21-5496-1177

URL <http://www.fujielectric.com.cn/>

### Shanghai Electric Fuji Electric Power Technology (Wuxi) Co., Ltd.

Research and development for, design and manufacture of, and provision of consulting and services for electric drive products, equipment for industrial automation control systems, control facilities for wind power generation and photovoltaic power generation, uninterruptible power systems, and power electronics products

Tel +86-510-8815-9229

### Wuxi Fuji Electric FA Co., Ltd.

Manufacture and sales of low/high-voltage inverters, temperature controllers, gas analyzers, and UPS

Tel +86-510-8815-2088

### Fuji Electric (Changshu) Co., Ltd.

Manufacture and sales of electromagnetic contactors and thermal relays

Tel +86-512-5284-5642

URL <http://www.fujielectric.com.cn/csfe/>

### Fuji Electric (Zhuhai) Co., Ltd.

Manufacture and sales of industrial electric heating devices

Tel +86-756-7267-861

URL <http://www.fujielectric.com.cn/fez/>

### Fuji Electric (Shenzhen) Co., Ltd.

Manufacture and sales of photoconductors, semiconductor devices and currency handling equipment

Tel +86-755-2734-2910

URL <http://www.sz.fujielectric.com.cn/>

### Fuji Electric Dalian Co., Ltd.

Manufacture of low-voltage circuit breakers

Tel +86-411-8762-2000

### Fuji Electric Motor (Dalian) Co., Ltd.

Manufacture of industrial motors

Tel +86-411-8763-6555

### Dailan Fuji Bingshan Vending Machine Co., Ltd.

Development, manufacture, sales, servicing, overhauling, and installation of vending machines, and related consulting

Tel +86-411-8754-5798

### Fuji Electric (Hangzhou) Software Co., Ltd.

Development of vending machine-related control software and development of management software

Tel +86-571-8821-1661

URL <http://www.fujielectric.com.cn/fhs/>

### Fuji Electric FA (Asia) Co., Ltd.

Sales of electrical distribution and control equipment

Tel +852-2311-8282

### Fuji Electric Hong Kong Co., Ltd.

Sales of semiconductor devices and photoconductors

Tel +852-2664-8699

URL <http://www.hk.fujielectric.com/en/>

### Hoei Hong Kong Co., Ltd.

Sales of electrical/electronic components

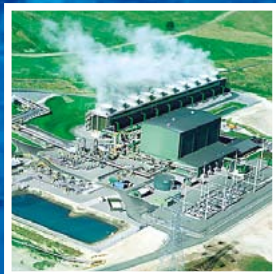
Tel +852-2369-8186

URL <http://www.hoei.com.hk/>

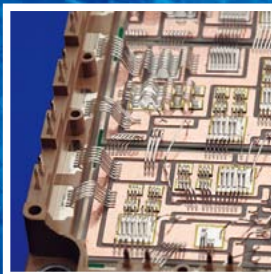


# *Innovating Energy Technology*

Through our pursuit of innovation in electric and thermal energy technology, we develop products that maximize energy efficiency and lead to a responsible and sustainable society.



Corrosion Resistant, Material, and Hot Water Utilization Technology  
Geothermal Power Plants



Device Technology  
Power Devices (IGBT)



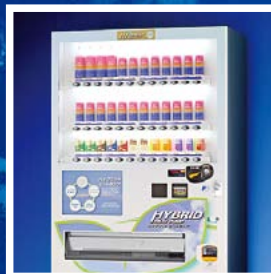
Power Electronics Technology  
Power Conditioning Systems (PCS)  
for Megasolar Plants



Power Electronics Technology  
Inverters



Power Electronics Technology  
Uninterruptible Power Supply  
Systems (UPS)



Heat Exchange and Refrigerant Control Technology  
Hybrid Heat Pump  
Vending Machines

**F** Fuji Electric